Role of pH-sensing (or Proton-Activated) Receptor - GPR4 and OGR1 in Intestinal Inflammation

Dissertation

zur
Erlangung der naturwissenschaftlichen Doktorwürde
(Dr. sc. nat.)

vorgelegt der

Mathematisch-naturwissenschaftlichen Fakultät

der

Universität Zürich

von

Yu WANG (王瑜)

aus China

Promotionskomitee:

Prof. Dr. med. Carsten A. Wagner (Vorsitz und Leitung der Dissertation)
Prof. Dr. med. Dr. phil. Gerhard Rogler (Koleiter der Dissertation)
Dr. rer. nat. Isabelle Frey-Wagner
Dr. rer. nat. Klaus Seuwen

Zürich, 2015

TABLE OF CONTENTS

TABLE OF CONTENTS **2**

SUMMARY **5**

ZUSAMMENFASSUNG **10**

CHAPTER 1 ..... **15**

INTRODUCTION **15**

1.1 INFLAMMATION AND IMMUNE RESPONSE 16

1.1.1 Introduction *16*

1.1.2 Th1 and Th2 cells in the adaptive immune system *18*

1.1.3 Overview of Th1, Th2, Th17 and Treg *21*

1.2 INFLAMMATORY BOWEL DISEASE (IBD) 23

1.2.1 A Brief Introduction to IBD *23*

1.2.2 Epidemiology *23*

1.2.3 Pathogenesis of IBD *24*

1.2.4 The intestinal mucosal immune system *25*

1.2.5 CD is a Th1/Th17 response and UC is a Th2-like response *30*

1.2.6 Overview of susceptibility loci implicated in IBD by GWAS *31*

1.3 IBD AND ACIDIC PH 35

1.3.1 Inflammation and acidic pH *35*

1.3.2 IBD and acidosis *38*

1.4 PROTON SENSING RECEPTOR FAMILY 42

1.5 MOUSE MODELS USED IN IBD STUDY 48

1.6 AIM OF THE PROJECT 51

CHAPTER 2 ..... **52**

PUBLICATIONS THAT CONTRIBUTED TO THAT WORK **52**

CHAPTER 3 ..... **55**

DISCUSSION **55**

3.1 **AMELIORATED COLITIS IN MICE LACKING GPR4 OR OGR1** 56

3.2 **THE PROPOSED MECHANISM OF GPR4 MEDIATED INFLAMMATION AGGRAVATION** 58

3.3 **SEVERAL LINES OF EVIDENCE TO SUPPORT THE DESTRUCTIVE ROLE OF ACTIVATED GPR4 IN THE PROGRESSION OF INFLAMMATION** 59

3.4 **PROGRESS IN GPR4 DOWNSTREAM SIGNALING PATHWAY STUDIES** 61

3.5 **PROGRESS IN DEVELOPMENT OF GPR4 INHIBITORS** 63

3.6 **OGR1 AND INFLAMMATION** 64

3.7 **GENDER DEPENDENT EFFECT OF OGR1** 65

3.8 **OTHER PROTON SENSORS AND THE DIGESTIVE SYSTEM** 66

CHAPTER 4 ..... **69**

FUTURE PERSPECTIVES **69**

REFERENCES **72**

CURRICULUM VITAE **81**

ACKNOWLEDGEMENTS **83**

LIST OF ABSTRACTS **86**

Summary

Inflammatory bowel disease (IBD), a common chronic inflammatory disorder of the gastrointestinal system, has been studied for decades. To clarify the pathogenesis of IBD and breakthrough the bottleneck of treatment remains a formidable task. It is widely acknowledged that inflammatory or tumor tissues exhibit elevated glucose uptake and local acidic pH due to hypoxia, excessive production and insufficient elimination of glycolytic metabolites. Recently, a novel family of proton sensing G-protein coupled receptors (GPCRs) including GPR4, ovarian cancer G protein coupled receptor 1 (OGR1, GPR68) and T-cell death associated gene 8 (TDAG8, GPR65) has been identified. All of these receptors are activated by protons in the physiological range around pH 7.4. The intraluminal gastrointestinal pH in patients with active IBD is significantly decreased. Local acidification, as low as pH 2.3, has been observed during intestinal inflammation and implicated in the pathogenesis and progression of IBD. The role of proton-activated GPCRs in the pathogenesis of inflammation is mostly unknown.

The aim of the thesis project is to unravel the relationship between pH receptors and IBD and to answer the question whether GPR4 and OGR1

may be involved in the pathogenesis of IBD. Here, we used two animal models to test our hypothesis; the dextran sulphate sodium (DSS) induced chronic colitis model and the IL10 KO mouse model, a spontaneous colitis model.

DSS was used to induce chronic colitis in GPR4 knockout mice (*Gpr4* $^{-/-}$, *in* Balb/c and C57Bl/6 background) and their respective wild-type controls (*Gpr4* $^{+/+}$, in Balb/c and C57Bl/6 background), to resemble ulcerative colitis (UC). Mice in both groups received 4 cycles of DSS treatment, while additional control groups of both genotypes received only normal water. In each cycle, 3% DSS was administered for 7 days in drinking water followed by 10 days of recovery with tap water. Mice were sacrificed after 5 weeks recovery after the last DSS cycle. Body weight was monitored and colon samples were collected for histology, cytokine mRNA expression, and myeloperoxidase (MPO) activity quantification. The colonoscopy score, colon length, and spleen weight were also used to assess the severity of colitis.

For the spontaneous colitis model, *Ogr1* $^{-/-}$ and *Gpr4* $^{-/-}$ mice (C57Bl/6) were crossed into interleukin-10 knockout (*IL-10* $^{-/-}$) mice (C57Bl/6), a spontaneous colitis model simulating Crohn's disease (CD), to generate *Gpr4* $^{+/+}$ */Ogr1* $^{-/-}$ */IL-10* $^{-/-}$ or *Gpr4* $^{-/-}$ */Ogr1* $^{+/+}$ */IL-10* $^{-/-}$ mice. The

development of rectal prolapse, a marker of severe intestinal inflammation, was followed over 200 days. The incidence of rectal prolapses in double knockout mice was compared with *IL-10* $^{-/-}$ from the same litters. Kaplan-Meier survival analysis was introduced to evaluate whether deficiency of pH receptors could change prolapse occurrence. Moreover, to eliminate the bias and influence of severe colitis and development of prolapse, another group of mice was sacrificed at age 80 days, before any of the mice developed prolapses. Severity of colitis was assessed by the conventional parameters cytokine mRNA expression, histological score, MPO activity, colon length, and spleen weight. Lamina propria leukocytes (LPLs) from large intestine in mice were freshly isolated and characterized by flow cytometry assay.

After induction of chronic DSS colitis in *Gpr4* $^{+/+}$ *and Gpr4* $^{-/-}$ mice, *Gpr4* $^{-/-}$ mice showed less body weight loss (p <0.05 *) and lower histology scores (p <0.001 ***) indicating less severe inflammation. No significant difference in MPO activity and spleen weight was found. In the spontaneous colitis model, Kaplan-Meier survival analysis showed a significantly delayed onset and progression of rectal prolapses in female *Gpr4* $^{+/+}$ */Ogr1* $^{-/-}$ */IL-10* $^{-/-}$ mice relative to female *Gpr4* $^{+/+}$ */Ogr1* $^{+/+}$ */IL-10* $^{-/-}$ mice (p = 0.002 **) whereas there was no difference in male mice (p = 0.776). In comparison with *Gpr4* $^{+/+}$ */Ogr1* $^{+/+}$ */IL-10* $^{-/-}$ mice, both female

and male *Gpr4* $^{-/-}$ */Ogr1* $^{+/+}$ */IL-10* $^{-/-}$ mice had a significantly delayed onset and progression of rectal prolapses (estimated median survival time: female: >200 days vs. 123 days; male: >200 days vs. 161 days; p =0.000 *** and p =0.007 **). These findings were confirmed by the histology scores and MPO activity test.

Our findings demonstrate that the deficiency of GPR4 attenuated colitis in the *IL-10* $^{-/-}$ mice model. Because the spontaneous colitis in *IL-10* $^{-/-}$ mice is mediated by T helper 1 (Th1) and T helper 17 (Th17) cells, we tested whetherin *Gpr4* $^{-/-}$ */Ogr1* $^{+/+}$ */IL-10* $^{-/-}$ mice the Th1, Th17 and T regulatory (Treg) subpopulation profile might differ from *IL-10* $^{-/-}$ mice in lamina propria lymphocytes (LPLs). The LPLs profiles in flow cytometric analysis demonstrated that the deficiency of GPR4 suppressed infiltration of CD4+ (T helper) cells, mainly Th1 cells, but not CD8+ (T cytotoxic) cells, which was confirmed by the cytokine expression data. Female *Gpr4* $^{-/-}$ */Ogr1* $^{+/+}$ */IL-10* $^{-/-}$ mice had a significantly lower Th1 cytokine IFN-γ mRNA expression in colon compared with their female *Gpr4* $^{+/+}$ */Ogr1* $^{+/+}$ */IL-10* $^{-/-}$ counterparts.

Taken together, these data suggested that GPR4 deletion in mice was followed by ameliorated colitis and reduced susceptibility in the DSS induced chronic colitis model and that the deficiency of both pH

receptors, either GPR4 or OGR1, attenuated spontaneous inflammation and modulated the severity of disease in the *IL-10* $^{-/-}$ model. There data, therefore, indicate an important pathophysiological role for these G-protein coupled receptors during the pathogenesis of mucosal inflammation.

In the end, a possible mechanism of GPR4-mediated inflammation aggravation is proposed. In the spontaneous colitis model, the additional deletion of GPR4 in *IL-10* $^{-/-}$ mice leads to the loss of the proton sensors and defective downstream signaling pathway, induces suppression of Th1 cells and less production of IFN-γ in colon, offers protection and reduces spontaneous inflammation, and finally delays the onset and progression of rectal prolapse. Therefore, in turn, activation of GPR4 is likely to exacerbate intestinal inflammation and trigger responses which promote inflammation via a pathway involving Gs-cAMP, Th1, and IFN-γ.

ZUSAMMENFASSUNG

Chronisch Entzündliche Darmerkrankungen (CEDs) befinden sich als häufige gastrointestinale Krankheitsentitäten seit Jahrzehnten im Fokus der Forschung. Es bleibt dennoch schwierig die Pathogenese vollständig zu erklären und die Entwicklung weiterer Behandlungsstrategien ist notwendig. Es gilt als gesichert, dass entzündetes sowie tumoröses Gewebe verstärkt Glukose aufnimmt und von einem sauren Milieu umgeben ist. Dies wird erklärt durch Hypoxie, eine exzessive Produktion von Glykolysemetaboliten mittels anaerober Glykolyse und einer insuffizienten Eliminierung dieser Metabolite.

Kürzlich wurde eine neue Familie Protonen-aktivierter G-Protein gekoppelter Rezeptoren (GPCRs) identifiziert, welche GPR4, den Ovarian cancer G-protein coupled receptor 1 (OGR1, GPR68) sowie T-cell death asscociated gene 8 (TDAG8, GPR65) beinhaltet. All diese Rezeptoren werden durch Protonen innerhalb des physiologischen Bereichs um pH 7,4 aktiviert und könnten eine Rolle in der Aufrechterhaltung des pH Gleichgewichts spielen bzw in der Messung des lokalen pH.

Messungen belegen, dass der intraluminale Darm-pH-Wert bei Patienten, welche an einem aktiven Schub einer chronisch entzündlichen Darmerkrankung leiden, signifikant saurer ist. Die pH-Wert Erniedrigung bis hin zu einem pH von 2.3 sind lokal auf den entzündeten Darmabschnitten begrenzt und es, ist anzunehmen, dass diese pH-Wert Veränderung in der Pathotgenese wie auch im Verlauf von CEDs eine bedeutende Rolle spielt. Die Rolle von Protonen-aktivierten GPCRs in der

Pathogenese von Entzündungen ist weitestgehend unbekannt.

Ziel dieser Arbeit ist vornehmlich die Beantwortung zweier Kernfragen. Besteht ein Zusammenhang zwischen pH-Rezeptoren und CEDs und sind GPR4 sowie OGR1 an der Pathogenese von CEDs beteiligt? Um unsere Hypothese zu überprüfen testeten wir zwei Mausmodelle. Einerseits das Dextransulphat (Dextran Sulphat Sodium, DSS) induzierte chronische Kolitismodell und andererseits das spontane Kolitismodell in IL10 KO Mäusen.

Mit DSS wurde in GPR4 knockout Mäusen (*Gpr4* $^{-/-}$, im Balb/c und C57Bl/6 Hintergrund) und Wildtyp Mäusen (*Gpr4* $^{+/+}$, ebenfalls im Balb/c und C57Bl/6 Hintergrund) eine Kolitis induziert, welche der humanen Kolitis Ulcerosa ähnelt. Während die Tiere in der Kontrollgruppe gewöhnliches Trinkwasser angeboten bekamen, erhielten die Tiere in beiden Versuchsgruppen eine Behandlung mit vier DSS-Zyklen. In den ersten sieben Tagen jedes Zyklus wurde dem Trinkwasser 3%iges DSS zugesetzt, gefolgt von zehn Erholungstagen mit normalem Trinkwasser. Die Mäuse wurden nach 4 Zyklen der 3%-DSS-Behandlung und einer abschliessenden fünfwöchigen Erholung getötet. Für die Evaluation der Krankheitsschwere wurde der Gewichtsverlauf protokolliert, ein Koloskopiescore erhoben und die Darmlänge sowie das Milzgewicht gemessen. Zudem wurden Kolonproben für die histologische Aufarbeitung entnommen und mRNA Level bestimmter Zytokine sowie die Myeloperoxidaseaktivität (MPO) bestimmt.

Für die spontane Kolitis wurden *Ogr1* $^{-/-}$ und *Gpr4* $^{-/-}$ Mäuse (C57Bl/6) jeweils mit Interleukin-10 knockout (*IL-10* $^{-/-}$, C57Bl/6) Mäusen gekreuzt um *Gpr4* $^{+/+}$ */Ogr1* $^{-/-}$ */IL-10* $^{-/-}$ bzw. *Gpr4* $^{-/-}$ */Ogr1* $^{+/+}$ */IL-10* $^{-/-}$ Doppelknockouts zu erhalten. Diese Tiere dienten als Modell für einen Morbus Crohn ähnlichen Krankheitsverlauf. Über einen Zeitraum von 200 Tage wurde die Entwicklung eines Rektumprolaps als Indikator einer schweren intestinalen Entzündung erfasst. Die Inzidenz des Rektumprolaps in den Doppelknockout-Tieren wurde mit den *IL-10* $^{-/-}$ Tieren aus der gleichen Zuchthaltung verglichen. Mithilfe der Überlebenszeitanalyse nach Kaplan-Meier wurde evaluiert ob ein Ausschalten derpH-Rezeptoren GPR4 oder OGR1 die Prolapsrate beeinflusst. Um die Pathogenese der Colitis zu einem Zeitpunkt zu vergleichen bei dem weder bei den Doppelknockout Tieren noch bei den *IL-10* $^{-/-}$ Mäusen bereits ein Prolaps aufgetreten war, wurden weitere Mäuse im Alter von 80 Tagen getötet.. Zur Evaluation der Krankheitsschwere wurden die gewöhnlichen Parameter, herangezogen. Neben der Bestimmung des Histologiescores und der MPO-Aktivität wurde die mRNA Expression diverser Zytokine sowie die Kolonlänge und das Milzgewicht gemessen. Lamina propria Leukozyten (LPLs) aus dem Dickdarm wurden frisch isoliert und mittels Durchflusszytometrie charakterisiert.

Nach Induktion der chronischen DSS Kolitis in *Gpr4* $^{+/+}$ *und Gpr4* $^{-/-}$ Mäusen weist ein geringerer Gewichtsverlust (p <0.05 *) sowie ein niedrigerer Histologiescore in den Knockouttieren (p<0.001 ***) auf eine weniger schwere Kolitis hin. MPO-Aktivität und Milzgewicht unterschieden sich jedoch nicht signifikant. Im spontanen Kolitismodell

zeigte die Prolapszeitanalyse nach Kaplan-Meier ein signifikant verspätetes Auftreten von Rektumvorfällen in weiblichen *Gpr4* $^{+/+}$ */Ogr1* $^{-/-}$ */IL-10* $^{-/-}$ Mäusen verglichen mit *Gpr4* $^{+/+}$ */Ogr1* $^{+/+}$ */IL-10* $^{-/-}$ Mäusen (p = 0.002 **). Dagegen konnte dieser Unterschied nicht in männlichen Tieren festgestellt werden (p = 0.776). Verglichen mit *Gpr4* $^{+/+}$ */Ogr1* $^{+/+}$ */IL-10* $^{-/-}$ Mäusen, trat ein Rektumprolaps bei *Gpr4* $^{-/-}$ */Ogr1* $^{+/+}$ */IL-10* $^{-/-}$, ungeachtet ihres Geschlechts, später auf (geschätzte mittlere Überlebenszeit: weiblich > 200 Tage vs. 123 Tage; männlich: >200 Tage vs. 161 Tage; p =0.000 *** and p =0.007 **). Unterstützt wird diese Beobachtung durch die Ergebnisse des Histologiescores sowie der MPO-Aktivitätsmessung.

Unsere Untersuchungen konnten zeigen, dass eine GPR4 Defizienz eine Abschwächung der Kolitis im *IL-10* $^{-/-}$ Mausmodell bewirkt. Die weiteren Untersuchungen konzentrierten sich auf die Klärung der zugrundeliegenden Mechanismen. Da die spontane Kolitis in *IL-10* $^{-/-}$ Mäusen durch T1- sowie T17-Helferzellen (Th1 & Th17) unterhalten wird, testeten wir die Hypothese, dass sich Th1, Th17 und regulatorische T-Zellen (Treg) der Lamina propria Lymphozyten (LPLs) des Darms sich in *Gpr4* $^{-/-}$ */Ogr1* $^{+/+}$ */ IL-10* $^{-/-}$- von *Gpr4* $^{+/+}$ */Ogr1* $^{+/+}$ */IL-10* $^{-/-}$-Mäusen unterscheiden. Die LPLs Profile in der Durchflusszytometrieanalyse demonstrierten, dass die GPR4 Defizienz mit einer verminderten Infiltration CD4+ T-Helfer Zellen, vornehmlich Th1 Zellen, nicht aber CD8+ zytotoxischer T-Zellen einhergeht. Diese Ergebnisse wurden durch die Resultate der Zytokinexpressionsmessungen bestärkt. Weibliche *Gpr4* $^{-/-}$ */Ogr1* $^{+/+}$ */IL-10* $^{-/-}$ Mäuse wiesen eine signifikant niedrigere Th1 INF-γ mRNA Zytokinexpression in Darmgewebe, verglichen mit den

entsprechenden weiblichen *Gpr4* $^{+/+}$ */Ogr1* $^{+/+}$ */IL-10* $^{-/-}$ auf.

Zusammenfassend weisen die Resultate darauf hin, dass der GPR4 Knockout mit einer abgeschwächten Kolitis und einer reduzierten Anfälligkeit für die durch DSS induzierte Kolitis in Mäusen einhergeht. Das Fehlen der GPR4 oder OGR1 pH-Rezeptoren verbesserte die spontane Entzündung und modulierte die Krankheitsschwere im *IL-10* $^{-/-}$ Modell. Zusammenfassend legen diese Daten eine bedeutende pathophysiologische Rolle der G-Protein gekoppelten Rezeptoren in der mukosalen Entzündung nahe.

Abschliessend seien mögliche Mechanismen genannt, welche Erklärungsansätze für die GPR4-vermittelte Entzündung bieten. Die zusätzliche Deaktivierung von GPR4 in *IL-10* $^{-/-}$ Mäusen führt zu einem Verlust von Protonensensoren und einem gestörten nachgeschalteten Signalweg. Sie bewirkt zudem eine Suppression von Th1 Zellen und eine geringere Produktion von IFN-γ im Darm. Letztlich stellt das Fehlen von GPR4 einen "Schutzfaktor" dar, der die Entwicklung einer spontanen Kolitis reduziert und das Auftreten sowie die Progression eines Rektumprolaps verzögert. Andersherum, deutet dies auf eine pro-inflammatorische Rolle von GPR4 und OGR1 in der Pathogenese von CED dar. Dies führt zu der Annahme, dass eine Aktivierung von GPR4 die Verschlechterung einer Kolitis bewirkt und entzündungsunterhaltenden Prozesse fördert.

Chapter 1

Introduction

1.1 Inflammation and immune response

1.1.1 Introduction

What is the inflammation? "*Inflammation is a protective response which intended to eliminate the initial cause of cell injury, as well as the necrotic cells and tissues resulting from the original insults*" [1]. The protection and elimination finally can be accomplished by diluting, destroying and neutralizing the harmful pathogens. These functions are mediated by a complex host response called inflammation [1].

In general, the process of inflammation can be defined by the five "R" [2]: (1) Recognition of the toxic pathogens, (2) Recruitment of leukocytes, (3) Removal of the agent, (4) Regulation of the response, and (5) Repairing of the tissue functions.

In the initial step of protection, the innate immune system is activated by the chemical properties of the antigen, and it offers a fast and nonspecific defense mechanisms. These mechanisms include physical barriers such as physical (skin and mucosa), biochemical (i.e. complement, lysozyme and interferons), and immune system cells (e.g. neutrophils, monocytes, macrophages, natural killer [NK], and natural killer-T [NKT] cells) that attack foreign cells in the body [1]. If the innate immune response is insufficient to facilitate the clearance of the foreign pathogen, the response will shift toward a more complex and efficient process – the acquired or adaptive immune response [3]. The adaptive response recognizes the specific antigens through an antigen presenting process and enables B cell lymphocyte to mediate a humoral immune

response, whereas T cells lymphocyte mediate a cellular immune response [3].

Due to the defense efforts of both the innate and the adaptive immune system, and all the immune cells and antibodies from the cellular and humoral immune responses, the toxic pathogens are removed from the body. Meanwhile, the repair process is started to fix the tissue functions. The repair process includes three different levels [4]: regeneration, healing and/or fibrosis. Regeneration means new generations of tissues replace the damaged components and tissue functions essentially return to a normal state. If the injured tissue is not able to completely restitute, healing and fibrosis will provide enough structural stability that the injured tissue is usually able to function.

Inflammation can be categorized into acute and chronic inflammation [1]. Acute inflammation is rapid in onset and of short duration, lasting from a few minutes to a few days. In the context of acute inflammation, the main inflammatory reactions are composed of several vascular reactions and cellular responses [2]: heat (color), redness (rubor), swelling and pain (tumor and dolor). The pathology of acute inflammation is characterized by vascular changes, edema, and predominant neutrophil infiltration. The outcome of acute inflammation is either elimination of the stimuli followed by returning of the host to the normal condition and repair of the tissue function, or persistent stimulation resulting in chronic inflammation if the stimuli cannot be eliminated immediately. The duration of chronic inflammation lasts from weeks to years. The prolonged host response to persistent stimulus can lead to continuous

immune cell recruitment and tissue damage. In pathology, chronic inflammation is characterized by tissue destruction; angiogenesis and fibrosis; infiltration with macrophages, lymphocytes and plasma cells.

Although inflammatory reactions help clearing the stimuli, inflammation and subsequent repair processes themselves sometimes can cause substantial damage to the host body as well [1, 2, 4, 5]. During severe inflammation, the host innate immune system mediates a strong reaction, e.g. damage and tissue destruction, in an attempt to clear the infections and other harmful stimuli, which exert a negative or irreversible effect on tissue functions. Injury also might be caused by auto-antigens in autoimmune diseases, or by harmless environmental antigens in allergic disorders.

In short, the function of inflammation to the host body can be a double-edged sword. On one hand, it is a beneficial host response. On the other hand, it is itself capable of bringing tissue damage. In this sense, the immune system must be fine-tuned to maintain homeostasis.

1.1.2 *Th1 and Th2 cells in the adaptive immune system*

When the first line of defense (e.g. mucosa) is broken through, invasive bacteria will have to be eliminated by macrophages in their lysosome by endocytosis [3]. And then, antigen presenting cells (APCs) (e.g. dendritic cells, macrophages and B lymphocyte) present the antigen peptides to the T cell receptor of T lymphocytes, thereby activating T cells. IL-1 secreted by macrophages helps activating T helper cells ($CD4^+$); whereas IL-2 secreted by activated T helper cells regulates proliferation and

differentiation of T helper 1 (Th1) and T helper 2 (Th2) subsets [6-10]. Th1 cells secreting IFN-γ and TNF- directly activate macrophages, nature killer cells (NK) and cytotoxic T cells ($CD8^+$) [11], which are commonly known as cell-mediated immunity [3, 6, 9, 10]. Th2 cells, primarily producing IL-4, induce proliferation and differentiation of B cells into antibody secreting plasma cells and memory B cells, which are called humoral immunity [3, 8, 12]. Regulatory cytokines IFN-γ and IL-10 suppress Th2 and Th1 responses, respectively [3, 6-8, 10].

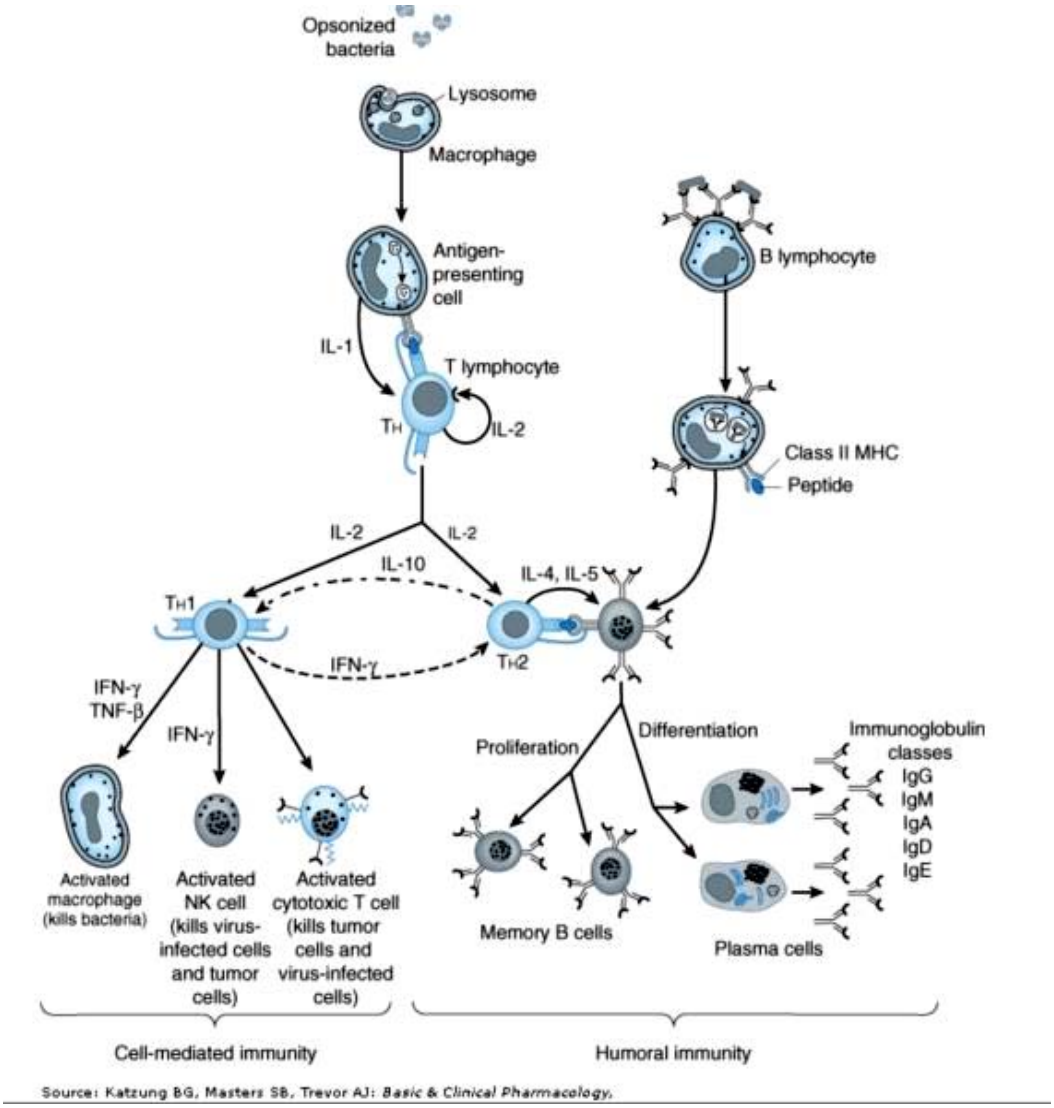

Figure 1 *Schematic overview of molecular interaction between cell-mediated and humoral immune responses* [3].

Both cell-mediated and humoral immune responses constitute the adaptive immune system, the highly specific and sophisticated defense system, which allows humans to better cope with the hostile environment [3, 7, 8, 12]. The cellular immunity protects the body by activating macrophages and natural killer cells, enabling them to destroy pathogens and form endosomes; by activating cytotoxic T cells that are able to induce apoptosis in tumor cells and virus infected cells; and by stimulating immune cells to secrete a variety of cytokines that up-regulate or down-regulate the function of other immune cells involved. The humoral immunity is also called the antibody-mediated system due to the production of specific antibodies [3, 12]. The plasma cells produce huge amounts of antibodies that will bind to the antigens and drive the target microorganisms for destruction. B memory cells remain the "memory" for the specific antigen that can be used to mobilize the immune system faster if the body meets the antigen later again [12].

It should be emphasized that Th2 cells, bridging the gap between T and B cells (Figure 1), are essential to stimulate IgE production [3, 6, 9, 12]. The humoral immunity will not be activated in the absence of Th2 cells, which is why the cellular cooperation between T and B cells is required for the production of antibodies.

1.1.3 Overview of Th1, Th2, Th17 and Treg

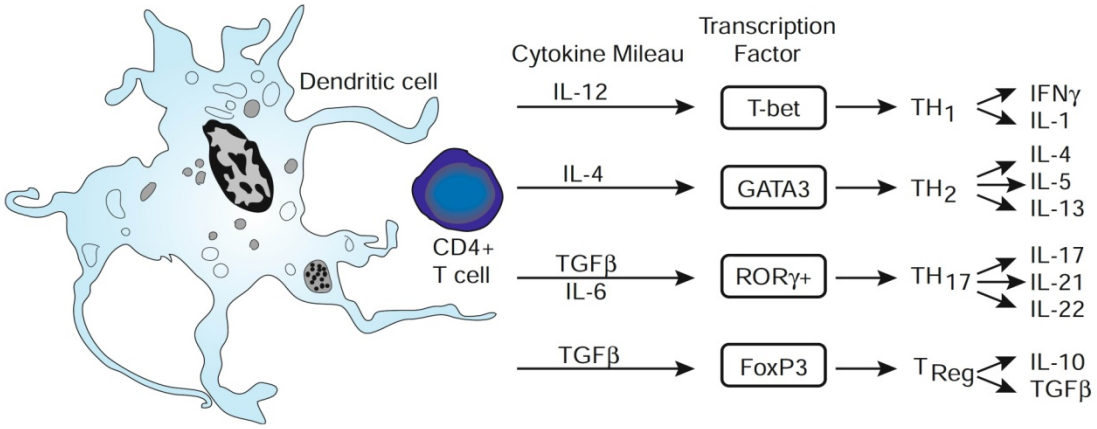

Figure 2 *The cytokine environment during antigen presentation controls T-cell differentiation by regulation of specific transcription factor activation* [5].

Based on the array of cytokines (e.g. IFN-γ or IL-4) produced by T lymphocytes, T helper cells are classically grouped into Th1 and Th2 cells subsets [6-10]. More recent studies have further broadened our knowledge of T cells. Nowadays, immunologists generally acknowledge that T helper cells are not restricted to Th1 and Th2 cells. A new subset of T cells (Th17) [13], which are characterized by producing IL-17 and IL-22, but not IFN-γ or IL-4, emerged to mediate chronic inflammatory disorders in collaborations with Th1 and Th2 cells [14, 15]. These three T helper cells (Th1, Th2 and Th17) have also been called T effector cells (T effector) [6-11, 13].

T effector cells are able to generate an antigen specific T cell immune response to eliminate antigens [9]. But, uncontrolled or excessive immune responses can lead to continuous inflammatory cell recruitment and tissue damage too, if persistent and unregulated, can finally result in

organ dysfunction. There must be some ways to control or prevent auto-immune responses. Besides the anti-inflammatory cytokine IL-10, T regulatory (Treg) cells are present as inhibitors and suppressors of the immune responses [16, 17], which are characterized by the high and stable expression of $CD25^+$ and FoxP3 [18, 19]. The in-vivo animal models provided some evidence for the presence and functions of Treg. The complete Treg depletion in Treg knockout mice led to profound autoimmunity and lethal autoimmune disease, which demonstrates that Treg suppression plays an indispensable role in the immune homeostasis [20].

In general, T cell differentiation is a complex process, depending on the local cytokine environment and the regulation of specific transcription factor activation. Figure 2 shows how Naïve $CD4^+$ T cells can be differentiated into 3 effector T cells and Treg cells subgroups [5]. In Th1 pathway, IL-2 and IL-12 induces Th1 differentiation, which promotes cell-mediated Th1 response. Compared with antibody-mediated Th2 response, Th1 response characterized by IFN-γ production along with T-bet transcription factor expression, is a more effective and stronger response [3]. But, long term of Th1 response will be devastating to the host, and the immune response therefore must be shift to a relatively mild response for the tissue. That is Th2 response, which requires GATA3 transcription factor expression [5]. In terms of Th17, Th17 differentiation depends on the expression of $ROR\gamma^+$ transcription factor and the exposure to transforming growth factor β (TGF-β) [5, 13]. While Treg pathway, as the above picture shows, relies on the expression of transcription factor FoxP3 plus TGF-β [16, 17]. All these four T cell subtypes are major components of immune systems.

1.2 Inflammatory Bowel Disease (IBD)

1.2.1 *A Brief Introduction to IBD*

Inflammatory Bowel Disease (IBD) [21-24] is a chronic disorder and inflammation of the colon and small intestine characterized by abdominal pain, vomiting, diarrhea, intestinal bleeding, anemia, body weight loss and various associated complaints or diseases like rheumatoid arthritis (RA), sclerosing cholangitis, ankylosing spondylitis, iritis/uveitis, pyoderma gangrenosum and erythema nodosum [25].

IBD is conventionally divided into two major types: Crohn's disease (CD) and ulcerative colitis (UC). The main difference between Crohn's disease and Ulcerative colitis is the location and nature of the inflammation (Figure 3) [26]. Crohn's disease may affect any part of the gastrointestinal tract, from mouth to anus, in spite of the majority of the cases starting in the terminal ileum. Ulcerative colitis, in contrast, is restricted to the colon and the rectum. Histologically, ulcerative colitis is restricted to the mucosa (epithelial lining of the gut), while Crohn's disease affects the whole bowel wall [23, 24].

1.2.2 Epidemiology

It is estimated that as many as 1.4 million people in the United States and 2.2 million in Europe are suffering from IBD, based on a study in 2004 [27]. IBD's peak onset is in persons 15 to 30 years of age. There seems to be slight gender related differences in IBD incidence. Ulcerative colitis is slightly more common in males, whereas Crohn's disease shows a

slight female predominance [27].

	Typical UC features	Typical CD features
Clinical	Frequent small-volume diarrhea with urgency	Diarrhea accompanied by abdominal pain and malnutrition
	Predominantly bloody diarrhea	Stomatitis
		Abdominal mass
		Perianal lesions
Endoscopic and radiological	Diffuse superficial colonic inflammation	Discontinuous transmural asymmetric lesions
	Involvement of rectum, but this can be patchy	Mainly involving ileum and right-sided colon
	Shallow erosions and ulcers	Cobblestone appearance
	Spontaneous bleeding	Longitudinal ulcer
		Deep fissures
Histopathological	Diffuse inflammation in mucosa or submucosa	Granulomatous inflammation
	Crypt architecture distortion	Fissures or aphthous ulcers can be seen; often transmural inflammation
Serological markers	Antineutrophil cytoplasmic antibodies	Anti-*Saccharomyces cerevisiae* antibodies

Figure 3 *Features for differentiating between UC and CD* [26]

1.2.3 Pathogenesis of IBD

There are two major hypotheses on IBD pathogenesis [28, 29]: 1. IBD is caused by abnormal and excessive immunological responses to the normal intestinal microflora. For example, the disorders of the mucosal innate immune system cause IBD, caused by events such as NOD2 polymorphisms, functional disorders of NOD2 or defective NOD2/CARD 15 signaling pathways. 2. IBD is alternatively caused by primary abnormal changes in the intestinal microflora. The changes in the composition of intestinal microflora result in pathogenic responses and mucosal inflammation. For instance, many IBD mouse model exhibit the features of bacteria driven inflammation, supporting the latter hypothesis. Being such a complex, chronic and relapsing disorder, to

clarify the pathogenesis of IBD remains a formidable task, however [21-25]. Both hypotheses require further evaluation and validation [28, 29].

1.2.4 *The intestinal mucosal immune system*

The intestinal mucosal immune system is composed of three major lymphoid areas (Figure 4) [30, 31]: 1. Lamina propria lymphocytes (LPLs), which lie beneath the epithelium and the basement membrane in the intestinal villi, constituting the mucosa with the epithelium; 2. Intraepithelial lymphocytes (IELs), which locate between the columnar epithelial cells; 3. Peyer's patches (PP), which are embedded in the gut wall. These three parts (LPLs, IELs and PP) constitute a complex network, the gut-associated lymphoid tissue (GALT), to respond to pathogens and insults in the gastrointestinal (GI) system.

Obviously, the intestinal epithelium within the GI tract plays a key role in the homeostasis maintenance of the intestinal immune system. Intestinal epithelial cells form a physical barrier against the massive invasion of bacteria and other antigens. An intact mucosal barrier and its integrity depend on intercellular tight junctions between cells, which help seal the paracellular space.

Under normal conditions [21, 22], the mucus layer secreted by the goblet cells, antimicrobial peptides (e.g. α-defensins) secreted by the paneth cells and IgA provide enough protection against bacterial invasion. In IBD [21], in contrast, the immune responses damage the mucus layer, reduce the production of antibodies and defensins, and increase the exposure to

luminal bacteria.

Under normal circumstances [21, 22], the initial immune response to intestinal bacteria is precisely regulated, and the regulation mechanism will decide whether there will be immune tolerance or triggering of a defensive response. Pattern recognition receptors, such as toll like receptors, and nucleotide oligomerization domain (NOD) like receptors [32], sensing NOD proteins, are essential to identify innate microbial signals and pathogen-associated molecular patterns (PAMPs). And then dendritic cells present antigens to naïve $CD4^+$ T cells in PP and drive the differentiation of $CD4^+$ T cells into regulatory T cells (Treg) and T helper cells (Th1, Th2 and Th17) with the assistance of cytokines, e.g. transforming growth factor β (TGF-β) and interleukin 10 (IL-10). The mentioned subtypes of $CD4^+$ T cells together with specific cytokines circulate to the intestinal lamina propria area and carry out effector functions (Figure 4) [21, 22].

The intestinal mucosal immune system forms a complex network [33]. Normally, the innate and adaptive immune cells in thelamina propria secrete a variety of cytokines, including anti-inflammatory cytokines, e.g. TGF-β and IL-10, which suppress the immune responses, and pro-inflammatory cytokines, e.g. tumor necrosis factor-α (TNF-α), IL-1β, IL-6, IL-12 and IL-23, which limit the exposure to luminal bacteria and protect the epithelium cells and tight junctions against toxic pathogens. Meanwhile, the regulatory T cells (Treg) and effector T cells subgroups (Th1, Th2 and Th17) are believed to hedge with each other by their cytokines and chemokines [21]. The balance between Treg and effector T

cells subgroups (Th1, Th2 and Th17) are tightly regulated to maintain the intestinal homeostasis as mentioned before [6, 7, 9].

In IBD, on the one hand, due to the continued epithelium injury, the integrity of the mucosal barrier is broken and the permeability through epithelial cells is substantially increased, causing defective regulation of tight junctions, increasing bacteria invasion and the significant amplification of the immune responses (Figure 5B) [21]. On the other hand, the intestinal homeostatic equilibrium is completely disrupted during IBD. Innate cells in IBD produce increased levels of pro-inflammatory cytokines, TNF-α, IL-1β, IL-6, IL-12 and IL-23 [33]. These cytokines accelerate the differentiation/activation of effector T cells subgroups (Th1, Th2 and Th17) and bring the inadequate suppression of Treg [34]. The marked expansion and proliferation of the lamina propria area is accompanied by intensive helper T cells infiltration, especially pro-inflammatory T cells subpopulations (Th1 and Th17) [13], which significantly exacerbate the inflammatory responses, and additional leukocyte recruitment by chemokine attraction, ultimately form an inflammation cycle (Figure 5B) [21, 22].

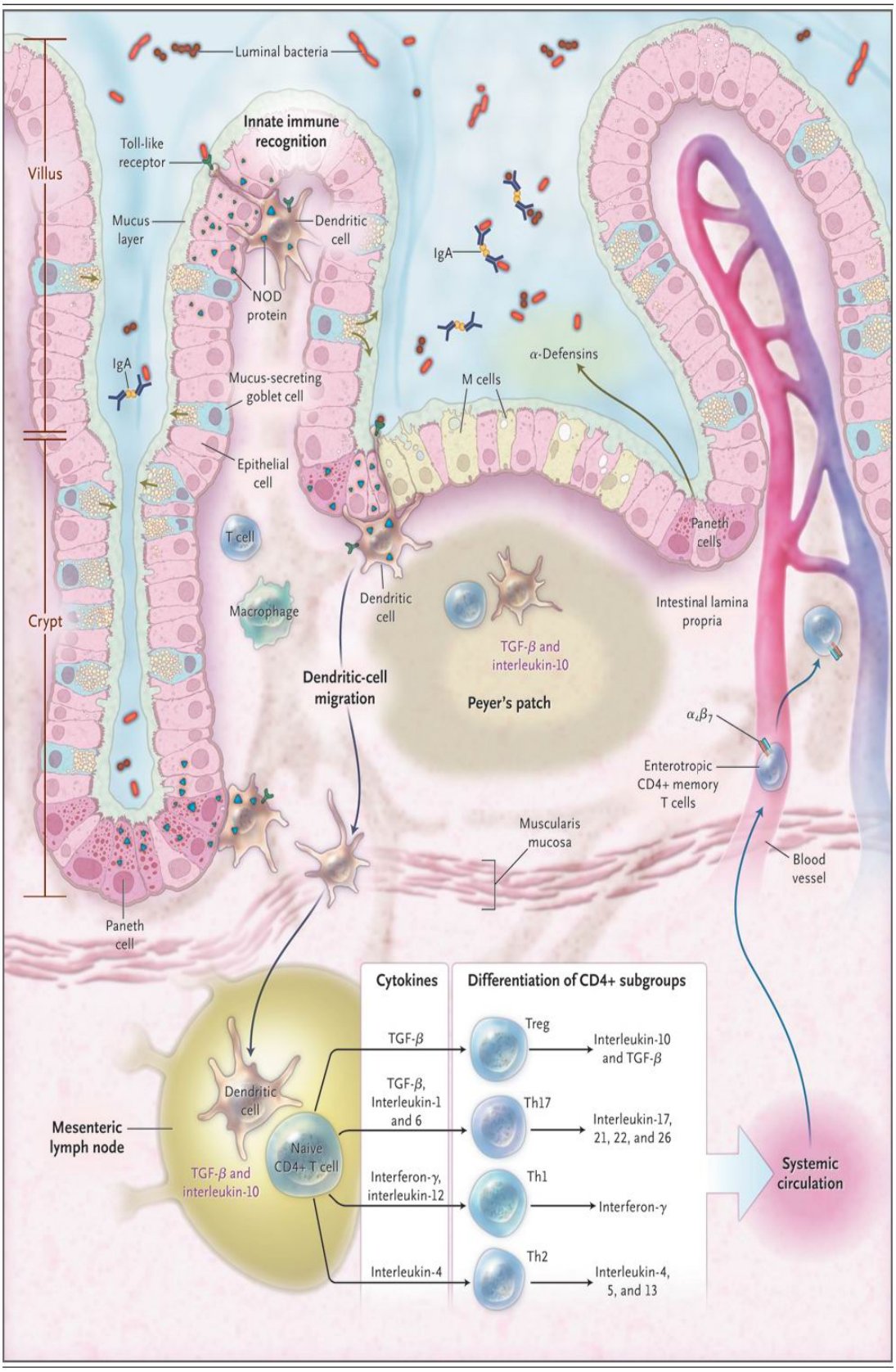

Figure 4 *The intestinal mucosal epithelium cells and innate immune recognition under normal circumstances* [21].

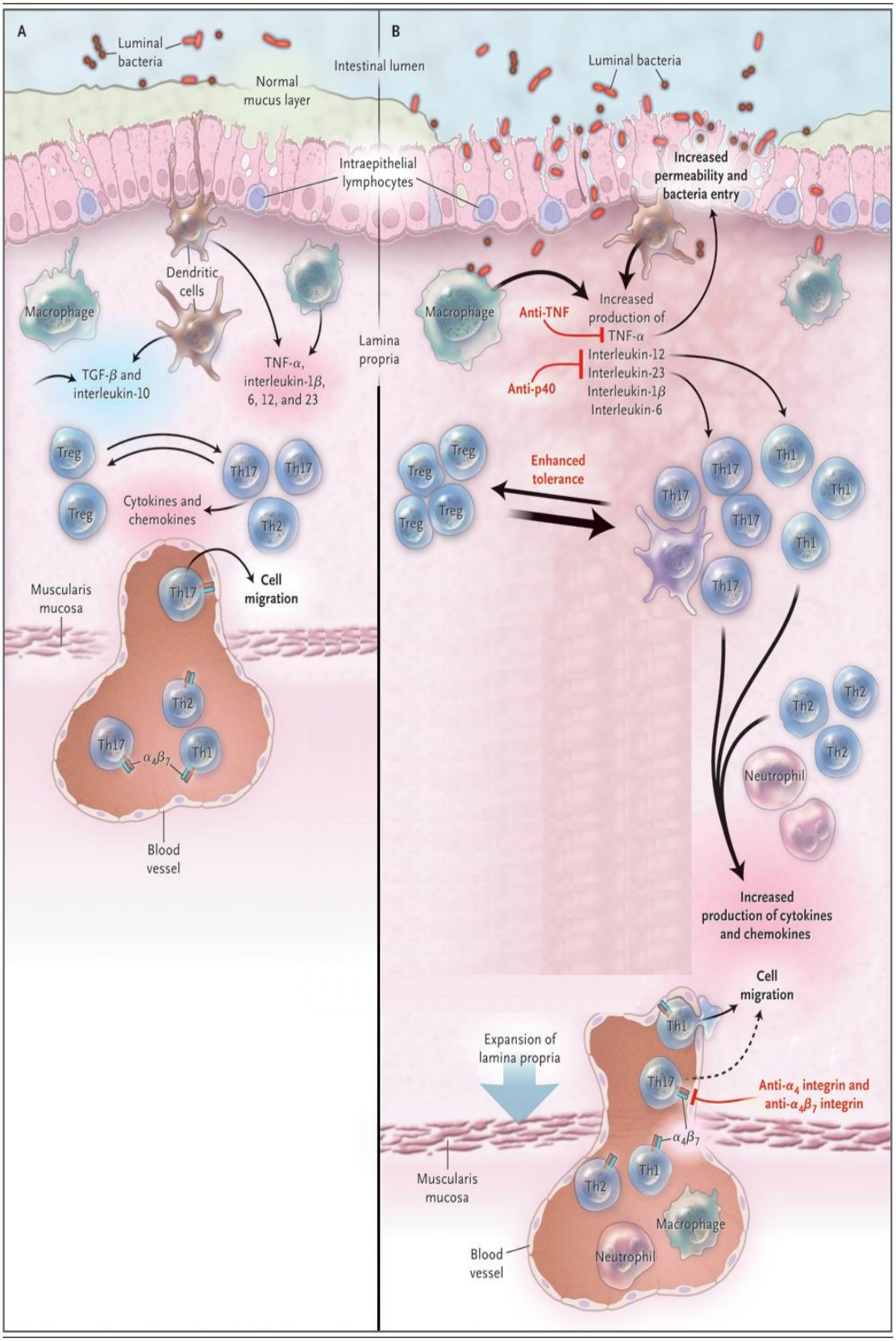

Figure 5 *The intestinal mucosal immune system in normal condition (A) and in IBD (B).* The picture was taken from [21].

1.2.5 *CD is a Th1/Th17 response and UC is a Th2-like response*

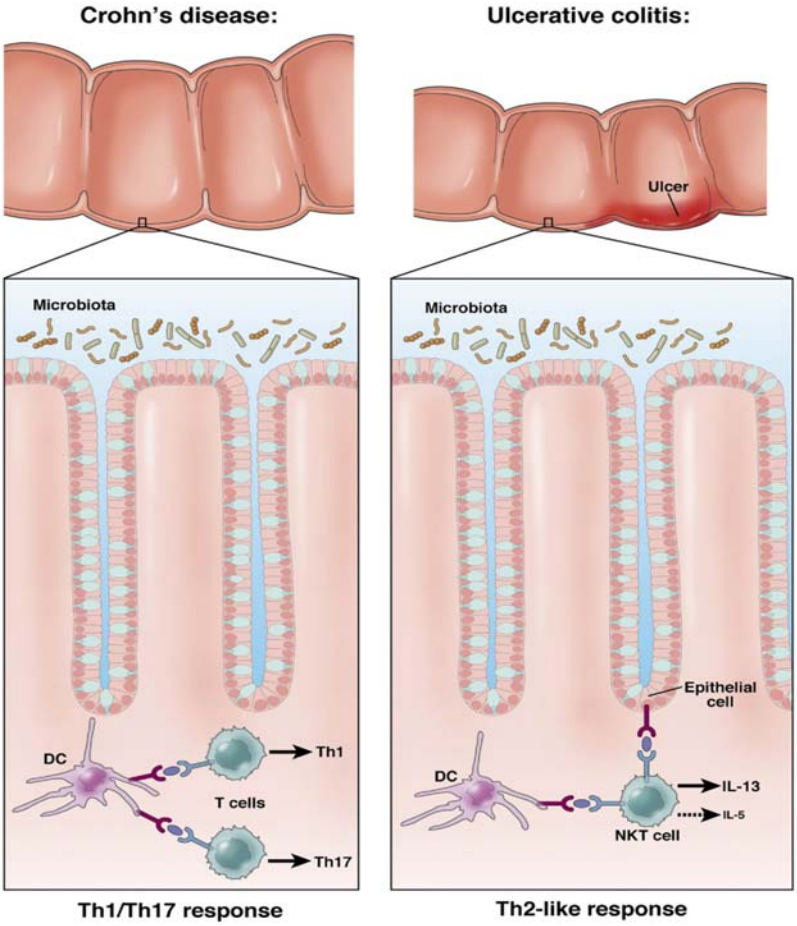

Figure 6 *The basic dichotomy of cytokine secretion profiles in CD and UC* [35], that means CD is a Th1/Th17 response and UC is a "Th2 like" response.

The helper T cells are differentiated into Th1 and Th2 cells, characterized by different cytokine secretion profiles, e.g. IFN-γ and IL-4 respectively [6, 7, 10]. From this angle, a new classification scheme that CD differs from UC was quickly established, in which CD seemed to be a Th1/Th17 response driven disease whereas UC seemed to be a Th2-like response (Figure 6).

In the new classification scheme [35], CD is dominated by the production of IFN-γ and IL-12/IL-23, looking like a Th1/Th17 response. UC, in contrast, is

driven by a “Th2-like” response with the normal IFN-γ production. The dendritic cells in UC present their antigens to NKT cells and induce the production of the cytokines IL-13 and IL-5, which primarily play pro-inflammatory roles. Because another signature cytokine IL-4 from Th2 cells is not increased in UC, it is better to call UC a ‘Th2-like” response rather than an absolute Th2 response [35].

The concept of distinguishing CD and UC undoubtedly contributes to our better understanding of the fundamentals of disease and pathogenesis. But the division between CD and UC is not so absolute, it still awaits further studies to prove and develop [35].

1.2.6 *Overview of susceptibility loci implicated in IBD by GWAS*

Our current knowledge of IBD mainly stems from the combination of clinical studies, in vivo mouse model studies and genome-wide association studies (GWAS) [36]. In the past decade, GWAS has been proven to be a powerful tool for geneticists and biomedical researchers to discover susceptibility genes, opening a door to potential treatments by unveiling the unexpected functional and mechanistic pathways in disease processes [37].

In detail, GWAS, using large case control samples and several hundred thousand genetic markers, uncover new genomic regions/locations (loci) associated with a given trait such as the susceptibility to complex diseases [37], such as IBD. In contrast with single gene disorders, complex

disease is usually caused by many genetic and environmental factors working together, each having a relatively small effect but leading to onset of the disease if interacting with each other [38].

Table 1 Loci or genes detected by genome-wide association scans in IBD [36].

IBD related processes	
Epithelial barrier	GNA12*,HFA4A,CDH1,ERRFL1, MUC19, ITLN1*
Restitution	REL,PTGER4,NKX2-3,STAT3,ERRFI1, HNF4A, PLA2G2A/E
Solute transport	SLC9A4, SLC22A5, SLC22A4*,AQP12A/B, SLC9A3, SLC26A3
Paneth cells	ITLN1*, NOD2*, ATG16L1*, XBP1*
Innate mucosal defense	NOD2*, ITLN1*, CARD9*,REL, SLC11A1, FCGR2A*/B
Immune cell recruitment	CCL11/CCL2/CCL7/CCL8, CCR6, IL8RA/IL8RB, MST1*
Antigen presentation	ERAP2*, LNPEP, DENND1B
IL-23/Th17	IL23R*, JAK2, TYK2*, STAT3, ICOSLG, IL21, TNFSF15*
T-cell regulation	NDFIP1, TNFSF8, TAGAP, IL2, IL2RA,TNFRSF9, PIM3, IL7R*, IL12B, IL23R*,PRDM1, ICOSLG, TNFSF8, IFNG, IL21
B-cell regulation	IL5, IKZF1, BACH2, IL7R*, IRF5
Immune tolerance	IL10, IL27*, SBNO2, CREM,IL1R1/IL1R2, NOD2*
Cellular responses	
Autophagy	ATG16L1*, IRGM, NOD2*,LRRK2, CUL2, PARK7, DAP
ER stress	CPEB4, ORMDL3,SERINC3, XBP1*
Intracellular logistics	VAMP3, KIF21B, TTLL8,FGFR1OP, CEP72, TPPP
Cell migration	ARPC2, LSP1, AAMP
Apoptosis/necroptosis	FASLG, THADA*,DAP, PUS10, MST1*
Carbohydrate metabolism	GCKR*, SLC2A4RG
Oxidative stress	PRDX5, BACH2, ADO, GPX4, GPX1*, SLC22A4, LRRK2, NOD2*, CARD9*, HSPA6, DLD, PARK7, UTS2*, PEX13

Recent advances in GWAS have provided substantial insight into the maintenance of mucosal homeostasis and the pathogenesis of IBD, which re-define and revolutionize our knowledge [36]. So far, GWAS and Meta analysis from IBD have successfully identified 99 non-overlapping genetic risk loci [36, 39-41]. Among those loci, 71 were reported in CD and 47 were reported in UC, including 28 risk loci which are shared between CD

and UC [36, 39-41]. The genetic risk loci and corresponding genetic variants suggest the importance of innate immunity, autophagy and phagocytosis in the disease susceptibility.

Comprehensive analysis of the risk loci and candidate genes discloses several pivotal steps in intestinal homeostasis (Table 1) [36], including ① innate immune system functions: epithelial barrier, epithelial restitution, solute transport, Paneth cells and secretion of defensins, innate mucosal defense; ② adaptive immune system functions: immune cell recruitment, antigen presentation, IL-23/Th17, T-cell regulation, B-cell regulation, and immune tolerance; ③ cellular responses: autophagy, endoplasmic reticulum (ER) stress, intracellular logistics, cell migration, apoptosis/necroptosis, carbohydrate metabolism, oxidative stress and reactive oxygen species (ROS) generation (Table 1).

Interestingly, in a recent GWAS effort, T-cell death associated gene 8 (TDAG8, GPR65), one of the members of the proton sensing receptor family, has been identified as a susceptibility gene and risk locus in CD (Table 2) [40, 41].

Table 2 The representative confirmed Crohn's disease risk loci and corresponding odds ratios [40, 41].

dbSNP ID	Chromsome	Gene Name	Odds ratio (95% CL)	Amino acid substitution
rs8005161	14q35	GPR65/TDAG8	1.23 (1.16~1.31)	IIE 231 LEU
rs11209026	1p31	IL23R	2.66 (2.36~3.00)	ARG 391 GLN
rs2076756	16q12	NOD2	1.53 (1.46~1.60)	--
rs3024505	1q32	IL-10	1.12 (1.07~1.17)	--

The potential for variants identified in GWAS to predict the risk of complex disease has been expected, but the application is still controversial. And the confirmation of loci's role and causality awaits detailed fine-mapping, expression and functional studies [38-41].

1.3 IBD and acidic pH

1.3.1 *Inflammation and acidic pH*

In the human body, most acids come from carbohydrate and fat metabolism, which generates huge amounts of CO_2 accompanied with the ATP generating and aerobic respiration. Then, CO_2 dissolves in the water to create carbonic acid (H_2CO_3) and dissociates into H^+ and HCO_3^- [42].

$$CO_2 + H_2O \leftarrow (H_2CO_3) \rightarrow H^+ + HCO_3^-$$

Normally acid base balance is maintained by intracellular and extracellular buffering and by the pulmonary and renal systems [42]. Higher H^+ concentrations drive the equation back to the left and generate more CO_2. In turn, overproduction of CO_2 pushes the equation forward to the right side and creates a more acidic environment. Hereinto, CO_2 concentration is tightly controlled by pulmonary ventilation, and H^+ and HCO_3^- density could be finely controlled by renal elimination and regeneration of bicarbonate [42].

In clinical practice, acid based disorders can be divided into two categories [43]: isocapnic acidosis (e.g. metabolic acidosis caused by excessive metabolic acids) and hypercapnic acidosis (e.g. respiratory acidosis due to carbon dioxide accumulation). The major reasons for isocapnic acidosis include: increased acid production, acid ingestion, and decreased renal acid excretion (e.g. kidney failure), GI or renal HCO_3^- loss (e.g. diarrhea or taking carbonic anhydrase inhibitors). The reasons for

respiratory acidosis are decreased ventilation and chronic obstructive pulmonary disease [42].

During inflammation, the following factors contribute to extracellular local acidification [44-48] :

1. The hypoxia and ischemic condition in inflammed tissues and high level of metabolic activity of immune cells in acute or chronic inflammation result in a switch to anaerobic glycolysis and subsequent accumulation of lactate and glycolytic metabolites, finally inducing lactic acidosis.
2. The massive infiltration of leukocytes, mainly neutrophil and macrophage, produce huge amount of protons during the activation of the respiratory burst. Meanwhile myeloperoxidase (MPO) uses the reactive oxygen species hydrogen peroxide (H_2O_2) to produce abundant hypochlorous acid.
3. The accumulation of short chain fatty acids, particularly succinic acid, which are the by-products of microbial metabolism in inflammatory tissues, reduces intracellular pH and impairs superoxide and hydrogen peroxide by inhibiting neutrophil respiratory burst.
4. As mentioned before, in respiratory infections, decreasing CO_2 ventilation aggravates the acidosis. Or in the condition of colitis and diarrhea, vast HCO_3^- loss does the same job.

Just as inflammation can induce local acidification or in severe sepsis also acidosis, in turn, acidic environment worsen the inflammation and aggravate the inflammatory response through immune cells (Figure 7). It

has been reported that low extracellular pH induces the activation of neutrophils and accelerated the maturation of dendritic cells [44-48]. Extracellular acidification was found to induce human neutrophil activation by a mechanism dependent on the activation of P13K/Akt and ERK pathways, and low pH intensifies acute inflammatory responses by delaying spontaneous apoptosis of neutrophils and extending the neutrophil functional lifespan [44, 45]. And the work from same group proved that extracellular acidosis increased endocytosis by dendrictic cells (DCs) and improved the antigen presenting ability by upregulating expression of cell surface proteins involved in antigen presentation and promoting the efficacy of MHC class-1 restricted antigen presentation [46, 47]. The transient exposure of human dendritic cells to pH 6.5 significantly improved its antigen presenting ability and activated the P13K/Akt and MAPK pathway via a strict p38 MAPK dependent manner. Interestingly, DCs exposure to pH 6.5 also induces a dramatic increase in the production of IL-12 and IFN-γ, but not IL-4, favoring a Th1 immunity pathway [48].

For other immune cells, e.g. monocytes, low extracellular pH (pH 6.5) stimulates the production of IL-1β by human monocytes through a caspase-1 dependent pathway, but not affecting the production of other pro-inflammatory cytokines such as TNF-α and IL-6 [49]. Rubartelli et al reported the same association that acidic extracellular pH (pH 5.7) stimulated IL-1β production while alkaline extracellular pH (pH 8.2) reversed this process [50]. The authors imply that extracellular acidosis induced activation of immune cells might derive from the activation of specific proton sensors expressed in these immune cells [50].

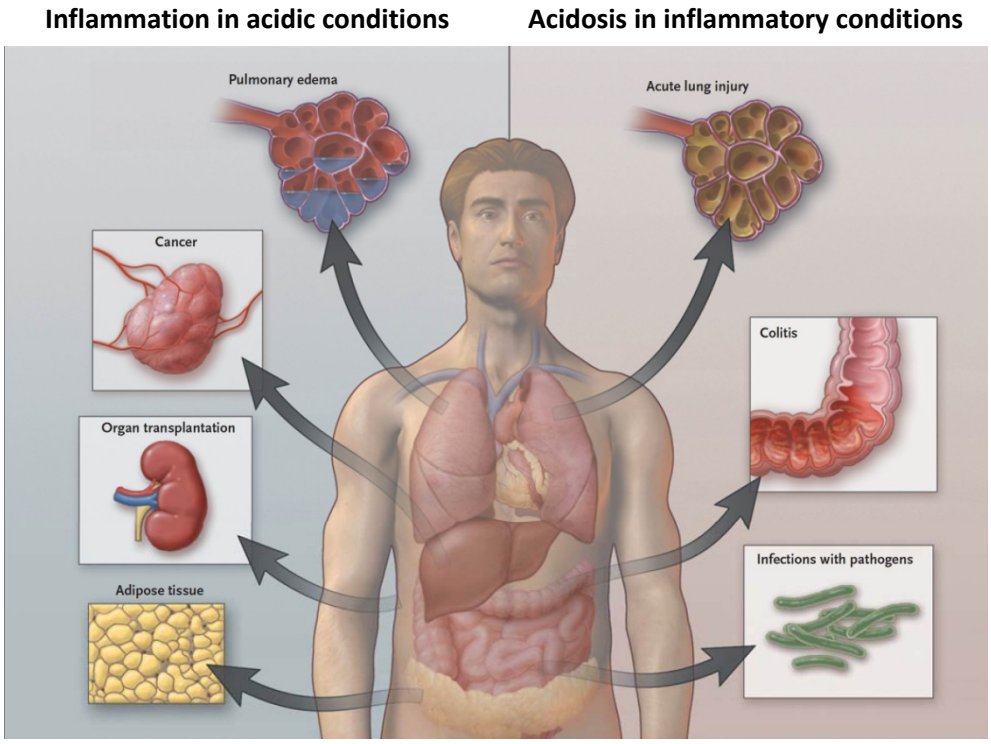

Figure 7 *The relationship between acidosis and inflammation, adapted from* [51]. An overview of clinical conditions characterized by tissue acidosis and hypoxia that causes inflammation (left) and inflammatory diseases leading to tissue acidosis and hypoxia (right).

1.3.2 *IBD and acidosis*

The tissue and blood pH is maintained in a range around pH 7.4 mainly through regulation of respiration and renal acid extrusion [42]. In contrast, the luminal pH value in the normal gastrointestinal tract shows a progressive increase in pH from the duodenum to the ileum, and a decrease in the caecum, and finally a slow rise again along the colon to the rectum (Figure 8).

Very interesting, Fallingborg et al reported that intraluminal colonic pH values in patients with active UC were significantly lower than in normal subjects [52]. In his study, intraluminal gastrointestinal pH was measured by

the radiotelemetry capsule method in seven patients with active UC. Three out of seven patients showed very low pH levels (lowest values 2.3, 2.9, and 3.4) in the proximal parts of the colon (Figure 9). Another three patients showed normal pH values in the colon [52]. Whereas, all of these pH levels were normal in the stomach and small intestine other than colon, suggesting lower pH value might be an indicator of severe disease activity of the colitis. Raimundo et al reported similar findings (luminal pH as low as 4.7 in right colon) in patients with both active and inactive UC [53]. Nugent et al also reported colonic luminal pH value dropped to less than 5.5 in two of six patients with active UC [54].

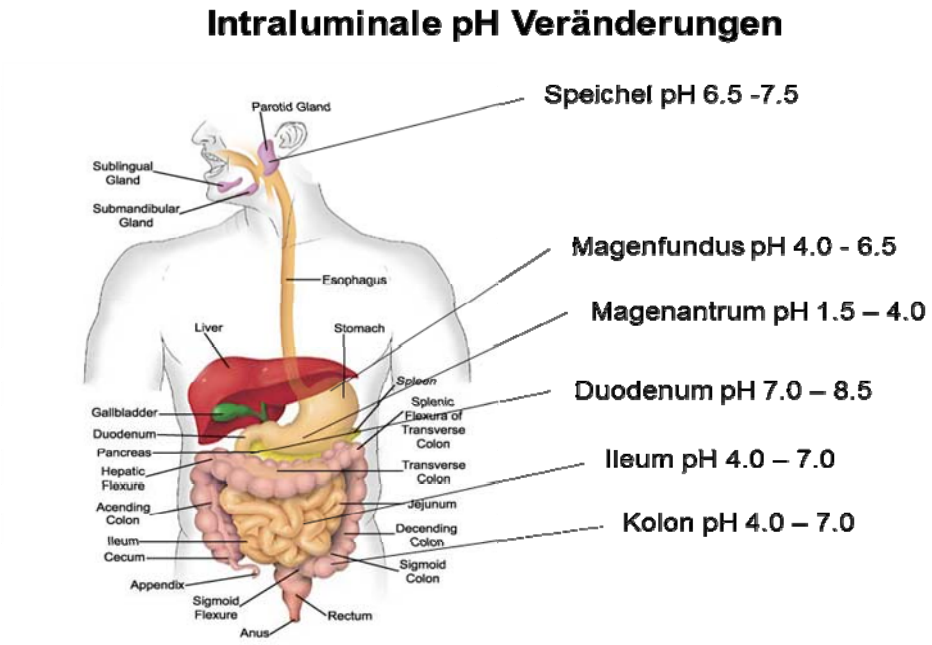

Figure 8 *Gastrointestinal pH profile of the normal subject.* The picture was taken from [55] and was modified to indicate pH range.

For CD patients, in one study in 1997, acidic colonic luminal pH was found similar as in active UC patients. Three out of four CD patients had lower pH values in the right (pH 5.3) and left colon (pH 5.3) than normal controls (pH 6.8) [54]. The authors also suggested that the reduced

intracolonic pH impaired bioavailability of 5-ASA (5-aminosalicylic acid, medication for IBD) in a pH dependent manner and substantially affected the efficacy of pH dependent colonic release and absorption of drugs [54]. These data indicated the pH controlling system in the gastrointestinal system may correlate with the IBD occurrence and intraluminal pH levels might be an indicator of severity of IBD.

Nevertheless there are still some discussions on the range of the intestinal luminal pH in IBD patients [56-58].

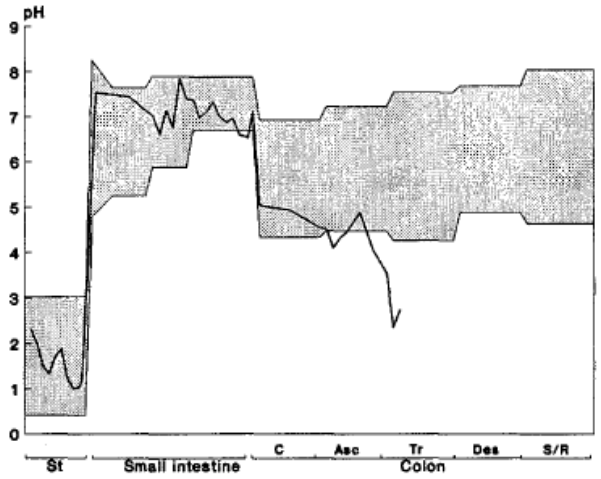

Figure 9 *Gastrointestinal pH profile of a patient with active UC* [52]. Shadow area represents mean values in healthy subjects. St: stomach, C: cecum, Asc: ascending colon, Tr: transverse colon, Des: descending colon, S/R: sigmoid colon and rectum. The study demonstrates that very low intraluminal pH levels in the colon occur in a patient with active ulcerative colitis. This might be an indicator of severe activity of the disease. A radiotelemetry capsule was used, and its location was determined by fluoroscopy.

First, whether or not the intestinal luminal pH in IBD patients is more acidic is still controversial in the academic community. Press et al [56] reported the right colonic luminal pH in 11 patients with active UC (mean values7 - 7.19), which are higher than those in normal controls (mean

value 5.88). Similarly, the left colonic luminal pH in UC patients was slightly higher than in normal controls too. Ewe et al [57] also stated inflammation did not decrease intraluminal pH in IBD, and that the median pH in the terminal ileum of patients with CD was 7.5 vs. 7.7 and in the rectum in UC 7.8 vs. 7.2 in the controls.

Second, we cannot rule out the influence of diets and dietary patterns changing luminal pH values due to the onset of IBD [58]. Diet significantly affects gut pH. For example, the increased intake of dietary fiber would aggravate acidosis by providing a carbohydrate meal to colonic flora [59, 60]. The hydrogen and bicarbonate ion secreted by intestinal mucosa are the major determinants of the normal luminal pH. Other factors involved are lactate production, bacterial fermentation of carbohydrates and mucosal absorption of short chain fatty acids. During severe inflammation, reduced mucosal bicarbonate secretion, increased bacterial lactate production, and decreased short chain fatty acids might also contribute to the low pH in IBD patient's colon [59, 60].

1.4 Proton Sensing Receptor Family

The receptors GPR4 and OGR1 (ovarian cancer G protein coupled receptor 1, GPR68) were identified about 15 years ago during the efforts to clone novel G protein coupled receptors [61]. TDAG8 (T-cell death associated gene 8, GPR65) acting as an upregulated gene after glucocorticoid treatment of T cells was identified in 1996 [62]. All of the three receptors share a high similarity at amino acid level (Figure 10). The three GPCRs were originally characterized as a protein group regulating physiological responses to the lipid messengers Sphingosylphosphorylcholine (SPC) and Lysophosphatidylcholine (LPC) and psychosine. But the key evidence publications have been retracted since 2005 [63-67]. In contrast, accumulating evidence showed that all three GPCRs (GPR4, OGR1 and TDAG8) are activated by protons in the physiological range around pH 7.4 and may play a crucial role in pH homeostasis [61, 68].

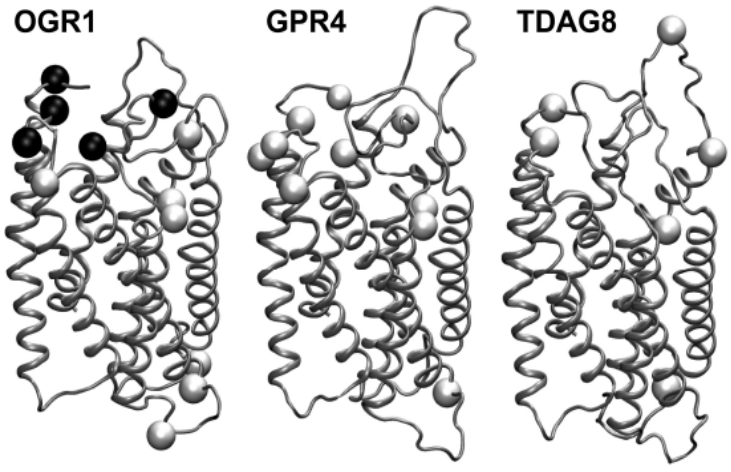

Figure 10 *The receptor backbone model for OGR1, GPR4 and TDAG8, with all histidines residues highlighted* [61]. Structural studies of three pH receptors (in silico modeling) suggested that histidines residues (ball-like structures) in all three receptors may play a pivotal role in proton binding and pH sensing. The hypothesis was confirmed by site-directed

mutagenesis studies in OGR1 [61, 68].

The three pH-sensing receptors seem to be relevant for physiological process developed in later evolution because they are found in mammalian species and vertebrates including Xenopus, Fugu, zebrafish and chicken, but not in Drosophila, C. elegans, or plasmodium [61]. In humans, OGR1 mRNA shows a low abundance in a wide range of tissues but is significantly highly expressed in lung, gastrointestinal tract, kidney, bone, and the nervous system. GPR4 shows significantly high abundance in endothelial cells despite it also is found in kidney, white adipose tissue, and lung. Very interesting, TDAG8 appears to be restricted to the immune system and bone, including peripheral blood leukocytes, spleen, lymph nodes, thymus, and osteoclasts which may play biological roles in the immune response and bone remodeling during local or systemic acidosis [62, 69, 70].

A more detailed recent analysis from Dr. Klaus Seuwen's lab (Novartis Institute for Biomedical Research) showed that the proton-activated receptor OGR1 acts via the Gq pathway and results in IP_3 formation and calcium mobilization in OGR1 overexpressing cells. OGR1 is inactive at pH 7.8 and fully activated at pH 6.8. Half maximal activation of the IP_3 formation by OGR1 expressed in CCL39 cells occurred at pH 7.48 [68]. For GPR4 and TDAG8, activation is through the Gs pathway and intracellular cAMP accumulation [61, 69, 70]. Half maximal activation of cAMP formation by GPR4 expressed in HEK293 occurred at pH 7.53. The pH sensing properties of TDAG8 were independently reported by two Japanese groups [69, 70]. Both groups stated that the TDAG8 receptor is a proton

sensing receptor and responsive to extracellular pH changes. But, in regard to psychosine, there is a dispute over its function as a ligand or antagonist. One group insisted that psychosine can bind to the TDAG8 receptor and that psychosine can exert an inhibitory effect on receptor [70]. Another group argued that psychosine did not stimulate or inhibit cAMP formation at all [69]. However, the data from these experiments with several TDAG8 transfected cell lines showed cAMP was markedly accumulated in response to extracellular pH, with a peak response at approximately pH 6.5-7.0.

To date, there are not many studies on the functions of the 3 proton sensing receptors. Some studies focused on the relationship between receptors and tumor development or the kidney.

Quite a few evidence supported pH receptors enhanced tumor development via different pathways. It has been reported that GPR4 and TDAG8 were overexpressed in variety of human cancer tissues, indicating roles in driving or maintaining tumor formation [71, 72]. In-vitro overexpression of GPR4 or TDAG8 in HEK293 cells were found to lead to a transcriptional activation to promote tumor growth via SRE- and CRE-driven promoters [71]. And *Gpr4* $^{-/-}$ mice showed a significantly reduced angiogenesis in response to VEGF and the tumor growth is strongly reduced in *Gpr4* $^{-/-}$ mice [73]. The tumorigenesis of melanoma cells was found to be significantly inhibited in OGR1 deficient mice too [74]. TDAG8 on the surface of tumor cells was found to facilitate tumor development and overexpression of TDAG8 in mouse lewis lung carcinoma (LLC) cells enhanced tumor growth in animal models

depending on PKA and ERK activation [72]. But some other independent studies reported an inconsistent result. GPR4 activation by acidosis inhibited tumor cell migration and metastasis in genetically engineered GPR4-overexpressing B16F10 melanoma cells and TRAMP-C1 prostate cancer cells [75]. And OGR1 has been found to function as a novel metastasis suppressor gene for prostate cancer in an in-vivo mouse tumor cell migration model [76]. Thus, it is quite difficult to draw a logical and clear conclusion from a set of contradictory data. Consequently, more studies are needed to further understand the roles of these receptors in cancer biology.

In the renal system, GPR4 expression was widely observed in kidney cortex and kidney collecting ducts. *Gpr4* $^{-/-}$ mice showed a decreased net acid renal secretion and spontaneous metabolic acidosis. The finding suggested that the proton sensor GPR4 regulates acid secretion in kidney collecting duct [77]. A separate study demonstrated that chronic acidosis and GPR4 increase H^+-K^+-ATPase α subunit ($HK\alpha_2$) protein, implicating a regulatory role of GPR4 [78]. Previous work from our group also showed that OGR1 regulated the activity of two major plasma membrane proton transporters in proximal tubules, Na^+/H^+ exchanger (NHE_3) and H^+-ATPase [79], indicating a role in the regulation of renal pH homeostasis.

In addition to a possible involvement in tumor development and kidney function, several studies have demonstrated the function of proton activated receptors in immune processes of the lung, insulin secretion and sensitivity, and bone metabolism. The latest update included OGR1 deficiency attenuated glucose-stimulated insulin secretion in vivo in a pH

dependent manner while acidity and OGR1 activation enhanced glucose-stimulated insulin secretion under physiological conditions in vitro [80]. *Ogr1* $^{-/-}$ mice further showed a decreased insulin secretion but have unusual normal glucose tolerance [80]. Interestingly, Giudici et al reported GPR4 deficiency improved glucose tolerance and insulin sensitivity with comparable insulin levels but increased plasma leptin levels in mice [81]. The effect was maintained in aged mice but not in obese mice. These two studies indicated OGR1 might modulate glucose homeostasis by boosting insulin secretion whereas GPR4 might modulate it by lowering insulin sensitivity [80, 81].

Other research showed TDAG8 seemed to be a major regulator or influencer in asthma and osteoclatic bone metabolism [82-85]. TDAG8 knockout attenuated dexamethasone-induced inhibition of pro-inflammatory cytokine production, TNF-α, in mouse peritoneal macrophages and suggested that TDAG8 was partly involved in the steroid hormone induced anti-inflammatory function [82]. Mogi et al from the same group further reported TDAG8 mediates the extracellular acidity induced suppression of TNF-α and IL-6 through the Gs/cAMP/PKA signaling pathway in mouse peritoneal macrophages [83]. Kottyan et al reported [84] that the eosinophils, which are the most characteristic feature of asthmatic inflammation, responded to protons with improved cellular viability and reduced apoptosis in both human and mouse. Importantly, the effect was in a dose-dependent manner between pH 7.5 and 6.0. TDAG8, identified as the chief pH receptor, was found overexpressed in eosinophils. More interesting, the author demonstrated that the acidity induced enhanced eosinophil viability was

dependent on cAMP production and TDAG8 [84]. TDAG8-deficient mice had attenuated airway eosinophilia and increased apoptosis in two asthma mouse models, which further proved the decisive role of TDAG8 in asthmatic inflammation [84]. Besides, TDAG8 may also play a role in bone metabolism [85]. TDAG8 activation was suggested to inhibit osteoclastic bone resorption, which could act as a novel therapeutic approach for metabolic bone disease, e.g. osteoporosis or porous bone [85].

1.5 Mouse models used in IBD study

The available animal models of IBD can be divided into four classes (Table 3) [86-88]: 1. Inducible colitis models in mice with a normal immune system. 2. Spontaneous colitis models. 3. Adoptive transfer models in immuno-compromised hosts. 4. Genetically engineered models including knockout mice and transgenic mice. All of these animal models enable us to better understand the mechanisms and fundamentals of gastrointestinal inflammatory diseases. But, among these all, an ideal experimental model of IBD is supposed to mimic human IBD, either UC or CD. And it should be easy to induce, cost effective and highly reproducible. Unfortunately, there is no single model available that completely meets all of these criteria [87-89].

Trinitrobenzene sulfonic acid (TNBS) and Dextran sulfate sodium (DSS) induced colitis might be the most widely used animal models for IBD studies [86]. For the induction of chronic colitis, mice receive 4 cycles of 2-4 % DSS treatment. One cycle consists of feeding DSS in drinking water for 7 days followed by a period of 10 days drinking water without DSS [89, 90]. The colitis becomes evident when the mice lose weight and develop diarrhea. This model shares many similarities to human IBD in aetiology, pathology, pathogenesis and therapeutic responses. Both of the toxic chemicals directly damage the mucosal barrier and disrupt epithelial integrity. The DSS induced colitis model is a particularly suitable model for human IBD especially UC [89]. It has been reported that morphological studies suggest that the administered DSS was partially phagocytized by macrophages in the colonic mucosa and macrophages malfunction

contribute to the resulting colitis [91]. The chronic DSS induced colitis is considered to be caused by long term active lymphocytes and cytokines secreted by macrophages or Th1/Th2 cells [92]. However, susceptibility to DSS highly varies with the animal species and strains [93]. In mice, the C57BL/J6 strain of mice was found to be more susceptible to experimental colitis using DSS than Balb/c mouse [93]. So, it is necessary to introduce another IBD mouse model to the study.

Table 3 Overview of IBD animal models [86]

Genetically engineered models
Gene knockout mouse models
IL-2 knockout/IL-2 Rα knockout mice
IL-10 knockout mice
STAT3 knockout mice
T-cell receptor mutant mice
TNF-3′ UTR knockout mice
Trefoil factor-deficient mice
Transgenic mouse and rat models
IL-7 transgenic mice
STAT-4 transgenic mice
HLA B27 transgenic rats
Models of spontaneous colitis
C3H/HeJBir mice
SAMP/Yit mice
Inducible colitis models
Trinitrobenzene sulfonic acid-induced colitis
Oxazolone colitis
Dextran sulfate sodium colitis
Carrageenan colitis
Peptidoglycan-polysaccharide colitis
Adoptive transfer models
CD4+/CD45RB^{high} T-cell transfer colitis
Colitis induced by transfer of hsp60-specific CD8 T cells

IL, Interleukin; IL-2R, IL-2 receptor; TNF, tumor necrosis factor; UTR, untranslated region; hsp, heat-shock protein

IL-10 is a well known suppressor of Th1 cells and macrophage activation and it inhibits IL-12 and TNF-alpha production [94]. IL-10 also inhibits T cells proliferation and promotes the formation of antigen specific regulatory T cells [86]. *IL-10* $^{-/-}$ mice spontaneously develop chronic colitis and inflammation occurring in the whole intestine, which is supposed to

simulate CD [86, 88, 89]. DRA (downregulated in adenoma, a chloride sulfate anion transporter causing congenital chloride diarrhea when mutated) transporter expression was dramatically reduced in the surface epithelium of colon in IL-10 knockout mice, and the attenuation of DRA expression in *IL-10* $^{-/-}$ mice participate in the pathogenesis of diarrhea in colitis [95]. The disadvantages of the *IL-10* $^{-/-}$ mice model include that it takes several months to develop colitis making them unsuitable for acute colitis study and high throughput tests.

1.6 Aim of the project

The motivation to initiate the project arose from the clinical clues and previous studies in our research group. Since local acidification has been observed during IBD and has been implicated in the pathogenesis and progression of IBD; and since OGR1 and GPR4 are expressed along the gastrointestinal tract, we investigated the precise role of GPR4 and OGR1 in this study.

In preliminary experiments of the project, we found that both OGR1 and GPR4 mRNA are widely expressed in several mouse tissues including small intestine and colon. Robust expression of OGR1 mRNA was measured in small intestine and in colon (Wagner, unpublished data). More interesting, we found OGR1 and GPR4 mRNA were highly expressed in spleen possibly due to its abundant expression in various types of immune cells and leukocytes and cytokines TNF-α significantly upregulate OGR1 mRNA expression in Mono Mac 6 cells (Cheryl de Valliere, unpublished data). Taken together, considering both GPR4 and OGR1 are being expressed along the small and large intestine as well as in almost all immune cells, we hypothesized that these two proton sensing receptors, might participate in the pathogenesis of IBD.

The hypothesis was tested by using the following IBD mouse models and approaches:

1. dextran sulphate sodium (DSS) induced chronic colitis model
2. Spontaneous colitis model (*Gpr4* $^{-/-}$*/IL-10* $^{-/-}$ and *Ogr1* $^{-/-}$*/IL-10* $^{-/-}$)

Chapter 2
Publications That Contributed to That Work

The proton-activated receptor GPR4 modulates intestinal inflammation

Yu Wang[1,2*], Cheryl de Valliere[1*], Irina Leonardi[1], Sven Gruber[1,2], Alexandra Gerstgrasser[1], Achim Weber[3], Katharina Leucht[1], Lutz Wolfram[1], Martin Hausmann[1], Carsten Krieg[4,5], Koray Thomasson[4], Onur Boyman[4], Isabelle Frey-Wagner[1], Gerhard Rogler[1,2§], Carsten A. Wagner[2§].

* Yu Wang and Cheryl de Valliere contributed equally to this work

§ Gerhard Rogler and Carsten A. Wagner share last authorship

1 Division of Gastroenterology and Hepatology, University Hospital Zurich, Zurich, Switzerland.
2 Institute of Physiology, Zurich Center for Integrative Human Physiology (ZIHP), University of Zurich, Zurich, Switzerland.
3 Institute of Surgical Pathology, University Hospital Zurich, Zurich, Switzerland
4 Laboratory of Applied Immunobiology, University of Zurich, Zurich, Switzerland.
5 current address: Institute of Experimental Immunology, University of Zurich, Zurich, Switzerland.

Corresponding authors:
Prof. Dr. Carsten A. Wagner
University of Zurich
Institute of Physiology
Winterthurerstrasse 190
CH 8057 Zürich, Switzerland
Tel.: +41-44-5355023
Fax: +41-44-6356814
E-mail: wagnerca@access.uzh.ch

Prof. Dr. Dr. Gerhard Rogler
Division of Gastroenterology and Hepatology
University Hospital Zurich
Rämistrasse 100
CH-8091 Zurich
Switzerland.
Tel.: +41 (0)44 255 95 19
Fax: +41 (0)44 255 94 97
Email: gerhard.rogler@usz.ch

The proton-activated receptor

GPR4 modulates intestinal inflammation

Yu Wang (MA)[1,2*], Cheryl de Valliere (MA)[1*], Irina Leonardi (MA)[1], Sven Gruber[1,2], Alexandra Gerstgrasser (PhD)[1], Achim Weber (MD, Prof)[3], Katharina Leucht (PhD)[1], Lutz Wolfram(PhD)[1], Martin Hausmann (PhD)[1], Carsten Krieg (PhD)[4,5], Koray Thomasson[4], Onur Boyman (MD, Prof)[4], Isabelle Frey-Wagner (PhD)[1], Gerhard Rogler (MD-PhD, Prof)[1,2§], Carsten A. Wagner (MD, Prof)[2§].

* Yu Wang and Cheryl de Valliere contributed equally to this work

§ Gerhard Rogler and Carsten A. Wagner share last authorship

[1] Division of Gastroenterology and Hepatology, University Hospital Zurich, Zurich, Switzerland.

[2] Institute of Physiology, Zurich Center for Integrative Human Physiology (ZIHP), University of Zurich, Zurich, Switzerland.

[3] Institute of Surgical Pathology, University Hospital Zurich, Zurich 8091, Switzerland

[4] Laboratory of Applied Immunobiology, University of Zurich, Zurich, Switzerland.

[5] current address: Institute of Experimental Immunology, University of Zurich, Zurich, Switzerland.

Corresponding authors:

Prof. Dr. Carsten A. Wagner
University of Zurich
Institute of Physiology
Winterthurerstrasse 190
CH 8057 Zürich, Switzerland
Tel.: +41-44-5355023
Fax: +41-44-6356814
E-mail: Wagnerca@access.uzh.ch

Prof. Dr. Dr. Gerhard Rogler
Division of Gastroenterology and Hepatology
University Hospital Zurich
Rämistrasse 100
CH-8091 Zurich
Switzerland.
Tel.: +41 (0)44 255 95 19
Fax: +41 (0)44 255 94 97
Email: gerhard.rogler@usz.ch

Disclosures

The study was supported by cooperative project funding by the Zurich Center for Integrative Human Physiology (ZIHP) to O. Boyman, G. Rogler and C. A. Wagner.

Abstract

BACKGROUND: During active inflammation tissue and intraluminal intestinal pH is decreased in patients with inflammatory bowel disease (IBD). pH may play a role for IBD pathophysiology. Recently, proton sensing G-protein coupled receptors (GPCRs) were identified, including GPR4, OGR1 (GPR68), and TDAG8 (GPR65). We investigated whether GPR4, a prototype pH-sensing receptor, is involved in intestinal inflammation.

METHODS: The impact of a deletion of GPR4 was assessed in two models of colitis, the chronic dextran sulphate sodium (DSS) induced model and by crossbreeding into IL-10 deficient background. Colitis severity was assessed from body weight, colonoscopy, colon length, histological score, cytokine mRNA expression, and myeloperoxidase (MPO) activity. In the spontaneous colitis model, the incidence of rectal prolapse and phenotypic and functional lamina propria leukocytes (LPLs) characteristics were analyzed.

RESULTS: *Gpr4* $^{-/-}$ mice showed less body weight loss and lower histology score after induction of chronic DSS colitis. In *Gpr4* $^{-/-}$ */IL-10* $^{-/-}$ double knock-outs onset and progression of rectal prolapse were significantly delayed as compared to *Gpr4* $^{+/+}$ */IL-10* $^{-/-}$ mice. Similarly, histology scores and MPO activity were reduced in double KO mice. *Gpr4* $^{-/-}$ */IL-10* $^{-/-}$ mice further had a lower $CD4^+$ T-helper cell infiltration with significantly lower IFN-γ expression.

CONCLUSION: The deletion of the GPCR GPR4 ameliorates colitis in animal models indicating an important role for the regulation of mucosal inflammation and thus providing a new link between environmental factors such as luminal pH and the immune system. The therapeutic inhibition of GPR4 may be beneficial for the treatment of IBD.

Key Words: G-protein coupled receptor; pH receptors; GPR4; IBD; animal model.

Statement of conflict of interest

All authors declare that they do not have any conflicts of interest.

Authors contribution

YWang, CdeValliere, ILeonardi, SGruber, AGerstgrasser, KLeucht, LWolfram, MHausmann, CKrieg, KThomasson performed experiments; YWang, CdeValliere, ILeonardi, SGruber, AGerstgrasser, AWeber, KLeucht, LWolfram, MHausmann, CKrieg, OBoyman, IFrey-Wagner, GRogler, CAWagner analyzed data; OBoyman, IFrey-Wagner, GRogler, CAWagner planned experiments; OBoyman, GRogler, CAWagner obtained funding for the project; YWang, GRogler, CAWagner wrote the manuscript; all authors read and approved the manuscript

Abbreviations: CCL20, chemokine (C-C motif) ligand 20; CD, Crohn's disease; COX-2, prostaglandin-endoperoxide synthase 2; CXCL1, chemokine (C-X-C motif) ligand 1; CXCL2, chemokine (C-X-C motif) ligand 2; DSS, dextran sulphate sodium; GAPDH, glyceraldehyde-3-phosphate dehydrogenase; GPCR, G-protein coupled receptor; GPR4, G protein coupled receptor 4; H&E, hematoxylin and eosin; IBD, inflammatory bowel disease; ICAM-1, intercellular adhesion molecule 1; IFN-γ, interferon gamma; IL-10, interleukin 10; IL-18, interleukin 18; IL-6, interleukin 6; iNOS, nitric oxide synthase 2; LPLs, lamina propria leukocytes; MCP-1, chemokine (C-C motif) ligand 2; MPO, myeloperoxidase; OGR1, G protein coupled receptor 68; OR, odds ratio; PBS, phosphate buffered saline; RT-PCR, reverse transcription polymerase chain reaction; SELE, selectin, endothelial cell; TDAG8, G-protein coupled receptor 65; TNF-α, tumor necrosis factor alpha; UC, ulcerative colitis; VCAM1, vascular cell adhesion molecule 1. MEICS, murine endoscopic index of colitis severity

Introduction

A local acidification in the gut lumen as well as in the mucosa has been observed during intestinal inflammation and implicated in the pathogenesis and progression of inflammatory bowel disease (IBD). Fallingborg *et al.* reported that intraluminal colonic pH values in patients with active ulcerative colitis (UC) were significantly lower than normal subjects (lowest values 2.3, 2.9, and 3.4) in the proximal parts of the colon (1). Similarly, Raimundo *et al*. reported luminal pH as low as 4.7 in the proximal colon in patients with both active and inactive UC (2). Nugent and coworkers also reported a decrease of colonic luminal pH values to less than 5.5 in two of six patients with active UC (3). Also in patients with active Crohn's disease (CD) three out of four CD patients investigated had decreased pH value in the proximal colon (pH 5.3) and distal colon (pH 5.3) as compared to normal controls (pH 6.8) (3). While there is still some discussion about the range of the intestinal luminal pH in IBD patients (4),(5), it is widely accepted that inflammation is accompanied by tissue acidosis associated with glucose uptake due to hypoxia and excessive production and insufficient elimination of glycolytic metabolites. This indicates that during active IBD luminal and tissue pH is decreased. The (patho)physiological impact of these observations, however, has remained incompletely understood to date.

G protein-coupled receptors play an important role in regulating intestinal functions and have been implicated in the development and course of inflammatory bowel disease (6). Only recently, we found that the GPCR OGR1 plays a role in inflammatory bowel disease and that genetic deletion of OGR1 ameliorates the development of inflammatory bowel disease in the IL10 deficient IBD mouse model (7). OGR1 (ovarian cancer G protein coupled receptor 1, OGR1, GPR68) belongs to a novel family of proton-activated G protein-coupled receptors including also GPR4 and the T-cell death associated gene 8 (TDAG8, GPR65) (8-10). Accumulating evidence indicates that all of these three GPCRs (GPR4, OGR1 and TDAG8) are activated by protons upon a decrease of pH in the range of pH 7.6 (inactive) to pH 6.8 (fully activated) and may play a crucial role in pH homeostasis (8, 10).

GPR4 activation is transduced via the Ga_s pathway, followed by intracellular cAMP accumulation (8, 10). Half-maximal activation of cAMP formation by GPR4 expressed in HEK293 occurred at pH 7.55 [10]. Limited studies exist on the relationship between GPR4 and tumor development or regulation of metabolic acidosis in the kidney (11-17). The function of proton-activated receptors has been linked to inflammation(18) but the role of GPR4 in inflammatory disease has remained unknown. GPR4 mRNA was found to be widely expressed in a variety of mouse tissues including small intestine, colon, spleen, and localized to among other cell types to endothelial cells throughout the body. Considering GPR4 being expressed along the small and large intestine, we hypothesized that this proton-activated receptor might be involved in sensing local pH changes and may participate in the pathophysiology of IBD. Since local acidification of pH has been observed during IBD and the interaction between immune system and pH-sensing receptors is poorly understood, we postulate that GPR4 might be a player in mucosal inflammation during IBD.

Therefore, we examined the role of GPR4 in two models of colitis *in vivo*, the dextran sulphate sodium (DSS) induced chronic colitis model and the spontaneous colitis model in IL-10 deficient animals. Collectively, these data demonstrate that deletion of GPR4 is associated with ameliorated colitis and thus pH sensing plays an important role in the pathophysiology of IBD.

Methods and Materials

Human colonic biopsies

Biopsies of human colon were collected from patients during colonoscopy performed at the Division of Gastroenterology and Hepatology, University Hospital Zurich (Switzerland). CD patients (8 with severe, 7 with moderate inflammation and 14 in remission) and UC patients (5 with severe and 3 with moderate inflammation) underwent colonoscopy for assessment of inflammation and disease severity. Biopsies from patients with colitis were taken endoscopically from inflamed areas. The normal control tissues (17 controls) were from subjects undergoing colonoscopy as a screening procedure for colo-rectal cancer. The protocol for the study was approved by the ethics committee, University Hospital Zurich.

Genomic DNA extraction and genotyping

DNA extraction was done according to standard NaOH digestion. The PCR reactions used for GPR4 genotyping were set up with following oligonucleotides: 5'-atgggatcggccattgaacaa-3' (TS426), 5'-tcatcctgatcgacaagacc-3' (TS427), 5'- gctgccatgtggactctcga-3' (TS428), 5'-caggaaggcgatgctgatat-3' (TS429). TS426-TS427 is specific for neo (479 bps), and TS428-TS429 is specific for the GPR4 allele (302 bps).

Induction of chronic colitis with DSS

Gpr4 $^{-/-}$ mice (BALB/c and C57BL/6 background) were provided by Thomas Suply and Klaus Seuwen, Novartis, Basel. All transgenic strains were bred in the standard animal facility of the Institute of Physiology, University of Zurich. All animal experiments were performed in the Zurich Integrative Rodent Physiology (ZIRP) core facility according to the guidelines of the Swiss animal welfare law and approved by the Cantonal Veterinary Office Zurich, Switzerland.

Three experiments (2 experiments on a BALB/c and one on a C57/BL6 background) were performed with DSS (MP Biomedicals, LLC, Solon, OH,

USA) induced chronic colitis. Female mice at the age of 10-13 weeks and a body weight around 20g were used in the experiment. *Gpr4* $^{-/-}$ mice and wild-type mice received 3% DSS in drinking water for 7 days followed by 10 days recovery on water. Cycles were repeated three times. After the last cycle all animals were allowed to recover for 5 weeks and subsequently sacrificed for sample collection. Mice on water served as controls throughout the experiments.

Histological analysis was performed as described previously (19-21). The sections were stained with hematoxylin and eosin (H&E) and scored twice in a blinded fashion.

Gpr4 $^{-/-}$ /IL-10 $^{-/-}$ mice

Gpr4 $^{-/-}$ mice (C57BL/6) were bred to *IL-10* $^{-/-}$ mice (C57BL/6) with the goal to generate *Gpr4* $^{-/-}$ /*IL-10* $^{-/-}$ mice. Mice were routinely screened using PCR reactions for: IL-10 forward 5'-GTGGGTGCAGTTATTGTCTTCCCG-3' (oIMR0086), reverse 5'-GCCTTCAGTATA Grp4 forward AAAGGGGGACC-3' (oIMR0087), Grp4 reverse 5'-CCTGCGTGCAATCCATCTTG-3' (oIMR0088). In experiments WT littermates were used as controls. The onset and development of inflammatory markers, colitis and rectal prolapses was monitored over 200 days and data was analyzed using Kaplan-Meier analysis (log rank Mantel-Cox test). For the evaluation by histology, flow cytometry, and for the determination of cytokine (mRNA) expression profiles, some mice were sacrificed by cervical dislocation at 80 days of age.

Assessment of colonoscopy score in mice

Mucosal damage was assessed by the murine endoscopic index of colitis severity (MEICS) as described previously (20-23). Animals were anaesthetized intraperitoneally with a mixture of 90-120 mg of ketamine (Narketan 10%, Vétoquinol AG, Bern, Switzerland) and 8 mg of xylazine (Rompun 2%, Bayer, Zurich, Switzerland) per kg body weight and examined by colonoscopy (Karl Storz Tele Pack Pal 20043020, Karl Storz Endoskope, Tuttlingen, Germany).

Myeloperoxidase (MPO) activity assay

MPO activity was calculated by photoabsorbance, as previously described (20-21). Briefly, colon tissues were homogenized in 50 mM PBS (pH 6.0) with 0.5% hexadecyltrimethylammonium bromide (H-5882, Sigma). After performing three cycles of freeze-and-thaw, 20 µl of the homogenates supernatant were mixed with 280 µl of 0.02% dianisidine (D-3252, Sigma) solution. After 20 min incubation at room temperature, absorbance was measured at 460 nm. Protein concentration of the colon tissue supernatant was determined by Bradford protein assay (Bio-Rad). MPO activity was calculated as mean absorbance/incubation time/protein concentration.

RNA extraction and quantitative Real-Time RT-PCR

mRNA was extracted from colon and mesenteric lymph nodes tissue using the Qiagen RNeasy Mini Kit at a Qiacube workstation (Qiagen; Hilden, Germany) according to the manufacturer's instructions (20-21). cDNA was prepared from adjusted RNA samples (2µg/20µl reaction) using the TaqMan High Capacity Reverse Transcriptase Reagent Kit (Applied Biosystems; Forster City, CA, USA). Thermocycling conditions for reverse transcription were set at 25 °C for 10 minutes, 37 °C for 120 minutes, 85 °C for 5 seconds (TGradient thermocycler, Biomera; Goettingen, Germany).

Quantitative RT-PCR Taqman assays (7900 Fast Real Time PCR system, Applied Biosystems; Forster City, CA, USA) were performed under the following cycling conditions: 20 seconds at 95 °C, then 45 cycles of 95 °C for 3 seconds and 60 °C for 30 seconds with the TaqMan Fast Universal Mastermix. TaqMan assay probes for GPR4, TDAG8, OGR1, iNOS, IL-10, TNF-α, IFN-γ, IL-6, IL-18, MCP-1 (Life Technologies/ABI; Forster City, CA, USA) were used (Supplementary Table 1). RNA samples from individual animals were run in triplicates including a negative control (without cDNA). The comparative ΔCt method was applied to determine the quantity of the cytokines relative to the endogenous control GAPDH (mouse GAPDH, Mm03302249_g1, Reporter=VIC and Quencher=MGB) and a reference sample. The relative quantification value was expressed and shown as $2^{-\Delta Ct}$.

Preparation of lamina propria lymphocytes (LPLs)

Lamina propria lymphocytes (LPLs) were isolated from *Gpr4* $^{-/-}$ /*IL-10* $^{-/-}$, *Gpr4* $^{+/+}$ /*IL-10* $^{-/-}$ and *Gpr4* $^{+/+}$ /*IL-10* $^{+/+}$ mice at 80 days of age following a slightly modified protocol by Weigmann (24). Briefly, the dissected colon was washed with Ca^{+}- and Mg^{+}-free PBS. The tissue was cut and incubated in medium containing 20 mM EDTA (Sigma-Aldrich) for 30 min at 37° C under shaking. LPLs were isolated from the lamina propria by enzymatic digestion (in DMEME medium containing 300 U/mL collagenase type I, 2 mg/mL Hyaluronidase, 0.3 mg/ml DNase and 5 mM $CaCl_2.2H_2O$) for 15 min at 37 °C under shaking. The LPLs were purified by discontinuous Ficoll density-gradient centrifugation.

Flow Cytometric Analysis (FACS)

Single cell suspensions from lamina propria (LP) of mice were prepared as described above and stained for analysis by flow cytometry using PBS containing 4% FCS and 2.5 mM EDTA. At least 0.5×10^6 LP cells/well were stained at 4°C in the dark with the following fluorochrome-labeled monoclonal antibodies (all from BD): α-CD3, α-CD4, α-CD8, α-CD25, α-CD45.2, and α-CD161 (NK1.1). Viable cells were acquired on a FACS Canto II (BD Biosciences) and analyzed using FlowJo software (TriStar Inc).

Statistical Analysis

Statistical analyses were performed using GraphPad Prism 5 (Version 5.04, GraphPad Software Inc, San Diego, CA, US) and SPSS (8.0 for Windows; SPSS Inc, Chicago, IL, US). Groups of data were compared between genotypes using nonparametric Mann-Whitney U-test or Kruskal-Wallis one-way ANOVA followed by Dunn's multiple-comparison test. All data were expressed as the means ± SEM. Probabilities (*p*, two tailed) of $p < 0.05$ were considered statistically significant. Body weight comparison was performed using "General Linear Model, repeated measures", and the full

factorial model with type III sum of squares method(25). The “General Linear Model, repeated measures” integrated both “individual deviation of daily body weight” and “difference in genotype groups” into the analysis to avoid systemic bias (25).

For prolapse ratio comparison studies, statistical differences between genotypes were calculated by chi-square test with Fisher’s exact test (exact significance, two sided) and risk estimate test from contingency table. The prolapse survival analysis was performed using Kaplan-Meier prolapse-free survival analysis (log rank Mantel-Cox test) and estimated median prolapse-free survival time.

Results

GPR4 expression in the colon of normal subjects and IBD patients

Semiquantitative RT-qPCR confirmed mRNA expression of GPR4 in normal colon and IBD patients' colon. mRNA expression of GPR4 was significantly higher in the colon of patients with active UC (5.3-fold, $P< .05$ *) and in CD patients in remission (5.8-fold, $P< .001$ ***) (Figure 1.A). GPR4 expression in patients with CD was increased 2.7-fold and 2.5 fold (severe and moderate groups). In patients with active UC, a 3.1-fold (severe group) increase in the level of GPR4 expression was observed.

In mice, DSS-induced chronic colitis caused no upregulation of mRNA expression for the two other members of the pH receptor family, TDAG8 and OGR1, in colonic tissue, from both *Gpr4* $^{+/+}$ and *Gpr4* $^{-/-}$ mice (Figure 1.B). This indicates that these two pH receptors were not upregulated on mRNA level to compensate for the lack of GPR4 *in vivo.* Moreover, during acute colitis (7 days DSS) wildtype mice displayed increased TDAG8 expression, but no increase in GPR4 or OGR1 expression in the colon (Figure 1.C) This observation likely reflects immune cell infiltration, where TDAG8 is highly expressed.

DSS induced chronic colitis is attenuated in mice lacking Gpr4

Since GPR4 is expressed in human inflamed colonic tissue and other proton-activated receptors from the same family have been linked to inflammatory diseases, we tested the impact of genetic deletion of GPR4. Compared with *Gpr4* $^{+/+}$ mice, *Gpr4* $^{-/-}$ mice showed less reduction in body weight upon DSS treatment (Fig. 2). A total of 22 DSS treated *Gpr4* $^{+/+}$ (16 BALB and 6 C57BL/6) mice and 18 DSS treated *Gpr4* $^{-/-}$ (11 BALB and 7 C57BL/6) mice in 3 independent experiments were compared with 5 *Gpr4* $^{+/+}$ and 6 *Gpr4* $^{-/-}$ control mice (C57BL/6) receiving normal water. From day 62 to day 83 (22 days after the fourth DSS cycle) *Gpr4* $^{-/-}$ mice had lost clearly less body weight and showed an enhanced ability to regain weight ($F=2.980$, $P< .05$ *, Figure 2A). All 3 independent experiments showed qualitatively similar results: *Gpr4* $^{-/-}$ mice suffered less body weight loss, indicating a

protective effect of GPR4 deficiency (P< .05 for BALB (exp 1), P< .05 * for BALB (exp 2) and P< .01 ** for C57BL/6 background) independent of the genetic background.

Histological analysis provided evidence (Figure 2B) that *Gpr4* $^{-/-}$ +DSS mice had attenuated colonic inflammation. The total histological score for DSS treated *Gpr4* $^{-/-}$ mice (2.3 ± 0.38) was significantly lower as compared to DSS treated *Gpr4* $^{+/+}$ mice (4.9 ± 0.81) (P< .001, Supplementary Figure 1). Water control and *Gpr4* $^{-/-}$ mice showed almost no signs of inflammation. *Gpr4* $^{-/-}$ mice had lower scores for both epithelial injury and leukocyte infiltration (P< .001 for both) (Figure 2B and 2C). Again, all 3 experiments showed consistent results independent of genetic background.

In contrast DSS treated *Gpr4* $^{-/-}$ had slightly shorter colon lengths and a higher endoscopic MEICS score (P< .05, Supplementary Figure 2A and 2B). GPR4 deficiency did not change MPO activity and spleen weight upon DSS (Supplementary Figure 2C and 2D). Cytokine expression profiling for iNOS, IL-10, TNF-α, IFN-γ, IL-6, and MCP-1 was not different in colon and mesenteric lymph node tissues between *Gpr4* $^{+/+}$ and *Gpr4* $^{-/-}$ mice upon DSS induced colitis (Figure 3 and Supplementary Figure 2E).

Spontaneous colitis is attenuated in Gpr4/IL-10 double knock out animals

Next, we assessed the impact of GPR4 in a spontaneous colitis model. The occurrence of rectal prolapse as a sign of spontaneous colitis in IL-10 $^{-/-}$ mice was monitored for 200 days. In comparison with *Gpr4* $^{+/+}$ */IL-10* $^{-/-}$ mice, both female and male *Gpr4* $^{-/-}$ */IL-10* $^{-/-}$ mice, had a lower rectal prolapse incidence (female: 6.9%, n = 29 vs. 66.7%, n = 12, P< .001 , odds ratios of *Gpr4* $^{-/-}$/*Gpr4* $^{+/+}$ = 0.037 (95% CL 0.006-0.241); male: 24.4%, n=41 vs. 52.0%, n=25, P= .033, odds ratios = 0.298 (95% CL 0.103-0.859); chi-square test with Fisher's exact test/two sided). All mice were maintained in the same OHB room and all experiments were carried out during the same time period. No prolapses were observed in any control *Gpr4* $^{+/+}$ */IL-10* $^{+/+}$ mice in the breeding colonies for 200 days (n > 100 for each gender).

Kaplan-Meier prolapse-free survival analysis showed a significantly delayed onset of rectal prolapse in *Gpr4* $^{-/-}$ /*IL-10* $^{-/-}$ mice as compared to *Gpr4* $^{+/+}$ /*IL-10* $^{-/-}$ mice (estimated median prolapse-free survival time, female: >200 days vs. 123 days, $P < .001$; male: >200 days vs. 161 days, $P = .007$, log rank (Mantel-Cox) test, Figure 4A and Supplementary Figure 3A).

Figure 4B (and Supplementary Figure 3B) illustrate the level of granulocyte infiltration as measured by MPO activity in colon tissue of mice at 80 days of age. This age was chosen as none of the mice had developed a prolapse at this age. In *Gpr4* $^{-/-}$ /*IL-10* $^{-/-}$ male mice, MPO activity was significantly lower than that in *Gpr4* $^{+/+}$ /*IL-10* $^{-/-}$ male mice (0.013±0.068 vs. 0.53±0.101, $P < .05$). A similar trend was seen in female *Gpr4* $^{-/-}$ /*IL-10* $^{-/-}$ animals (Figure 4B). Compared with control *Gpr4* $^{+/+}$ /*IL-10* $^{-/-}$ mice, *Gpr4* $^{-/-}$ /*IL-10* $^{-/-}$ mice were not different with respect to colon length and relative spleen weight (except for *Gpr4* $^{-/-}$ /*IL-10* $^{-/-}$ female mice, $P < .05$, Figure 4C and D and Supplementary Figure 3C and 3D).

Histological analysis of murine colons from 80 days old mice showed that colons from male (histological score of 1.6±0.91) and female (1.6±0.93) *Gpr4* $^{+/+}$ /*IL-10* $^{+/+}$ mice were morphologically normal. *Gpr4* $^{-/-}$ /*IL-10* $^{-/-}$ male (2.3±0.68) and female (2.6±1.69) mice displayed significantly less mucosal injury and infiltration as compared to *Gpr4* $^{+/+}$ /*IL-10* $^{-/-}$ male (6.3±0.45) and female (6.5±1.12) mice ($P < .05$ for both), consistent with the prolapse ratio and prolapse-free survival analysis. (Figure 5 and Supplementary Figure 4).

Reduction of mucosal CD4+ T helper cell infiltrate upon Gpr4 deficiency

Spontaneous colitis in IL-10 deficient mice is mediated by Th1 and Th17 cell infiltration (26-27). In order to identify cellular players underlying the reduced colitis in GRP4$^{-/-}$ mice we subsequently measured cellular infiltrates in the lamina propria by flow cytometry. As shown in Figure 6 and Supplementary Figure 5, the percentage, the CD8 to CD4 ratios, as well as CD4+ T cell numbers were significantly higher in *Gpr4* $^{+/+}$ /*IL-10* $^{-/-}$ as compared to *Gpr4* $^{+/+}$ /*IL-10* $^{+/+}$ controls ($P < .01$, $P < .001$ and $P < .001$). *Gpr4* $^{+/+}$ /*IL-10* $^{-/-}$ mice had

significantly higher counts of CD4+ cells, but not CD8+ in the lamina propria. No changes of Treg, NK cells, CD45+ total immune cells, non-B & non-T cells, macrophages and monocytes/neutrophils in LPLs composition were observed among the three groups (Supplementary Table 2).

We further characterized cytokine mRNA expression in colon tissue and mesenteric lymph nodes using age-matched female (Figure 7 and Supplementary Figure 6) and male (Supplementary Figure 7) mice at 80 days of age. As shown in Figure 7**,** IFN-γ expression was significantly lower in *Gpr4* $^{-/-}$ /*IL-10* $^{-/-}$ mice (P< .05), which reconfirmed reduced Th1 -cell infiltrate in mice lacking GPR4. Furthermore, *Gpr4* $^{-/-}$ /*IL-10* $^{-/-}$ mice showed lower mRNA expression for iNOS, IL-6, MCP-1, CXCL2, CXCL1, SELE, VCAM1 as compared to *Gpr4* $^{+/+}$ /*IL-10* $^{-/-}$ mice (Figure 7).

Discussion

This is the first study on the (patho-)physiological function of the proton-activated G-protein coupled receptor GPR4 in the intestine and its impact on intestinal inflammation. We demonstrate that GPR4 deletion protects against experimental colitis in both DSS-induced chronic colitis and the IL-10-induced colitis.

According to the National Center for Biotechnology Information (NCBI) Gene Expression Omnibus (GEO) profile and Gene database (http://www.ncbi.nlm.nih.gov/sites/geo) and the BioGPS database of The Scripps Research Institute (http://biogps.org)) the human small intestine and colon express GRP4 at moderate levels. Here, we demonstrate that GPR4 mRNA is strongly up-regulated in the colons of IBD patients (Figure 1A and GEO Profile database ID: 12504653 and 4234799). In the chronic DSS colitis model (26-29), *Gpr4* $^{-/-}$ mice lost less body weight and had lower histology scores compared to WT littermates indicating less severe inflammation. In the spontaneous IL-10-mediated colitis model (30-32) lack of GPR4 significantly delayed onset and progression of rectal prolapses which could explain the protective role of Gpr4 deficiency in experimental colitis. As IL-10 is a well-known anti-inflammatory cytokine and suppressor for Th1 cells and macrophages (33), IL-10 knockout mice are thought to have a Th1-cell driven disease (26-27). Consistent with less Th1 cell infiltrate in *Gpr4* $^{-/-}$ */IL-10* $^{-/-}$ mice a significantly lower IFN-γ expression was found. Further, LPL-infiltration measured by flow cytometry demonstrated that GPR4 knockout partially reduced infiltration of CD4+ T cells. Finally, the anti-inflammatory effect of GPR4 deficiency seemed not to be mediated by elevated Treg levels as no significant changes in Treg numbers were observed between groups.

Therefore, in turn, activation of GPR4 is likely to exacerbate intestinal inflammation and trigger inflammatory responses via the Gs-cAMP-Th1-IFN-γ pathway. IFN-γ aggravates inflammation by increasing iNOS expression, activating macrophages and NK cells and inducing apoptosis (34-35). The

excessive production of glycolytic metabolites in inflamed tissue causes the accumulation of protons, which may further activate GPR4, forming a positive feedback loop which may lead to a vicious cycle. Thus blockade of GPR4 may be a promising new target for IBD treatment.

Recent data published on *Gpr4* $^{-/-}$ mice support the negative role of GPR4 activation during inflammation. *Gpr4* $^{-/-}$ mice showed an impaired response to VEGF-driven angiogenesis in a growth factor implant model and had less tumor growth (12). Moreover, both GPR4 knockout and GPR4 inhibition by specific siRNAs resulted in decreased VEGFR2 (VEGF receptor 2, the main signaling receptor for VEGF on endothelial cells) levels, which might be one of the reasons for a reduced angiogenic response to VEGF (12). In addition GPR4 may be involved in inflammation, autoimmunity and allergy. In vitro stimulation of GPR4 caused upreglation of many transcripts involved in inflammatory processes(36). Reduced immune responses and attenuated airway hyper-responsiveness were observed in GPR4 deficient mice following ovalbumin exposure (37). This was accompanied by a reduction in the number of eosinophils in broncho-alveolar lavage fluid (38). In the cigarette smoke-induced COPD mouse model, *Gpr4* $^{-/-}$ mice had accelerated elimination of airway inflammation and enhanced neutrophil clearance (39).In patients with systemic Sclerosis, expression of GPR4 correlates with the severity of lung disease (40).

Yang *et al*. found evidence that acidosis/GPR4 signaling regulates endothelial cell adhesion mainly through the Gs/cAMP/Epac pathway (41). The activation of GPR4 by acidosis up-regulated the expression of multiple adhesion molecules such as SELE, VCAM-1 and ICAM-1 in vitro and increased the adhesiveness of human umbilical vein endothelial cells (HUVECs) expressing endogenous GPR4. These adhesion molecules are involved in the binding of leukocytes (41). In our studies *Gpr4* $^{-/-}$ */IL-10* $^{-/-}$ mice expressed lower mRNA levels of iNOS, TNF-α, IFN-γ, IL-6, MCP-1, CXCL2, CXCL1, SELE and VCAM-1 which at least in part is in agreement with the mentioned *in vitro* observations. A regulation of the NF-κB pathway by

Gpr4-dependent signalling has been postulated (36) further supporting our findings.

In summary, our results demonstrate that *Gpr4* $^{-/-}$ deficiency protects from experimental colitis indicating an important pathophysiological role for the proton-activated receptor during the pathogenesis of mucosal inflammation. GPR4 may become a promising novel target for pharmacological IBD therapy.

Acknowledgement

We thank Prof. Dr. Burkhardt Seifert and Dr. Sarah R. Haile (Division of Biostatistics, University of Zurich) for the statistics support and advice. We also thank Dr. Klaus Seuwen, Novartis Institutes for BioMedical Research (NIBR), Basel, Switzerland, for his critical comments and valuable suggestions as well as for providing the Gpr4 KO mice. Parts of the study were presented at the Digestive Disease Week (DDW) 2011 (Chicago, IL) and DDW 2012 (San Diego, CA), and the Annual Meeting of the Swiss Physiological Society and Young Investigator Award 2012 (Fribourg, Switzerland).

Figure legends

Figure 1

GPR4 mRNA detection in colonic tissue from humans and mice.

(A) GPR4 mRNA was detected in colonic biopsies from controls (normal subjects), and patients with ulcerative colitis (UC), or Crohn's disease (CD) by real-time RT-PCR Taqman assays. A minimum of 5 patients per group was tested for quantification. **(B)** GPR4 mRNA detection in colonic tissues from wildtype mice or *Gpr4* $^{-/-}$ mice with water or DSS induced chronic colitis. **(C)** GPR4 mRNA detection in colonic tissues from wildtype mice or wildtype mice with acute DSS induced colitis (7 days). The relative amount of GPR4 mRNA was determined via normalization across all samples to the housekeeping control gene GAPDH. Groups of data were compared between control group and different individual group using the non-parametric Kruskal-Wallis one-way ANOVA followed by Dunn's multiple-comparison test. For quantification, values are mean ± SEM; n ≥ 5 per group; $P < .01$ **, $P < .001$ ***.

Figure 2

***Body* weight loss analysis and histological assessment of colonic inflammation.**

(A) *Gpr4* $^{-/-}$ mice, compared with *Gpr4* $^{+/+}$ mice, showed less relative body weight loss during DSS-induced chronic colitis. After 4 cycles of DSS treatment (last 22 days), *Gpr4* $^{-/-}$ mice exhibited clearly reduced gain of body weight ($F=2.980$, $P < .05$ *) than *Gpr4* $^{+/+}$ mice. The body weight changes are expressed as relative change of body weight in % relative to day 0. Histology scores were analyzed to assess the epithelial damage **(B)** and leukocyte infiltration **(C)** indicating less severe inflammation in *Gpr4* $^{-/-}$ mice with DSS. The right panel shows a representative histological section from wild-type or *Gpr4* $^{-/-}$ mice treated with DSS Data are representative of 3 independent experiments each with 6-8 female mice/ group.

Figure 3

Assessment of the colitis severity during DSS induced chronic colitis. The mRNA expression levels of iNOS, IL-10, TNF-α, IFN-γ, IL-6, and MCP-1 in colon from *Gpr4* $^{-/-}$ mice and *Gpr4* $^{+/+}$ mice with or without administration of DSS were not changed between genotypes for the same treatment. For quantification, values are mean ± SEM; n ≥ 5 per group; $P < .05$ *, $P < .01$ **, $P < .001$ ***. Data are representative of 3 independent experiments.

Figure 4

Development of IBD and progression to prolaps were reduced by the deletion of GPR4 from IL10 deficient mice.

(A) Kaplan-Meier prolapse-free survival curve showed delayed onset and progression of prolapses in female *Gpr4* $^{-/-}$ /*IL-10* $^{-/-}$ mice relative to female *Gpr4* $^{+/+}$ /*IL-10* $^{-/-}$ mice (estimated median prolapse-free survival time, >200 days vs. 123 days, $P = .000$ ***, log rank (Mantel-Cox) test). Black dotted lines, *Gpr4* $^{-/-}$ /*IL-10* $^{-/-}$ mice (6.9% prolapses, n=29, female); black solid line, *Gpr4* $^{+/+}$ /*IL-10* $^{-/-}$ mice (66.7% prolapses, n=12, female); grey dotted lines, *Gpr4* $^{+/+}$ /*IL-10* $^{+/+}$ mice (0% prolapses, n=31, female). No rectal prolapse was detected in the *Gpr4* $^{+/+}$ /*IL-10* $^{+/+}$ mice in these breeding colonies for 200 days (> 100 mice). Comparison of MPO activity in colon tissue **(B)**, colon length **(C),** and relative spleen weight **(D)** showed attenuated colitis in female *Gpr4* $^{-/-}$ /*IL-10* $^{-/-}$ mice (not significant but relative spleen weight, $P < .01$ **, Kruskal-Wallis one-way ANOVA followed by Dunn's multiple-comparison test).

Figure 5

Less histological damage in *Gpr4* $^{-/-}$ /*IL-10* $^{-/-}$ female mice.

(A) The total histology scores of distal colon of female *Gpr4* $^{-/-}$ /*IL-10* $^{-/-}$, *Gpr4* $^{+/+}$ /*IL-10* $^{-/-}$ and *Gpr4* $^{+/+}$ /*IL-10* $^{+/+}$ mice at 80 days of age are shown, indicating reduced inflammation in *Gpr4* $^{-/-}$ /*IL-10* $^{-/-}$ mice ($P < .05$, *Gpr4* $^{-/-}$ /*IL-10* $^{-/-}$ compared to *Gpr4* $^{+/+}$ /*IL-10* $^{-/-}$). **(B)** H&E stained sections showed the significant difference in the damage of epithelial integrity and intensity of the

leukocyte infiltration into inflamed sites. The total histology scores are representative for overall histology scores of distal colon (epithelial injury plus leukocyte infiltration). Data are presented as mean ± SEM; n ≥ 5 per group; $P < .05$ *, $P < .01$ **, $P < .001$ ***.

Figure 6

Suppression of IFN-γ-producing $CD4^+$ T helper cells in *Gpr4 $^{-/-}$ /IL-10 $^{-/-}$* mice.

LPLs were isolated from the colon of female *Gpr4 $^{-/-}$ /IL-10 $^{-/-}$*, *Gpr4 $^{+/+}$ /IL-10 $^{-/-}$* and *Gpr4 $^{+/+}$ /IL-10 $^{+/+}$* mice, stained to identify subpopulations and analyzed by FACS. LPLs profiles from FACS analysis demonstrated that ablation of GPR4 suppressed accumulation of $CD4^+$ (T helper) cells, mainly Th1 cells, but not $CD8^+$ (T cytotoxic) cells: quantification of $CD4^+$ T cells, percentage of $CD4^+$ cells in $CD3^+$ T cells, comparison of $CD4^+/CD8^+$ ratio, quantification of $CD8^+$ T cells, and percentage of $CD8^+$ cells in $CD3^+$ T cells. The difference between *Gpr4 $^{-/-}$ /IL-10 $^{-/-}$* and *Gpr4 $^{+/+}$ /IL-10 $^{-/-}$* did not reach statistical significance. Representative FACS results from more than 5 qualitatively similar experiments are shown; isolated LPLs from 3 female mice were pooled in each group. Data are presented as mean ± SEM; $P < .05$ *, $P < .01$ **, $P < .001$ ***.

Figure 7

Analysis of mRNA expression profiles of cytokines in colon from *Gpr4 $^{-/-}$ /IL-10 $^{-/-}$*, *Gpr4 $^{+/+}$ /IL-10 $^{-/-}$* and *Gpr4 $^{+/+}$ /IL-10 $^{+/+}$* mice.

The mRNA expression profiles of iNOS, IFN-γ, IL-6, MCP-1, CXCL1, and CXCL1 were analyzed by semi-quantitative RT-qPCR in colon tissue from of all three female strains (*Gpr4 $^{-/-}$ /IL-10 $^{-/-}$*, *Gpr4 $^{+/+}$ /IL-10 $^{-/-}$* and *Gpr4 $^{+/+}$ /IL-10 $^{+/+}$* mice). Th1 associated IFN-γ expression was significantly lower in colon of female *Gpr4 $^{-/-}$ /IL-10 $^{-/-}$* mice compared with female *Gpr4 $^{+/+}$ /IL-10 $^{-/-}$* mice

(*P*< .05 *, Kruskal-Wallis one-way ANOVA followed by Dunn's multiple-comparison test). Data are presented as relative expression normalized to the house-keeping gene GAPDH, n = 6-9 mice per group. Data are presented as mean ± SEM; *P* < .05 *, *P* < .01 **, *P*< .001 ***.

References

1. Fallingborg J, Christensen LA, Jacobsen BA, et al. Very low intraluminal colonic pH in patients with active ulcerative colitis. Dig Dis Sci. 1993;38:1989-1993

2. Raimundo AH, Evans DF, Rogers J, et al. Gastrointestinal pH profiles in ulcerative colitis. Gastroenterology. 1992;102:A681

3. Nugent SG, Kumar D, Rampton DS, et al. Intestinal luminal pH in inflammatory bowel disease: possible determinants and implications for therapy with aminosalicylates and other drugs. Gut. 2001;48:571-577

4. Press AG, Hauptmann IA, Hauptmann L, et al. Gastrointestinal pH profiles in patients with inflammatory bowel disease. Aliment Pharmacol Ther. 1998;12:673-678

5. Ewe K, Schwartz S, Petersen S, et al. Inflammation does not decrease intraluminal pH in chronic inflammatory bowel disease. Dig Dis Sci. 1999;44:1434-1439

6. Wasilewski A, Storr M, Zielinska M, et al. Role of G Protein-coupled Orphan Receptors in Intestinal Inflammation: Novel Targets in Inflammatory Bowel Diseases. Inflamm Bowel Dis. 2014

7. de Vallière C, Wang Y, Vidal S, et al. The G protein-coupled pH-sensing receptor OGR1 is a regulator of intestinal inflammation. Inflamm Bowel Dis. in press

8. Seuwen K, Ludwig MG, Wolf RM. Receptors for protons or lipid messengers or both? J Recept Signal Transduct Res. 2006;26:599-610

9. Choi JW, Lee SY, Choi Y. Identification of a putative G protein-coupled receptor induced during activation-induced apoptosis of T cells. Cell Immunol. 1996;168:78-84

10. Ludwig MG, Vanek M, Guerini D, et al. Proton-sensing G-protein-coupled receptors. Nature. 2003;425:93-98

11. Sin WC, Zhang Y, Zhong W, et al. G protein-coupled receptors GPR4 and TDAG8 are oncogenic and overexpressed in human cancers. Oncogene. 2004;23:6299-6303

12. Wyder L, Suply T, Ricoux B, et al. Reduced pathological angiogenesis and

tumor growth in mice lacking GPR4, a proton sensing receptor. Angiogenesis. 2011;14:533-544

13. Sun X, Yang LV, Tiegs BC, et al. Deletion of the pH sensor GPR4 decreases renal acid excretion. J Am Soc Nephrol. 2010;21:1745-1755

14. Codina J, Opyd TS, Powell ZB, et al. pH-dependent regulation of the alpha-subunit of H+-K+-ATPase (HKalpha2). Am J Physiol Renal Physiol. 2011;301:F536-543

15. Castellone RD, Leffler NR, Dong L, et al. Inhibition of tumor cell migration and metastasis by the proton-sensing GPR4 receptor. Cancer Lett. 2011;312:197-208

16. Brown D, Wagner CA. Molecular mechanisms of acid-base sensing by the kidney. J Am Soc Nephrol. 2012;23:774-780

17. Wagner CA. Metabolic acidosis: new insights from mouse models. Curr Opin Nephrol Hypertens. 2007;16:471-476

18. Okajima F. Regulation of inflammation by extracellular acidification and proton-sensing GPCRs. Cell Signal. 2013;25:2263-2271

19. Hausmann M, Obermeier F, Paper DH, et al. In vivo treatment with the herbal phenylethanoid acteoside ameliorates intestinal inflammation in dextran sulphate sodium-induced colitis. Clin Exp Immunol. 2007;148:373-381

20. Bentz S, Pesch T, Wolfram L, et al. Lack of transketolase-like (TKTL) 1 aggravates murine experimental colitis. Am J Physiol Gastrointest Liver Physiol. 2011;300:G598-607

21. Fischbeck A, Leucht K, Frey-Wagner I, et al. Sphingomyelin induces cathepsin D-mediated apoptosis in intestinal epithelial cells and increases inflammation in DSS colitis. Gut. 2011;60:55-65

22. Becker C, Fantini MC, Neurath MF. High resolution colonoscopy in live mice. Nat Protoc. 2006;1:2900-2904

23. Scharl M, Leucht K, Frey-Wagner I, et al. Knock-out of beta-glucosidase 2 has no influence on dextran sulfate sodium-induced colitis. Digestion. 2011;84:156-167

24. Weigmann B, Tubbe I, Seidel D, et al. Isolation and subsequent analysis of murine lamina propria mononuclear cells from colonic tissue. Nat Protoc. 2007;2:2307-2311

25. SPSS Inc. SPSS advanced statistics 17.0. 17.0 ed. Chicago, Ill.: SPSS

Inc.; 2007

26. Wirtz S, Neurath MF. Mouse models of inflammatory bowel disease. Adv Drug Deliv Rev. 2007;59:1073-1083

27. Hibi T, Ogata H, Sakuraba A. Animal models of inflammatory bowel disease. J Gastroenterol. 2002;37:409-417

28. Solomon L, Mansor S, Mallon P, et al. The dextran sulphate sodium (DSS) model of colitis: an overview. Comparative Clinical Pathology: Springer London; 2010:235-239

29. Okayasu I, Hatakeyama S, Yamada M, et al. A novel method in the induction of reliable experimental acute and chronic ulcerative colitis in mice. Gastroenterology. 1990;98:694-702

30. MacDonald TT. Gastrointestinal inflammation. Inflammatory bowel disease in knockout mice. Curr Biol. 1994;4:261-263

31. Bhan AK, Mizoguchi E, Smith RN, et al. Colitis in transgenic and knockout animals as models of human inflammatory bowel disease. Immunol Rev. 1999;169:195-207

32. Michelle E.A. Borm, Bouma. G. Animal models of inflammatory bowel disease. Drug Discovery Today: Disease Models: Elsevier; 2004:437-443

33. Moore KW, de Waal Malefyt R, Coffman RL, et al. Interleukin-10 and the interleukin-10 receptor. Annu Rev Immunol. 2001;19:683-765

34. Perez-Rodriguez R, Roncero C, Olivan AM, et al. Signaling mechanisms of interferon gamma induced apoptosis in chromaffin cells: involvement of nNOS, iNOS, and NFkappaB. J Neurochem. 2009;108:1083-1096

35. Schroder K, Hertzog PJ, Ravasi T, et al. Interferon-gamma: an overview of signals, mechanisms and functions. J Leukoc Biol. 2004;75:163-189

36. Dong L, Li Z, Leffler NR, et al. Acidosis activation of the proton-sensing GPR4 receptor stimulates vascular endothelial cell inflammatory responses revealed by transcriptome analysis. PLoS One. 2013;8:e61991

37. Seuwen; Klaus; (Basel CBEB, CH) ; Suply; Thomas; (Basel, CH) ; Wyder; Lorenza; (Basel, CH) ; Dawson King; Janet; (Basel, CH) ; Ludwig; Marie-Gabrielle; (Basel, CH) ; Mueller; Matthias; (Basel, CH) ; Nath; Puneeta; (Horsham, GB) ; Jones; Carol Elizabeth; (Horsham, GB). Inhibition of gpr4, US20100144835. In: USPTO, ed. USA; 2010:1-50

38. P Nath JM, M Freeman, C Poll, KH Banner, T Suply, A Trifilief, and C

Jones. Effect of GPR4 Inhibition in a Murine Model of Allergic Asthma. D22 MODULATORS OF INFLAMMATORY PATHWAYS IN AIRWAY DISEASE. American Thoracic Society 2009 International Conference. San Diego,CA, US: Am J Respir Crit Care Med; 2009:A5449

39. Puneeta Nath CS, Mark Freeman, Chris Poll, Katharine Banner, Thomas Suply, Alexandre Triffilief, Carol Jones. Effect of GPR4 inhibition in a murine tobacco smoke model of chronic obstructive pulmonary disease. British Pharmacological Society Winter Meeting December 2008. Brighton, UK: Proceedings of the British Pharmacological Society; 2008:017P

40. Assassi S, Wu M, Tan FK, et al. Skin gene expression correlates of severity of interstitial lung disease in systemic sclerosis. Arthritis Rheum. 2013;65:2917-2927

41. Chen A, Dong L, Leffler NR, et al. Activation of GPR4 by acidosis increases endothelial cell adhesion through the cAMP/Epac pathway. PLoS One. 2011;6:e27586

Figure 1

A

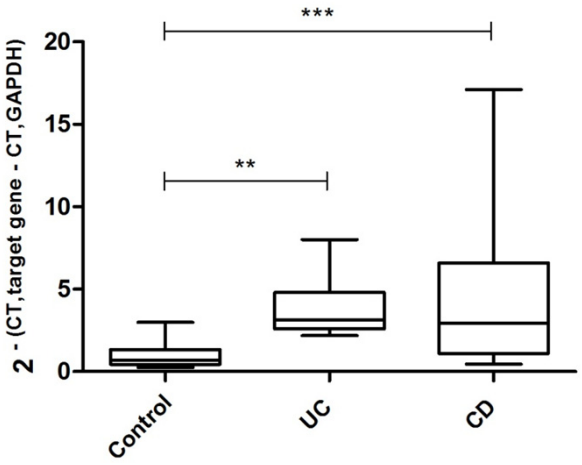
***
**
20
15
10
5
0
2 - (CT, target gene - CT, GAPDH)
Control
UC
CD

B

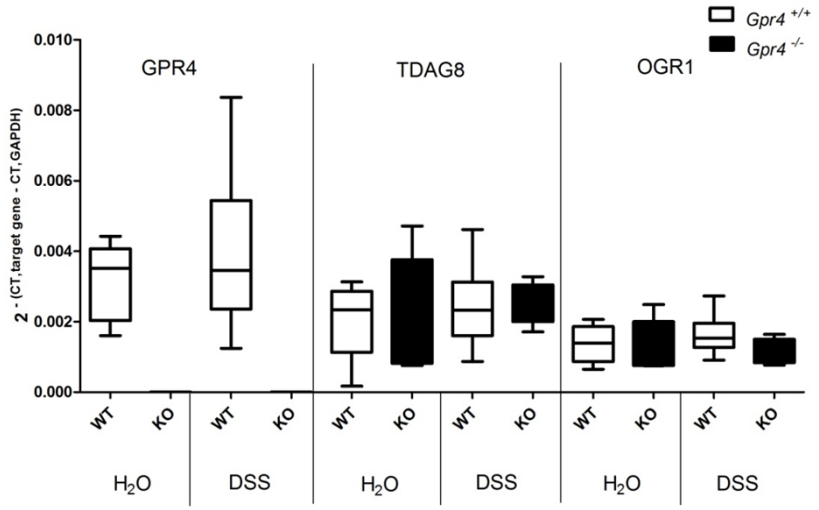
Gpr4 +/+
Gpr4 -/-
GPR4
TDAG8
OGR1
0.010
0.008
0.006
0.004
0.002
0.000
2 - (CT, target gene - CT, GAPDH)
WT
KO
H2O
DSS

C

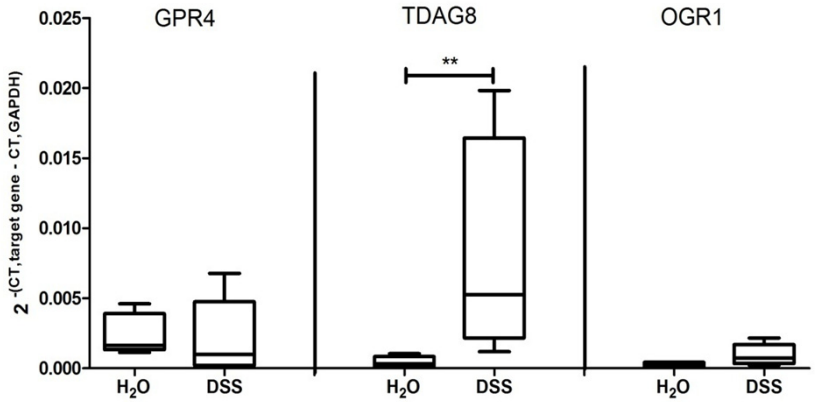
GPR4
TDAG8
OGR1
**
0.025
0.020
0.015
0.010
0.005
0.000
2 -(CT, target gene - CT, GAPDH)
H2O
DSS

Figure 2

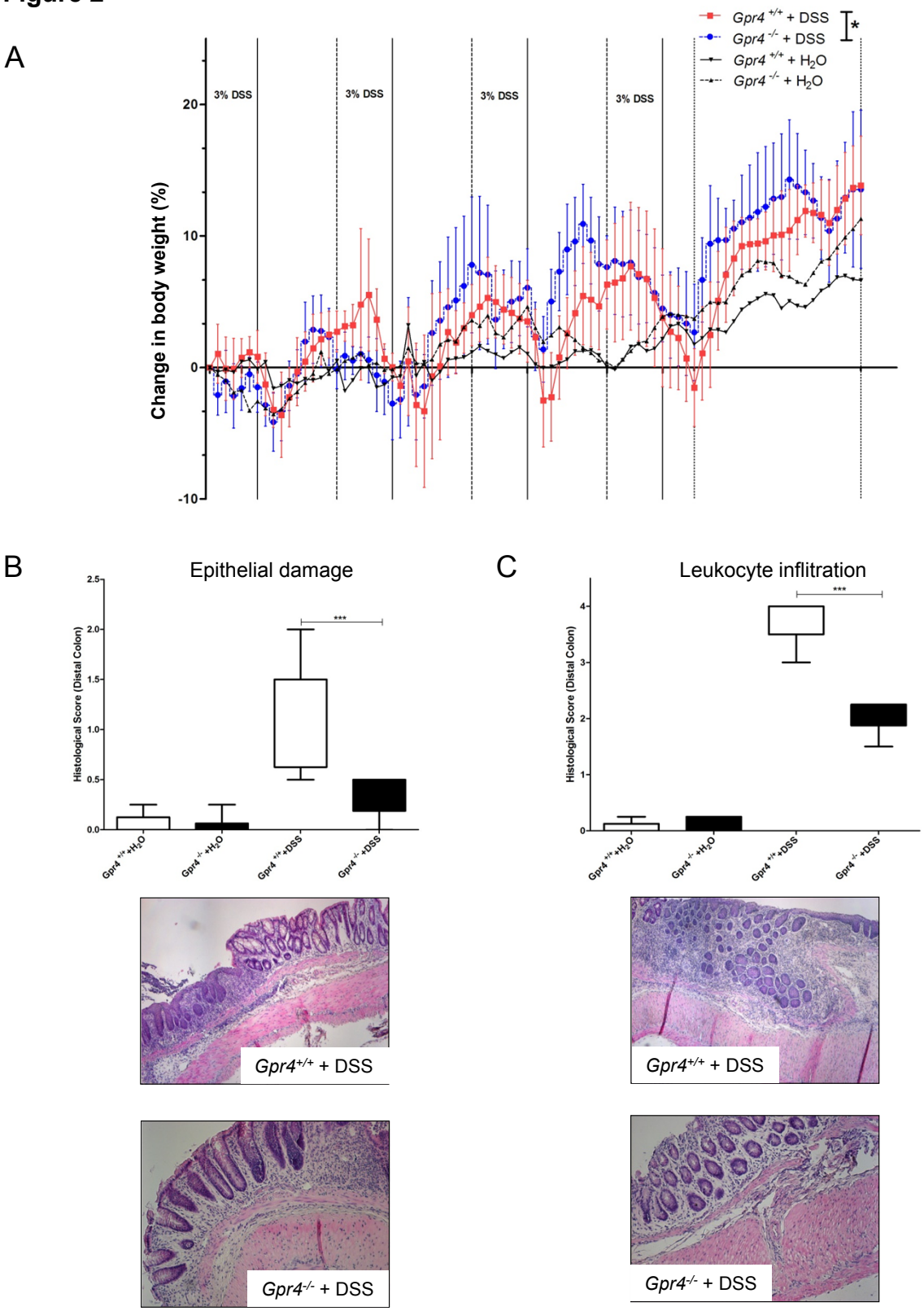
A
Gpr4 +/+ + DSS
Gpr4 -/- + DSS
Gpr4 +/+ + H2O
Gpr4 -/- + H2O
*
3% DSS
3% DSS
3% DSS
3% DSS
Change in body weight (%)
20
10
0
-10
B
Epithelial damage
Histological Score (Distal Colon)
***
Gpr4+/+ +H2O
Gpr4-/- +H2O
Gpr4+/+ +DSS
Gpr4-/- +DSS
C
Leukocyte inflitration
Histological Score (Distal Colon)
***
Gpr4+/+ +H2O
Gpr4-/- +H2O
Gpr4+/+ +DSS
Gpr4-/- +DSS
Gpr4+/+ + DSS
Gpr4+/+ + DSS
Gpr4-/- + DSS
Gpr4-/- + DSS

Figure 3

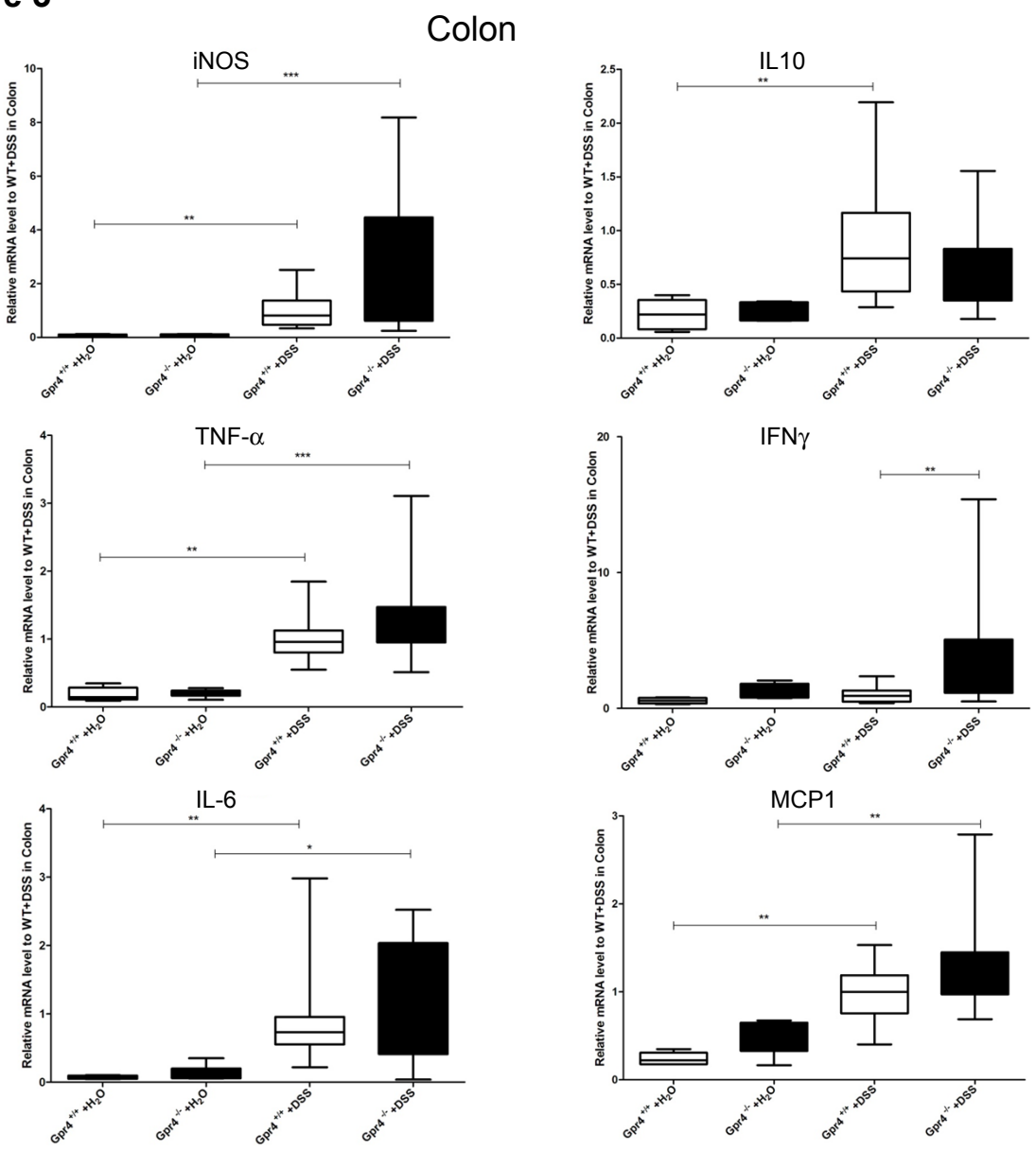
Colon
iNOS
IL10
TNF-α
IFNγ
IL-6
MCP1
Relative mRNA level to WT+DSS in Colon
Gpr4+/+ +H2O
Gpr4-/- +H2O
Gpr4+/+ +DSS
Gpr4-/- +DSS

Figure 4

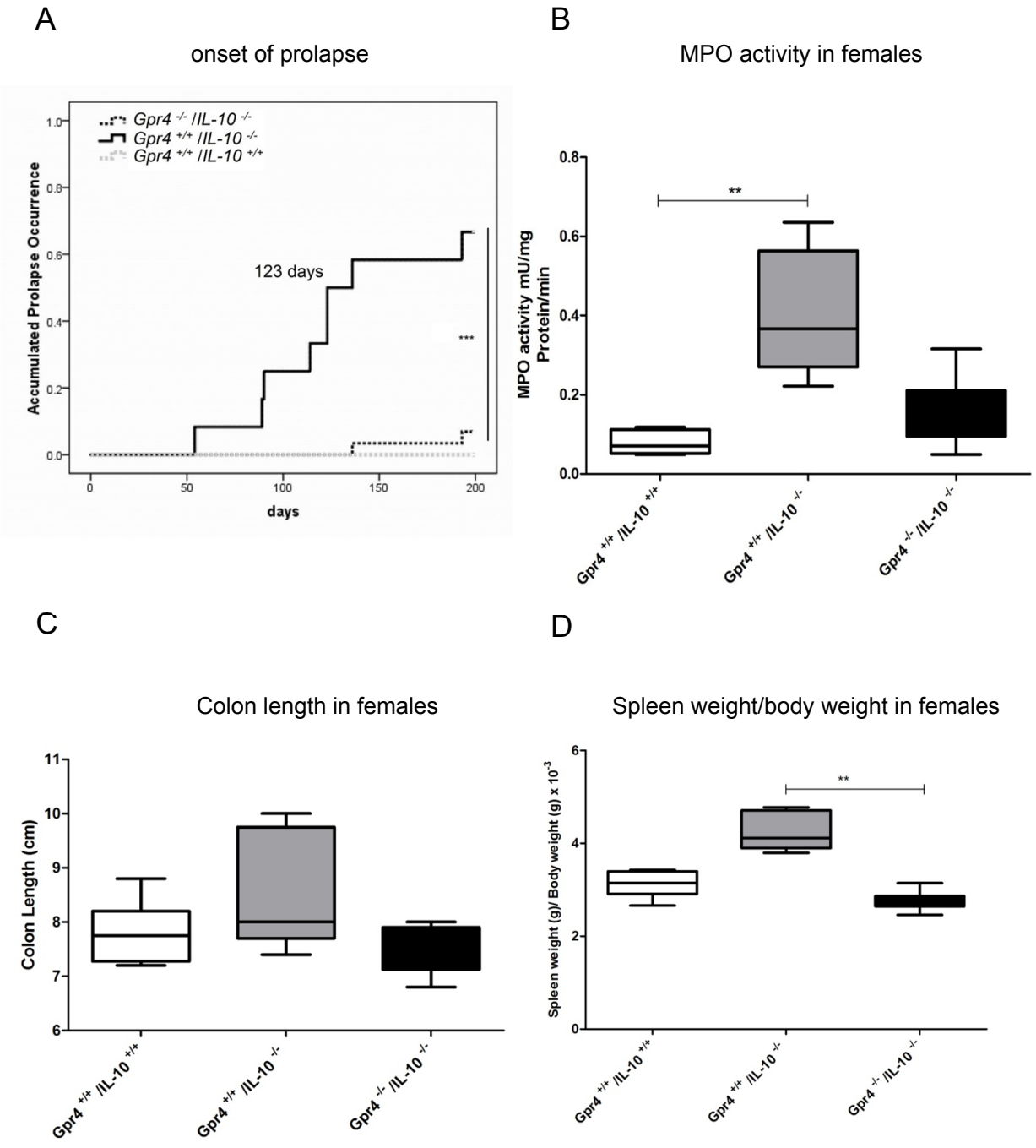
A
onset of prolapse
Gpr4 -/- /IL-10 -/-
Gpr4 +/+ /IL-10 -/-
Gpr4 +/+ /IL-10 +/+
Accumulated Prolapse Occurrence
123 days
***
days
B
MPO activity in females
MPO activity mU/mg Protein/min
**
Gpr4 +/+ /IL-10 +/+
Gpr4 +/+ /IL-10 -/-
Gpr4 -/- /IL-10 -/-
C
Colon length in females
Colon Length (cm)
Gpr4 +/+ /IL-10 +/+
Gpr4 +/+ /IL-10 -/-
Gpr4 -/- /IL-10 -/-
D
Spleen weight/body weight in females
Spleen weight (g)/ Body weight (g) x 10-3
**
Gpr4 +/+ /IL-10 +/+
Gpr4 +/+ /IL-10 -/-
Gpr4 -/- /IL-10 -/-

Figure 5

A

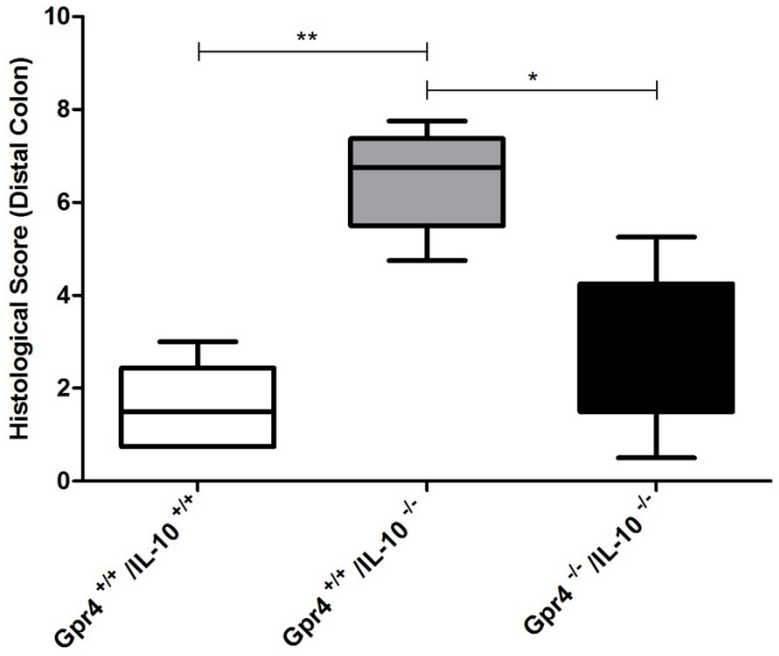

B

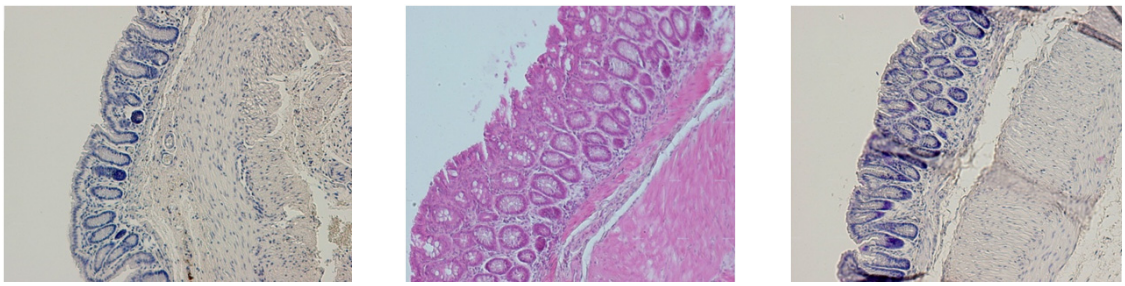

Gpr4$^{+/+}$ */IL-10*$^{+/+}$ *Gpr4*$^{+/+}$ */IL-10*$^{-/-}$ *Gpr4*$^{-/-}$ */IL-10*$^{-/-}$

Figure 6

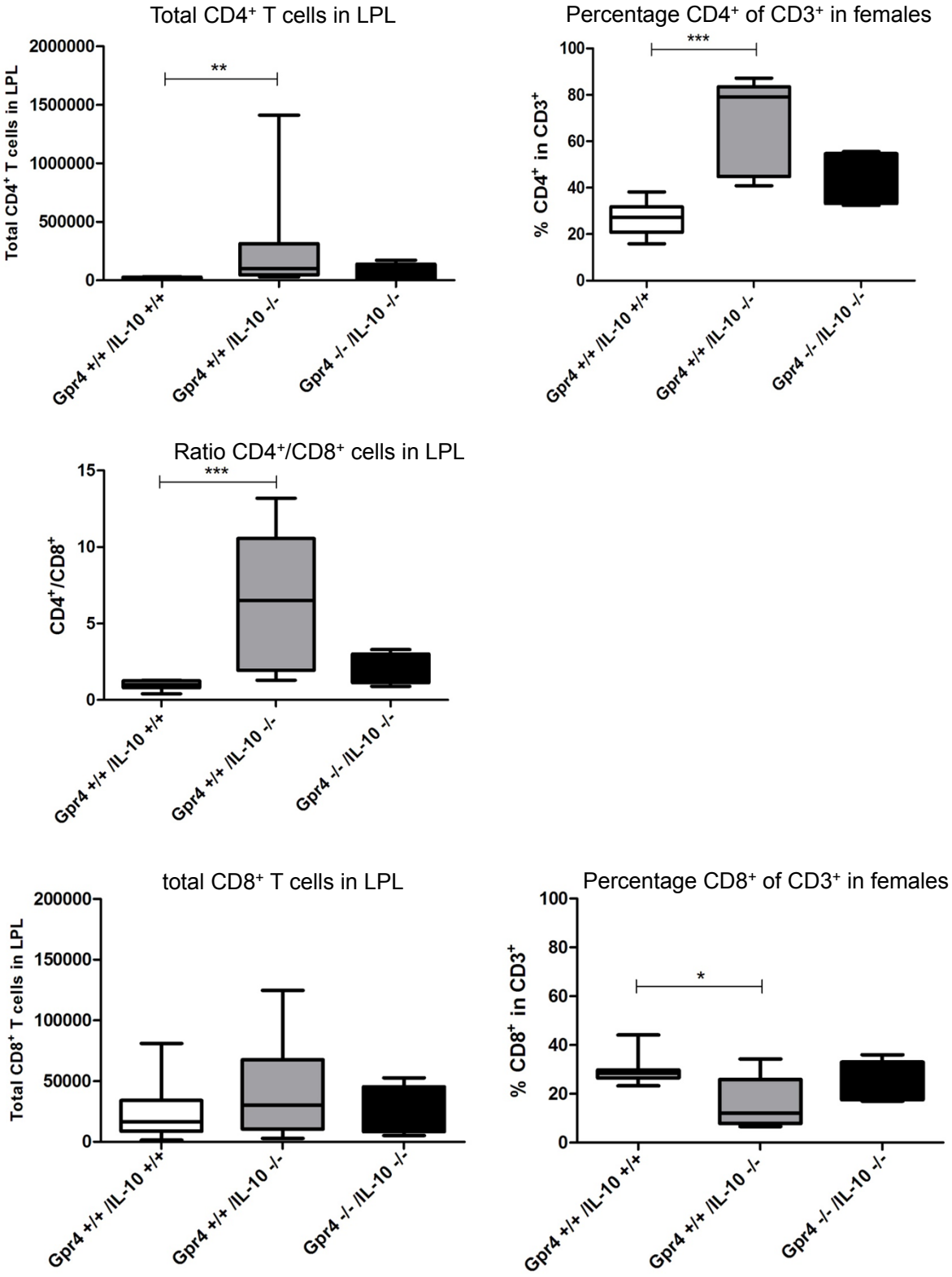
Total CD4+ T cells in LPL
Total CD4+ T cells in LPL
2000000
1500000
1000000
500000
0
**
Gpr4 +/+ /IL-10 +/+
Gpr4 +/+ /IL-10 -/-
Gpr4 -/- /IL-10 -/-
Percentage CD4+ of CD3+ in females
% CD4+ in CD3+
100
80
60
40
20
0
***
Gpr4 +/+ /IL-10 +/+
Gpr4 +/+ /IL-10 -/-
Gpr4 -/- /IL-10 -/-
Ratio CD4+/CD8+ cells in LPL
CD4+/CD8+
15
10
5
0
***
Gpr4 +/+ /IL-10 +/+
Gpr4 +/+ /IL-10 -/-
Gpr4 -/- /IL-10 -/-
total CD8+ T cells in LPL
Total CD8+ T cells in LPL
200000
150000
100000
50000
0
Gpr4 +/+ /IL-10 +/+
Gpr4 +/+ /IL-10 -/-
Gpr4 -/- /IL-10 -/-
Percentage CD8+ of CD3+ in females
% CD8+ in CD3+
100
80
60
40
20
0
*
Gpr4 +/+ /IL-10 +/+
Gpr4 +/+ /IL-10 -/-
Gpr4 -/- /IL-10 -/-

Figure 7

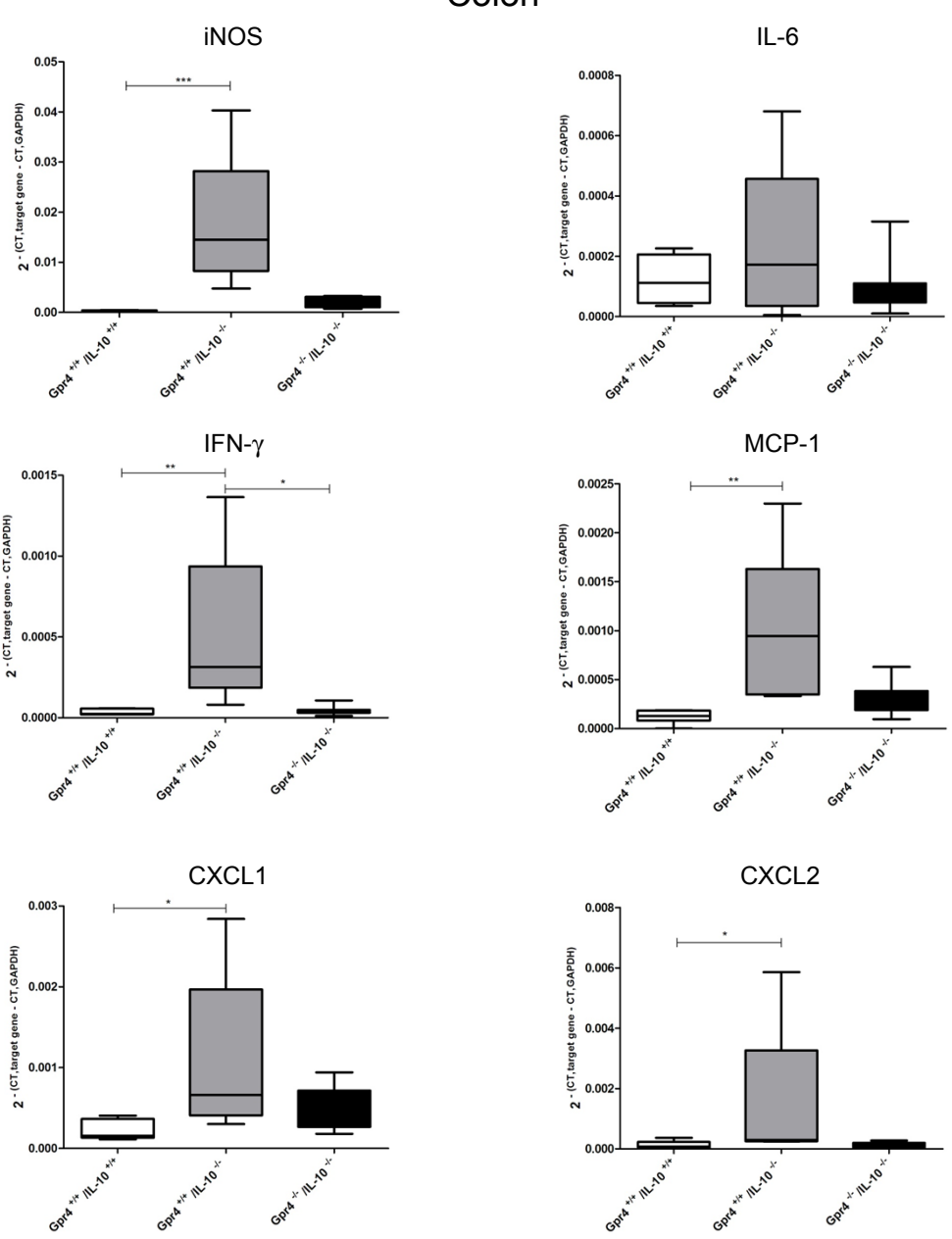
Colon
iNOS
IL-6
IFN-γ
MCP-1
CXCL1
CXCL2
2 - (CT,target gene - CT,GAPDH)
Gpr4 +/+ /IL-10 +/+
Gpr4 +/+ /IL-10 -/-
Gpr4 -/- /IL-10 -/-

The proton-activated receptor

GPR4 modulates intestinal inflammation

Yu Wang, Cheryl de Valliere, Irina Leonardi, Sven Gruber, Alexandra Gerstgrasser, Achim Weber, Katharina Leucht, Lutz Wolfram, Martin Hausmann, Carsten Krieg, Koray Thomasson, Onur Boyman, Isabelle Frey-Wagner, Gerhard Rogler, Carsten A. Wagner

SUPPLEMENTS

Supplement Table 1 List of TaqMan assay probes

Gene Symbol	Gene Name	Assay ID
GAPDH	Mouse glyceraldehyde-3-phosphate dehydrogenase	Mm03302249_g1
GPR4	Mouse G protein coupled receptor 4	Mm00558777_s1
TDAG8	Mouse TDAG8 (G protein coupled receptor 65)	Mm00433695_m1
OGR1	Mouse OGR1 (G protein coupled receptor 68)	Mm00558545_s1
iNOS	Mouse nitric oxide synthase 2	Mm01309893_m1
IL-10	Mouse Interleukin 10	Mm00439615_g1
TNF-α	Mouse tumor necrosis factor alpha	Mm99999068_m1
IFN-γ	Mouse interferon gamma	Mm00801778_m1
IL-6	Mouse Interleukin 6	Mm00446190_m1
IL-18	Mouse Interleukin 18	Mm00434225_m1
MCP-1	Mouse chemokine (C-C motif) ligand 2	Mm00441242_m1
CXCL2	Mouse chemokine (C-X-C motif) ligand 2	Mm00436450_m1
CCL20	Mouse chemokine (C-C motif) ligand 20	Mm01268754_m1
CXCL1	Mouse chemokine (C-X-C motif) ligand 1	Mm04207460_m1
SELE	Mouse selectin, endothelial cell	Mm00441278_m1
VCAM1	Mouse vascular cell adhesion molecule 1	Mm01320970_m1
COX-2	Mouse prostaglandin-endoperoxide synthase 2	Mm00478374_m1

Supplement Table 2 – FACS summary

	Gpr4 $^{+/+}$ /IL-10 $^{+/+}$	*Gpr4* $^{+/+}$ /IL-10 $^{-/-}$	*Gpr4* $^{-/-}$ /IL-10 $^{-/-}$
Total CD3$^+$ T cells in LPL	77700 ± 21030	366600 ± 168000	125700 ± 64930
CD3% in CD45$^+$	24.2 ± 3.7	29.0 ± 2.7	27.8 ± 3.0
Total CD45$^+$ T cells in LPL	311700 ± 67800	1293000 ± 545600	488200 ± 272800
CD45 % in viable single LPL	63.8 ± 8.4	83.7 ± 6.7	71.7 ± 12.2
Total Treg cells in LPL	7249 ± 1325	22140 ± 3446	16300 ± 9012
Treg % in CD4$^+$	35.9 ± 2.9	21.4 ± 2.6	24.3 ± 2.9

Supplementary Table 2

***Analysis of T Cell Subsets in Gpr4$^{+/+}$ /IL-10$^{+/+}$, Gpr4$^{+/+}$ /IL-10 $^{-/-}$* and *Gpr4 $^{-/-}$ /IL-10 $^{-/-}$* mice.**

Female mice were sacrificed at 80~110 days old and the tissues pooled from 3 mice in each group. LPLs were stained with labeled antibodies and analyzed by flow cytometry as described in methods. T cell subsets were stained with APC conjugated anti-CD45.2, FITC conjugated anti-CD3, PE conjugated anti-CD25, PB-Alexa 405 conjugated anti-CD4 and APC-Cy7 conjugated anti-CD8 and analyzed by FACS. There were no statistics significance in Total CD3$^+$ T cells in LPLs, CD3% in CD45$^+$, total CD45$^+$ T cells in LPLs , CD45 % in viable single LPLs, total Treg cells in LPLs, Treg % in CD4$^+$ between all three groups. Representative results of flow cytometric analysis of more than 5 independent experiments are shown. Data are presented as mean ± SEM.

Supplementary Figure 1

The total histology scores showed attenuated inflammation in GPR4 KO mice upon DSS colitis.

The total histology scores of distal colon for *Gpr4* $^{+/+}$ +H_2O, *Gpr4* $^{-/-}$ +H_2O, *Gpr4* $^{+/+}$ +DSS and *Gpr4* $^{-/-}$ +DSS mice are shown. The total histology scores are representative for overall histology scores of distal colon (epithelial injury plus leukocytes infiltration). Data are presented as mean ± SEM; n ≥ 5 per group; p

<0.05 *, p <0.01 **, p <0.001 ***.

Supplementary Figure 2

Assessment of the colitis severity during DSS induced chronic colitis. Colon length, colonoscopy scores, relative spleen weight, myeloperoxidase (MPO) activity and mRNA expression profiles of cytokines were assessed in *Gpr4*$^{+/+}$ and *Gpr4*$^{-/-}$ mice treated with water or DSS, respectively. Colon length **(A)** and colonoscopy scores **(B)** showed aggravated inflammation in *Gpr4* $^{-/-}$ mice upon DSS colitis. *Gpr4*$^{+/+}$ and *Gpr4* $^{-/-}$ mice showed similar relative spleen weight (spleen weight (mg) x 100 / body weight (g)) **(C)** and MPO activity in colonic tissue **(D)** upon DSS treatment. **(E)** The mRNA expression levels of iNOS, IL-10, TNF-α, lFN-γ, IL-6, IL-18 and MCP-1 in mesenteric lymph nodes from *Gpr4* $^{-/-}$ mice and *Gpr4* $^{+/+}$ mice with or without administration of DSS were not changed.. For quantification, values are mean ± SEM; n≥ 5 per group; *P* < .05 *, *P* < .01 **, *P* < .001 ***. Data are representative of 3 independent experiments.

Supplementary Figure 3

Development of IBD and progression of prolapse differ between *Gpr4* $^{-/-}$ */IL-10* $^{-/-}$ and *Gpr4* $^{+/+}$ */IL-10* $^{-/-}$ *male* mice.

(A) Kaplan-Meier prolapse-free survival curve showed delayed onset and progression of prolapse in male *Gpr4* $^{-/-}$ */IL-10* $^{-/-}$ mice relative to male *Gpr4* $^{+/+}$ */IL-10* $^{-/-}$ mice (estimated median prolapse-free survival time, >200 days vs. 161 days, ** *p*=0.007, log rank (Mantel-Cox) test). Black dotted lines, *Gpr4* $^{-/-}$ */IL-10* $^{-/-}$ mice (24.4% prolapses, n=41, male); black solid line, *Gpr4* $^{+/+}$ */IL-10* $^{-/-}$ mice (52.0% prolapses, n=25, male); grey dotted lines, *Gpr4* $^{+/+}$ */IL-10* $^{+/+}$ mice (0% prolapses, n=26, male). Comparison of MPO activity in colon tissue **(B),** colon length **(C)** and relative spleen weight **(D)** showed attenuated colitis in male *Gpr4* $^{-/-}$ */IL-10* $^{-/-}$ mice (not significant but MPO activity, *p*<0.05 *, Kruskal-Wallis one-way ANOVA followed by Dunn's multiple-comparison test).

Supplementary Figure 4

***Reduction* of histology scores in *Gpr4 $^{-/-}$ /IL-10 $^{-/-}$* male mice.**

The total histology scores of distal colon for male *Gpr4 $^{-/-}$ /IL-10 $^{-/-}$*, *Gpr4 $^{+/+}$ /IL-10 $^{-/-}$* and *Gpr4 $^{+/+}$ /IL-10 $^{+/+}$* mice at 80 days of age were shown, indicating reduced inflammation in *Gpr4 $^{-/-}$ /IL-10 $^{-/-}$* mice (p<0.05, *Gpr4 $^{-/-}$ /IL-10 $^{-/-}$* compared to *Gpr4 $^{+/+}$ /IL-10 $^{-/-}$)*. H&E staining sections (top panel) showed the significant difference in the damage of epithelial integrity and intensity of the leukocyte infiltration into inflamed sites. The total histology scores are representative for overall histology scores of distal colon (epithelial injury plus leukocytes infiltration). Data are presented as mean ± SEM; n ≥ 5 per group; p <0.05 *, p <0.01 **, p <0.001 ***.

Supplementary Figure 5

Suppression of IFN-γ-producing CD4^{+} T helper cells in *Gpr4 $^{-/-}$ /IL-10 $^{-/-}$* mice. Dot plots of the expression of CD4^{+} vs. CD8^{+} in LPLs isolated from female *Gpr4 $^{-/-}$ /IL-10 $^{-/-}$*, *Gpr4 $^{+/+}$ /IL-10 $^{-/-}$* and *Gpr4 $^{+/+}$ /IL-10 $^{+/+}$* mice are shown. LPLs were isolated and stained with anti-CD4 conjugated to PB-Alexa 405 and with anti-CD8 conjugated to APC-Cy7 and analyzed by FACS. Representative FACS results from more than 5 qualitatively similar experiments are shown; isolated LPLs from 3 female mice were pooled in each group.

Supplementary Figure 6

Analysis of mRNA expression profiles of cytokines in colon and mesenteric lymph nodes in female *Gpr4 $^{-/-}$ /IL-10 $^{-/-}$* and *Gpr4 $^{+/+}$ /IL-10 $^{-/-}$* mice . (A) The mRNA expression profiles of IL-18, SELE, CCL20, VCAM-1, and COX-2 were analyzed by semi-quantitative RT-qPCR in colon tissue from of all three female strains (*Gpr4 $^{-/-}$ /IL-10 $^{-/-}$*, *Gpr4 $^{+/+}$ /IL-10 $^{-/-}$* and *Gpr4 $^{+/+}$ /IL-10 $^{+/+}$* mice). **(B)** mRNA expression profiles of iNOS, TNF-α, IFN-γ, IL-6, CXCL1,

CXCL2, CCL20, MCP-1, VCAm-1, COX-2 in lymph nodes from same animals. (*P*< .05 *, Kruskal-Wallis one-way ANOVA followed by Dunn's multiple-comparison test). Data are presented as relative expression normalized to the house-keeping gene GAPDH, n = 6-9 mice per group. Data are presented as mean ± SEM.

Supplementary Figure 7

The mRNA expression profile of cytokines in colon (A) and mesenteric lymph nodes (B) between *Gpr4* $^{-/-}$ *IL-10* $^{-/-}$ and *Gpr4* $^{+/+}$ *IL-10* $^{-/-}$ *male* mice. iNOS, TNF-α, IFN-γ, IL-6, MCP-1, IL-18, CXCL2, CCL20, CXCL1, SELE, VCAM1 and COX-2 of all three male strains (*Gpr4* $^{-/-}$ */IL-10* $^{-/-}$, *Gpr4* $^{+/+}$ */IL-10* $^{-/-}$ and *Gpr4* $^{+/+}$ */IL-10* $^{+/+}$ mice) were determined by real time RT-PCR Taqman assay. Data represent copies of cytokine mRNA/GAPDH and mRNA amplification was representative of 6~9 mice per group. The homogenate of each mouse was tested in triplicates. Data are presented as mean ± SEM; p <0.05 *, p <0.01 **, p <0.001 ***.

Supplementary Figure 1

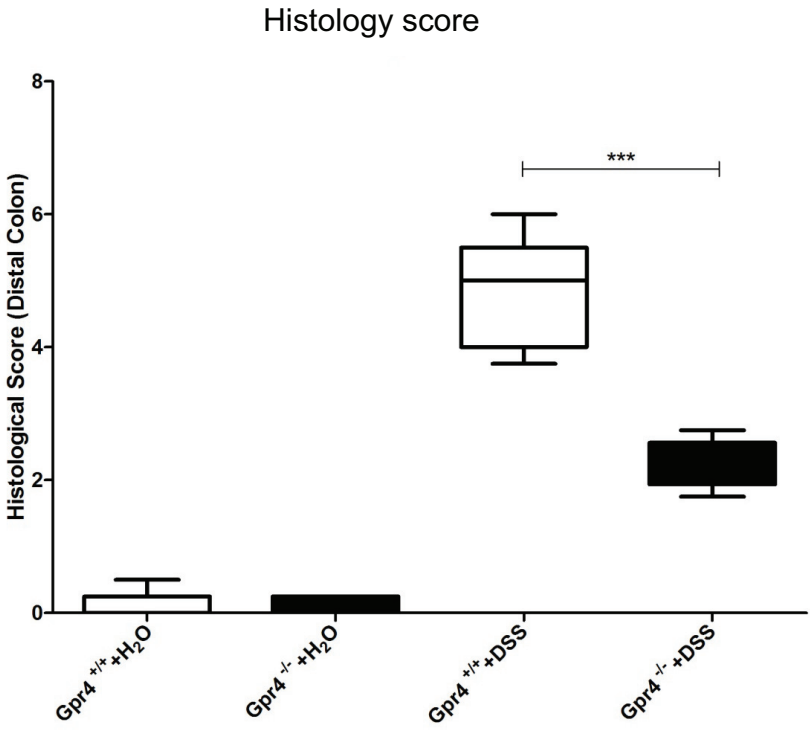

Supplementary figure 2

A

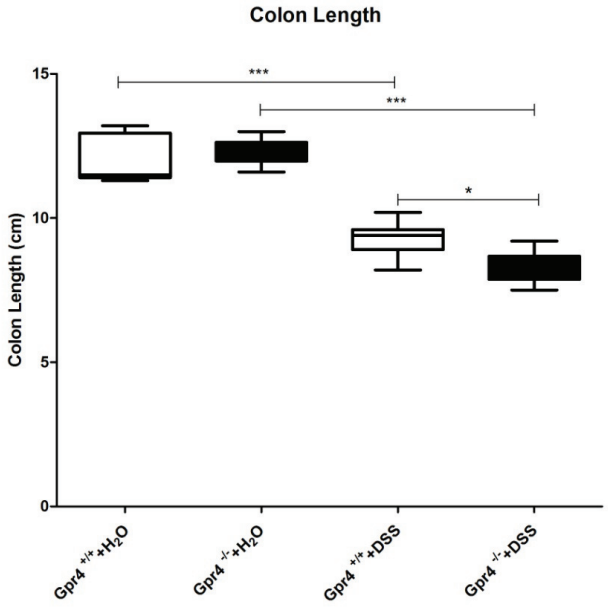

B

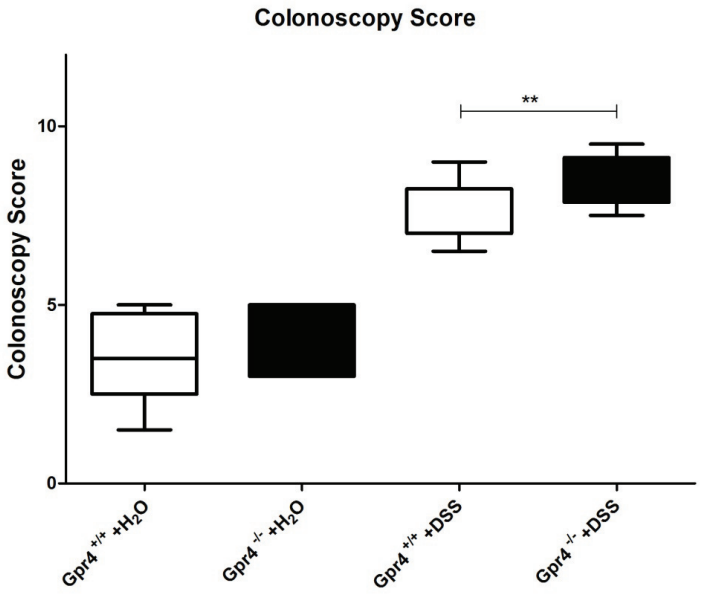

Supplementary figure 2 continued

C

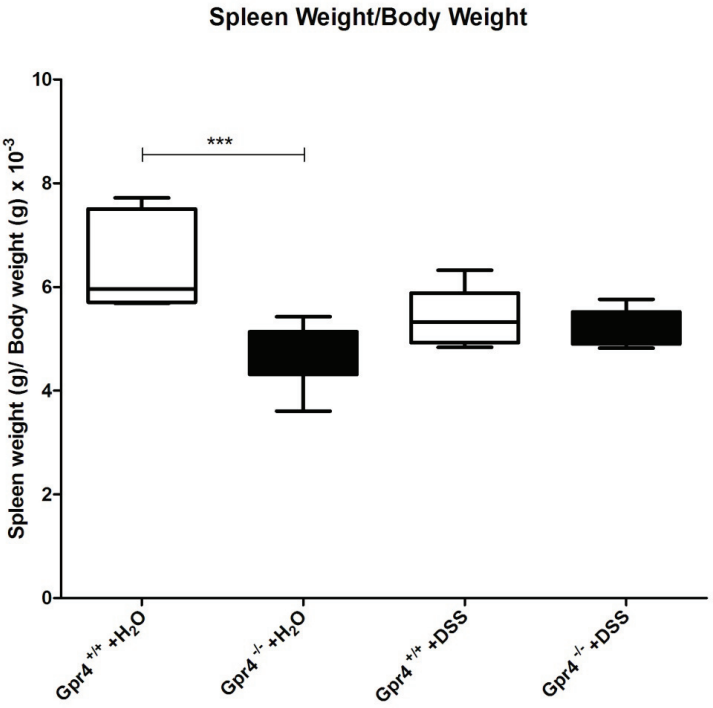

D

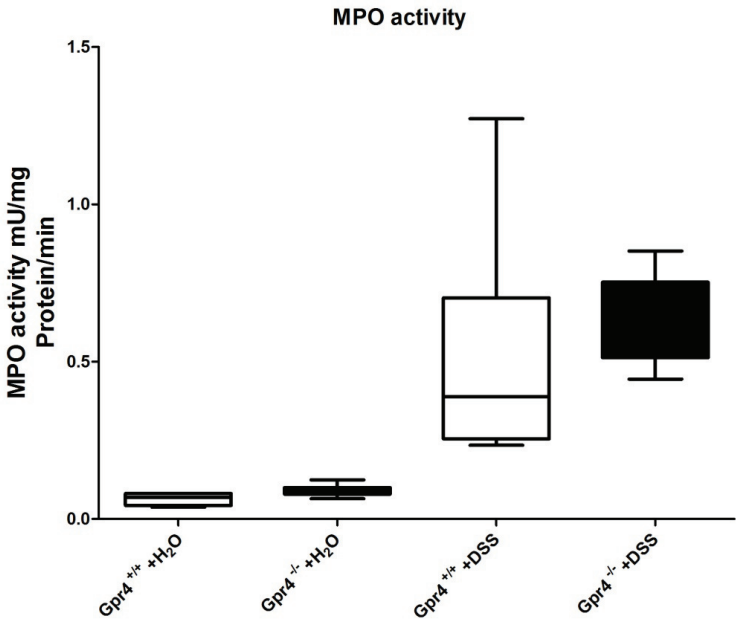

Supplementary figure 2 continued

E

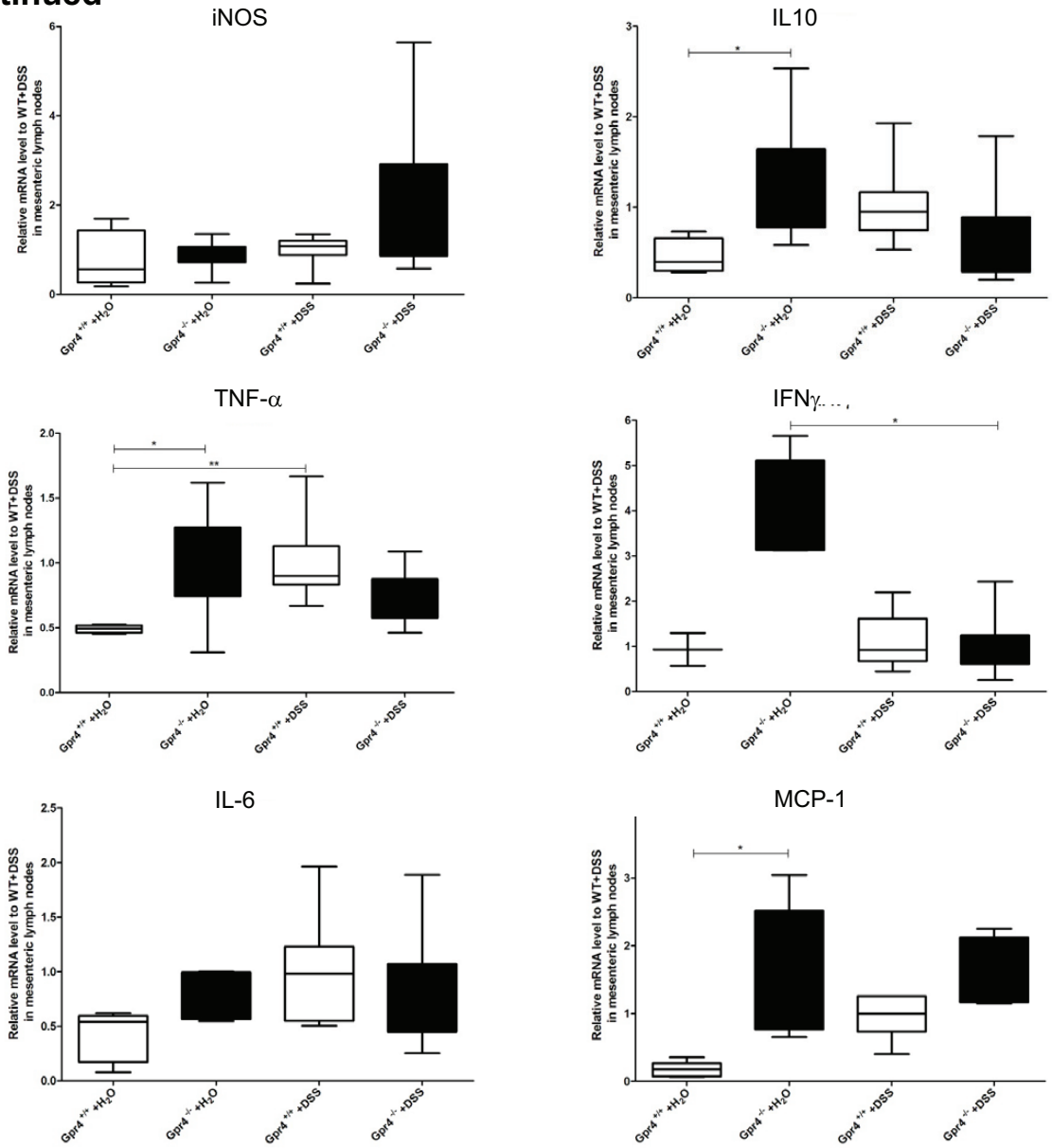

Supplementary Figure 3

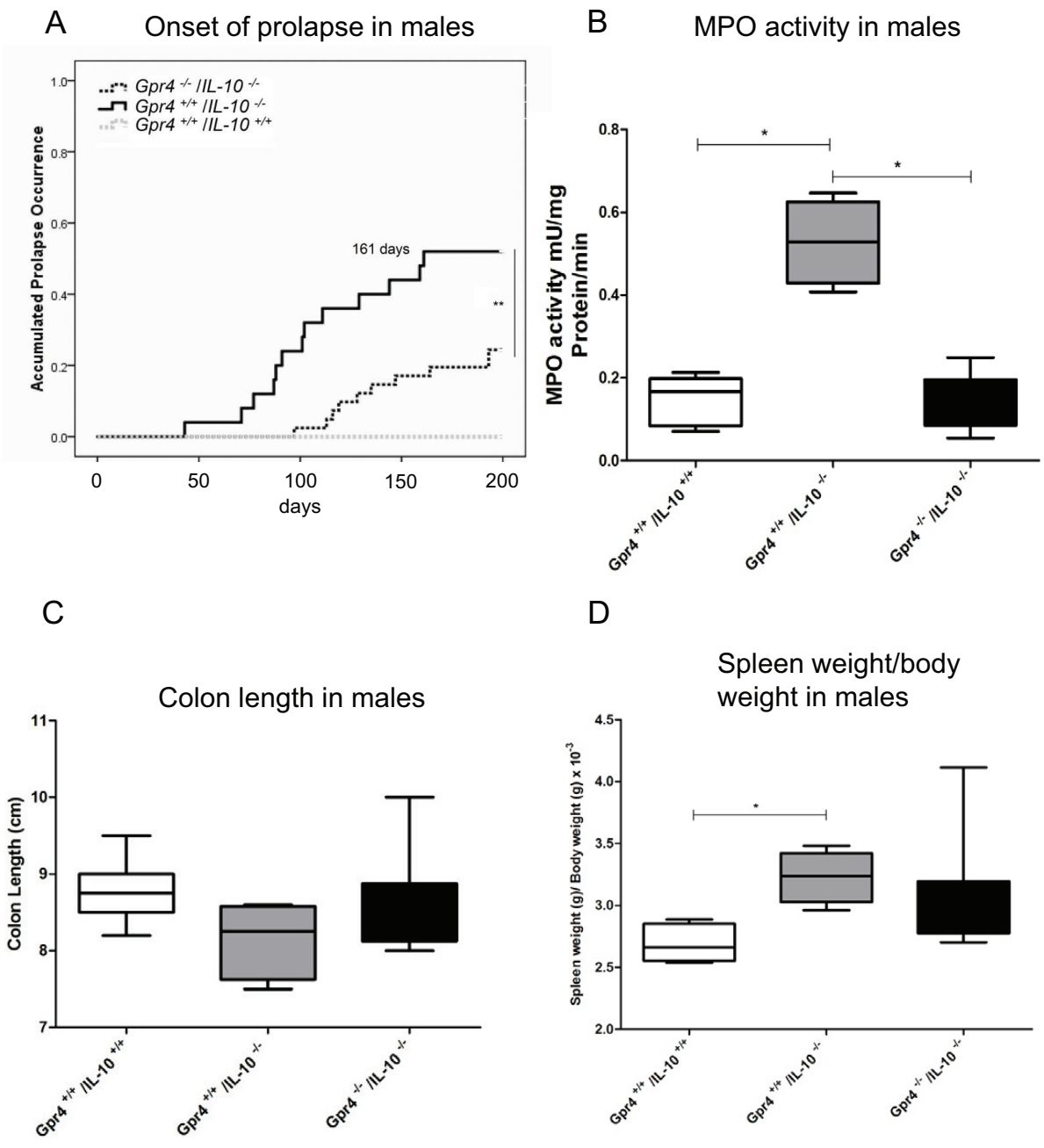

Supplementary Figure 4

A

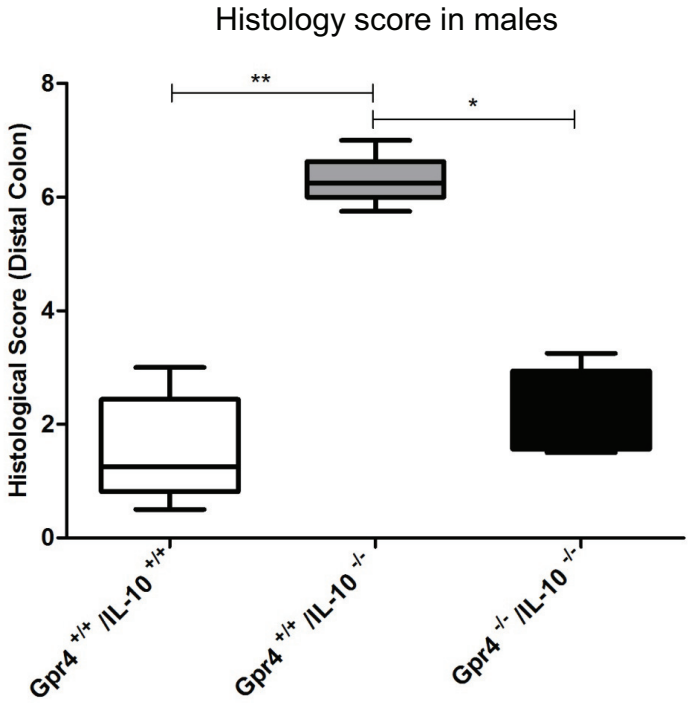

B

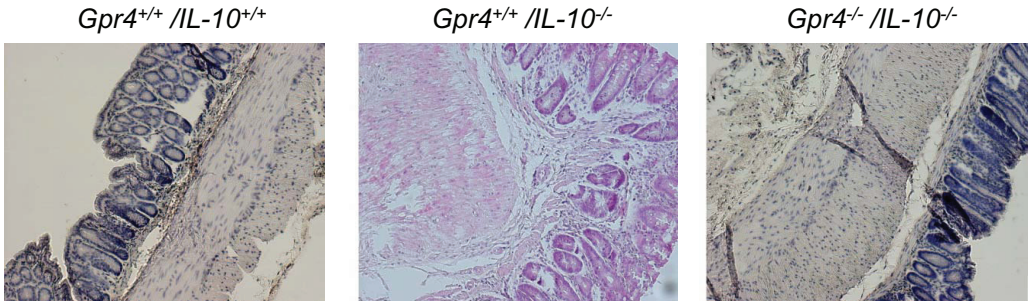

Supplementary Figure 5

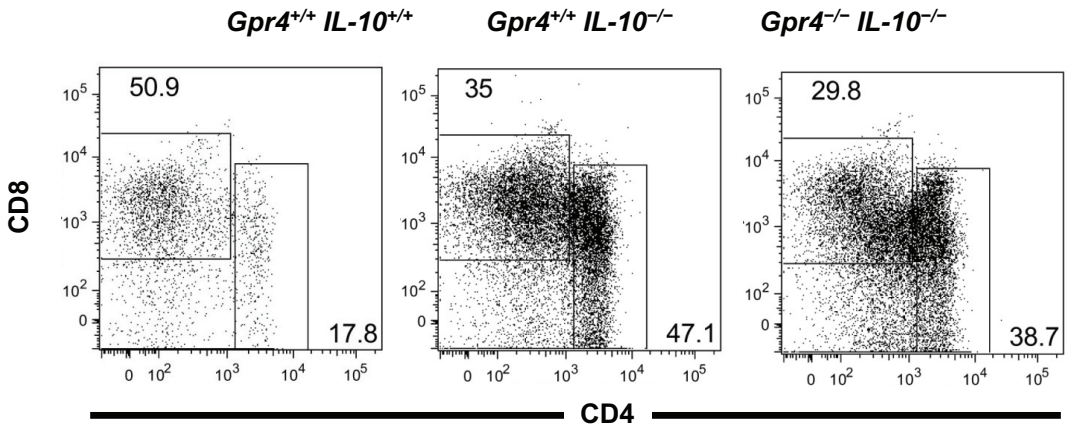

Supplementary figure 6 Colon, females

A

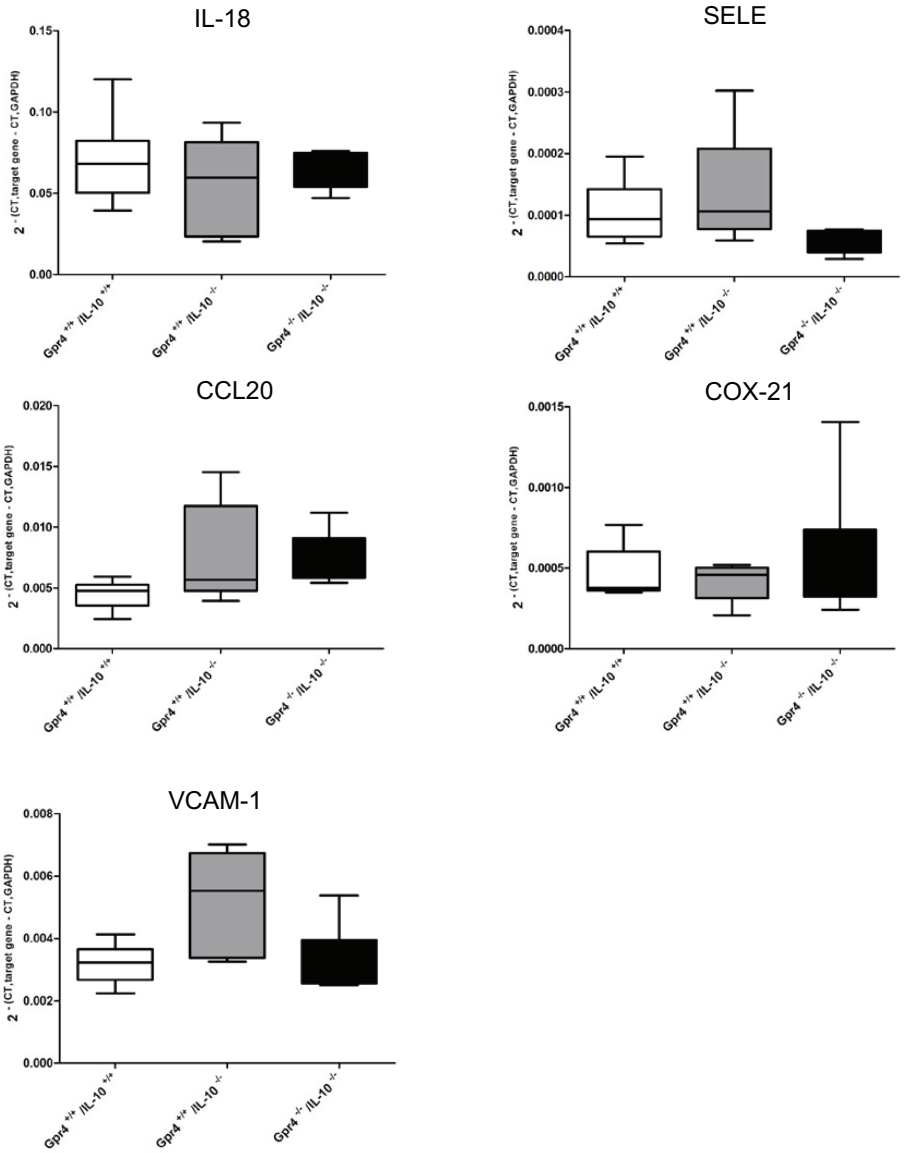

Supplementary figure 6 continued

lymph nodes, females

B

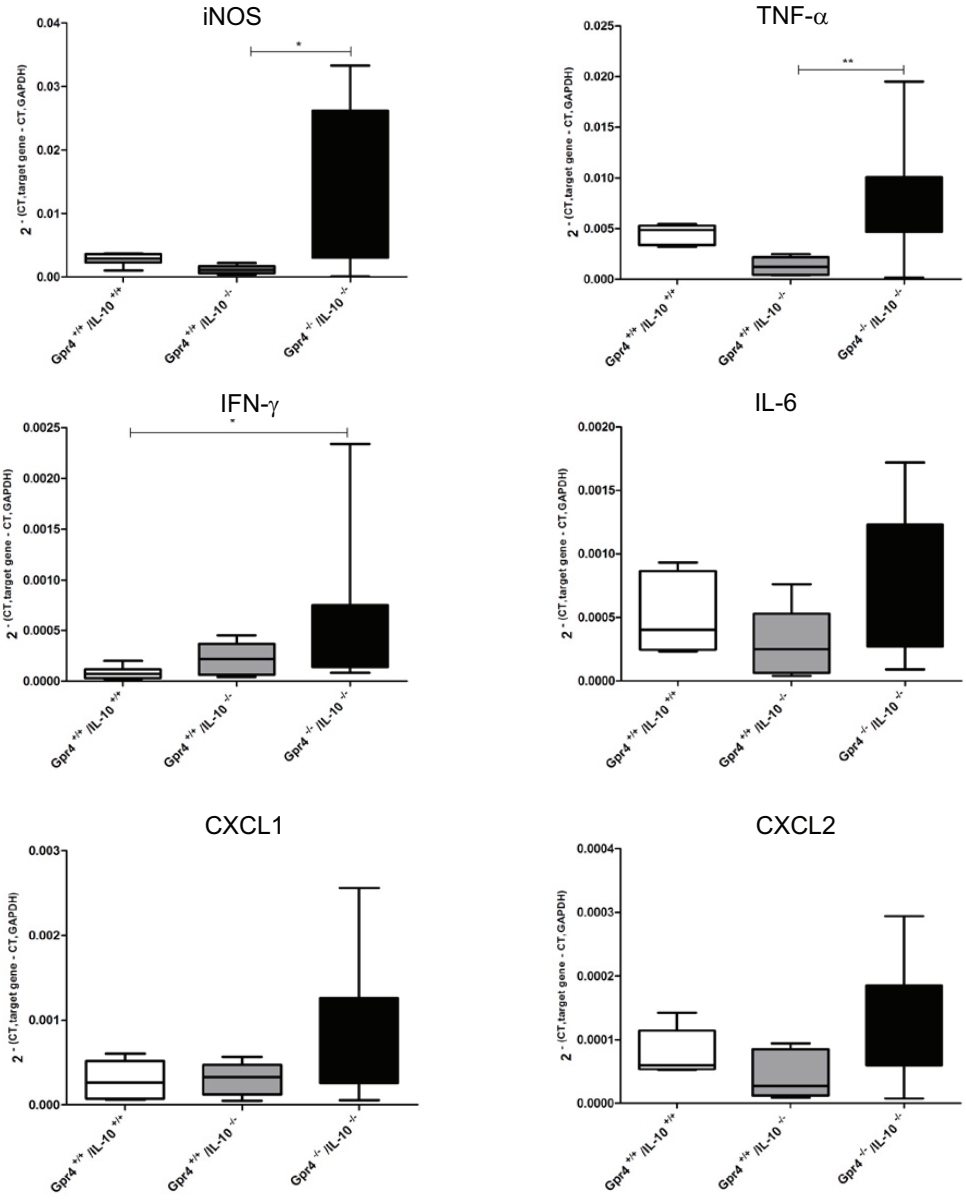

Supplementary figure 6 continued

lymph nodes, females

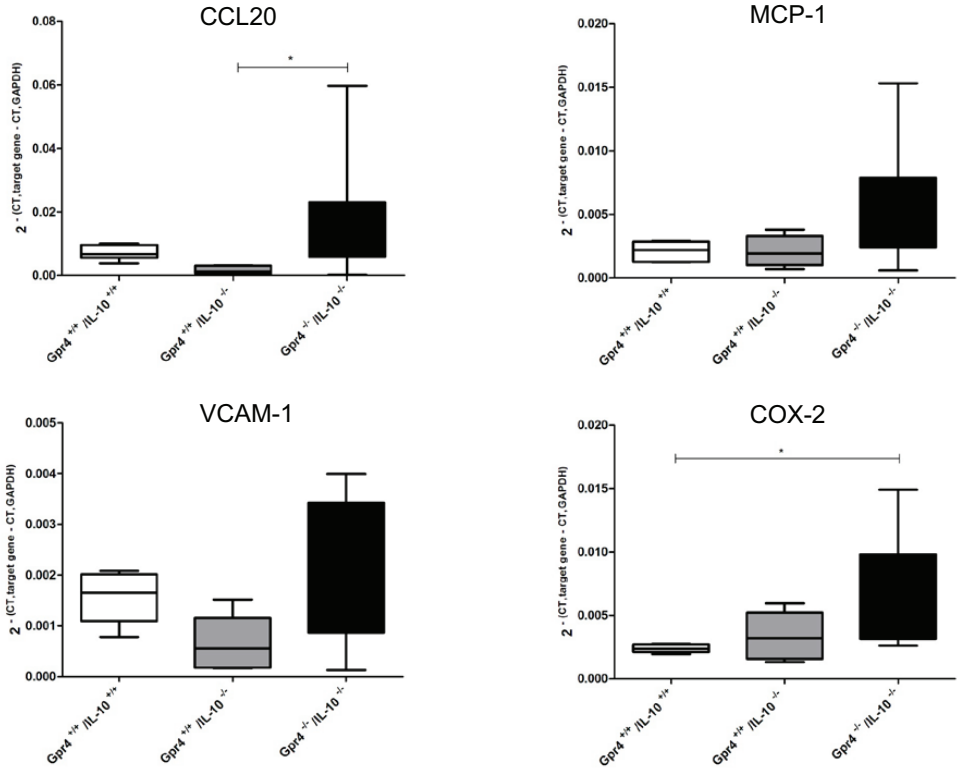

Supplementary Figure 7 Colon, males

A

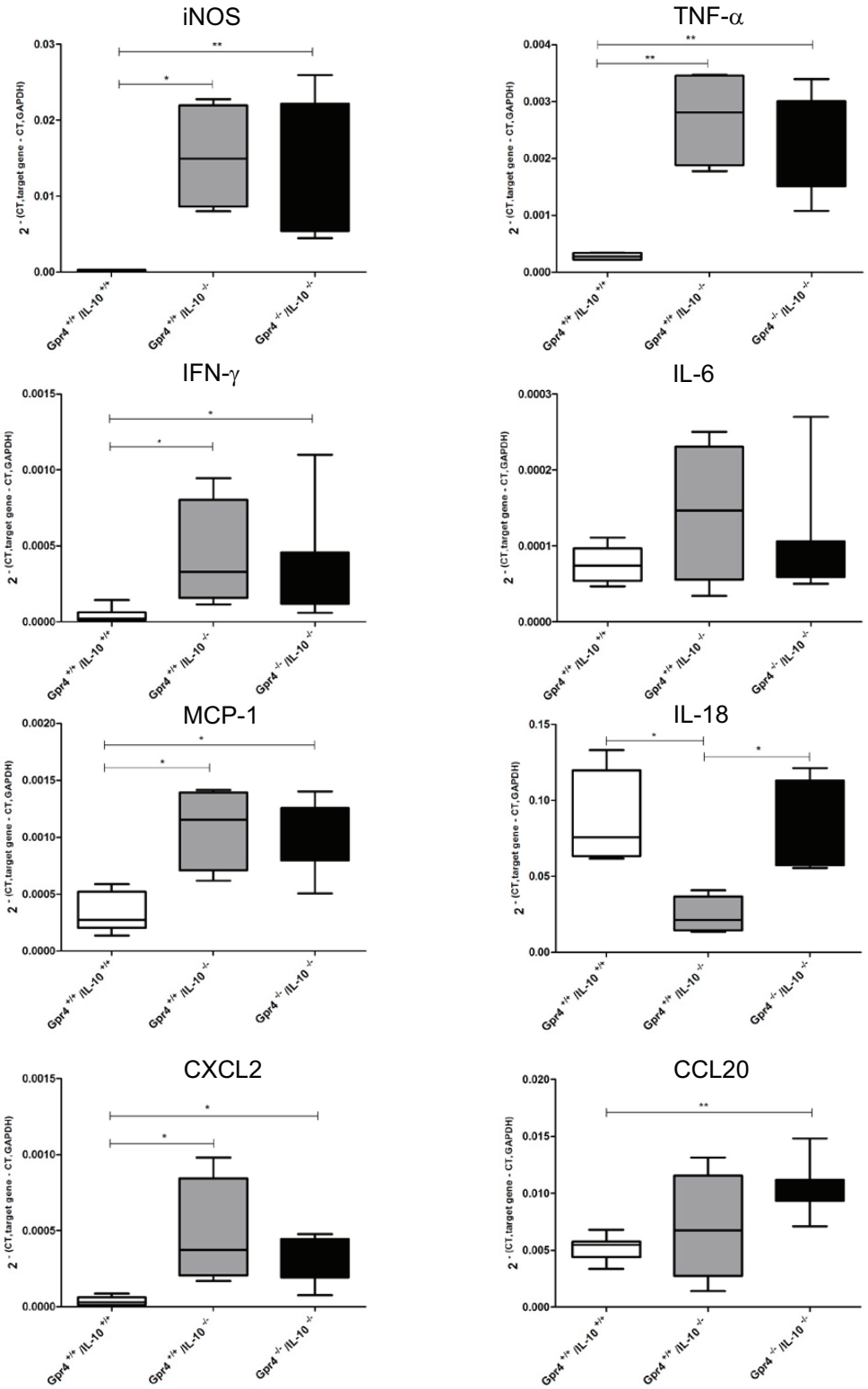

Supplementary Figure 7 continued Colon, males

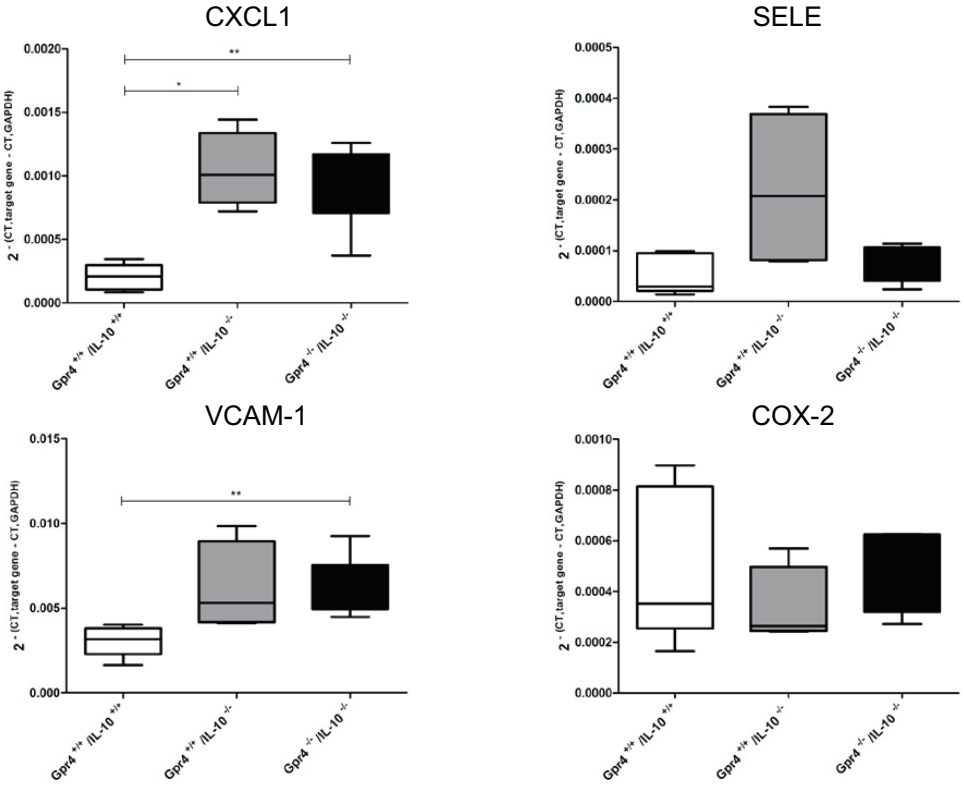

Supplementary Figure 7 continued Lymph nodes, males

B

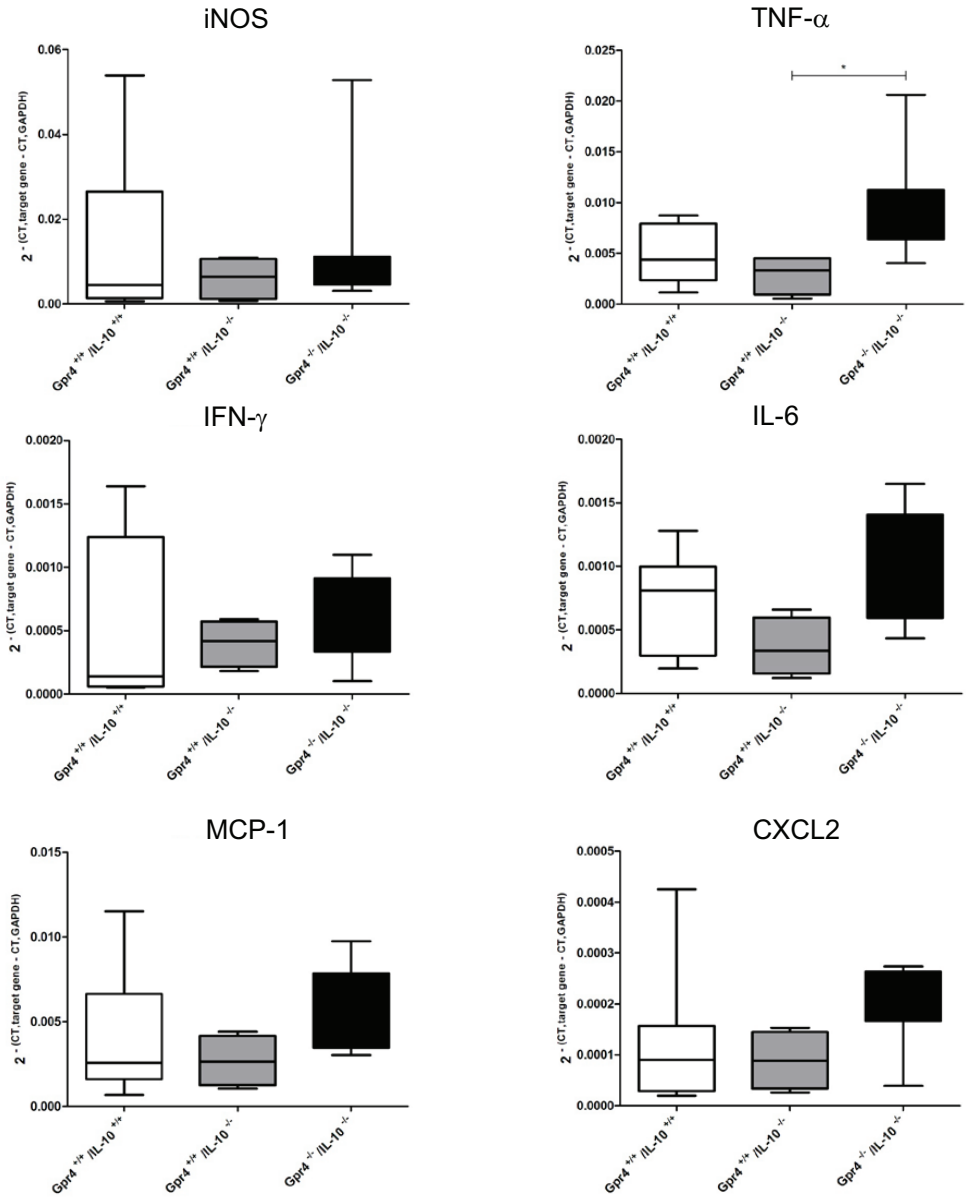

Supplementary Figure 7 continued

Lymph nodes, males

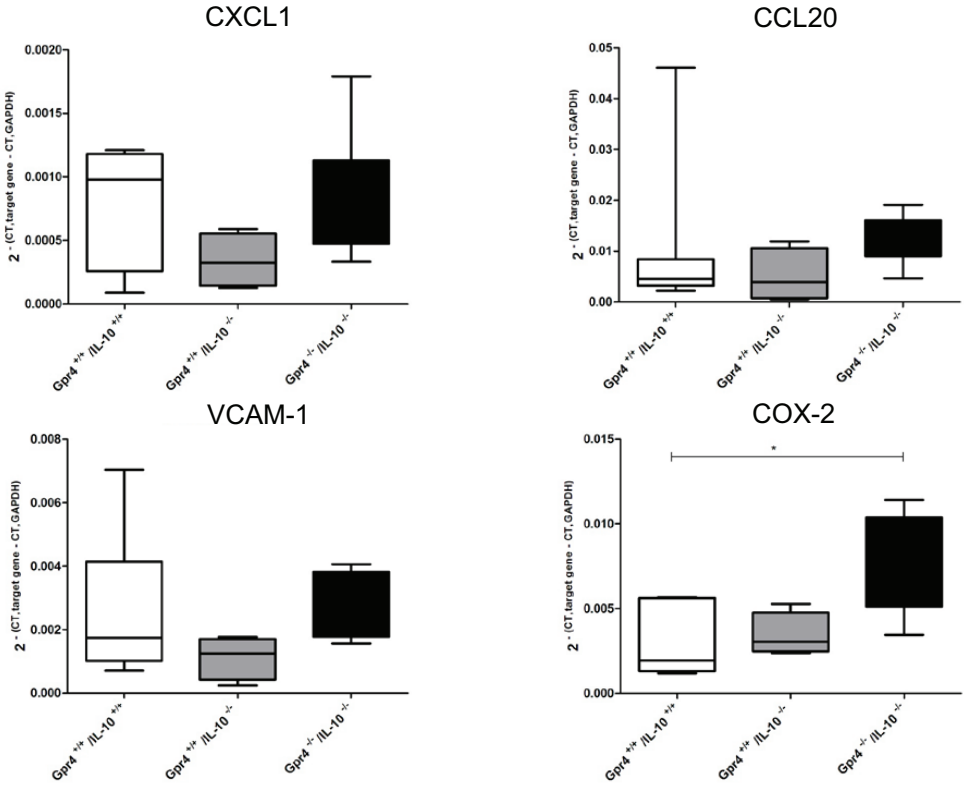

The G-protein-coupled pH-sensing OGR1 is a regulator of intestinal inflammation

Cheryl de Vallière[1*], Yu Wang[1,2*], Jyrki J. Eloranta[3] , Solange Vidal[4], Ieuan Clay[4], Marianne R. Spalinger[1], Anne Terhalle[1], Marie-Gabrielle Ludwig[4], Thomas Suply[4], Michael Fried[1], Gerd A. Kullak-Ublick[3], Isabelle Frey-Wagner[1], Michael Scharl[1], Klaus Seuwen[4], Carsten A. Wagner[2], Gerhard Rogler[1]

1 Division of Gastroenterology and Hepatology, University Hospital Zurich, Switzerland
2 Institute of Physiology, University of Zurich, Switzerland
3 Department of Clinical Pharmacology and Toxicology, University Hospital Zurich, Switzerland
4 Novartis Institutes for Biomedical Research, Basel, Switzerland

Corresponding author:

Gerhard Rogler, MD, PhD
Division of Gastroenterology and Hepatology
University Hospital Zürich
Rämistrasse 100
8091 Zürich
Switzerland
Tel. +41-(0)44-255-9477
E-mail: gerhard.rogler@usz.ch

* Cheryl de Vallière and Yu Wang contributed equally to this work.

INFLAMMATORY BOWEL DISEASES
Official Journal of the Crohn's & Colitis Foundation of America, Inc.

The G protein-coupled pH-sensing receptor OGR1 is a regulator of intestinal inflammation

Journal:	*Inflammatory Bowel Diseases*
Manuscript ID:	Draft
Wiley - Manuscript type:	Original Research Articles - Basic Science
Date Submitted by the Author:	n/a
Complete List of Authors:	de Vallière, Cheryl; University Hospital Zürich, Division of Gastroenterology and Hepatology Wang, Yu; University of Zürich, Institute of Physiology Eloranta, Jyrki; University Hospital Zurich, Department of Clinical Pharmacology and Toxicology Vidal, Solange; Novartis Institutes for Biomedical Research, Clay, Ieuan; Novartis Institutes for Biomedical Research, Spalinger, Marianne; University Hospital Zürich, Division of Gastroenterology and Hepatology Tcymbarevich, Irina; University Hospital Zürich, Division of Gastroenterology and Hepatology Terhalle, Anne; University Hospital Zürich, Division of Gastroenterology and Hepatology Ludwig, Marie-Gabrielle; Novartis Institutes for Biomedical Research, Suply, Thomas; Novartis Institutes for Biomedical Research, Fried, Michael; USZ, Gastroenterology Kullak-Ublick, Gerd; University Hospital Zurich, Department of Clinical Pharmacology and Toxicology Frey-Wagner, Isabelle; University Hospital Zürich, Division of Gastroenterology and Hepatology Scharl, Michael; University Hospital Zürich, Division of Gastroenterology and Hepatology Seuwen, Klaus; Novartis Institutes for Biomedical Research, Wagner, Carsten; University of Zürich, Institute of Physiology Rogler, Gerhard; University Hospital of Zürich, Division of Gastroenterology and Hepatology
Keywords:	Inflammation in IBD < Basic Science Areas, Animal Models of IBD < Basic Science Areas, Macrophages in IBD < Basic Science Areas, Signal Transduction Pathways < Basic Science Areas

The G protein-coupled pH-sensing receptor *OGR1* is a regulator of intestinal inflammation

Cheryl de Vallière[1*], Yu Wang[1,2*], Jyrki J. Eloranta[3], Solange Vidal[4], Ieuan Clay[4], Marianne R. Spalinger[1], Irina Tcymbarevich[1], Anne Terhalle[1], Marie-Gabrielle Ludwig[4], Thomas Suply[4], Michael Fried[1], Gerd A. Kullak-Ublick[3], Isabelle Frey-Wagner[1], Michael Scharl[1], Klaus Seuwen[4], Carsten A. Wagner[2], Gerhard Rogler[1]

[1]Division of Gastroenterology and Hepatology, University Hospital Zürich, Switzerland

[2]Institute of Physiology, University of Zürich, Switzerland

[3]Department of Clinical Pharmacology and Toxicology, University Hospital Zürich, Switzerland

[4]Novartis Institutes for Biomedical Research, Basel, Switzerland

Corresponding author:

Gerhard Rogler, MD, PhD
Division of Gastroenterology and Hepatology
University Hospital Zürich
Rämistrasse 100
8091 Zürich
Switzerland
Tel. +41-(0)44-255-9477
E-mail: gerhard.rogler@usz.ch

* Cheryl de Vallière and Yu Wang contributed equally to this work.

Abstract

Objective: A novel family of proton sensing G-protein coupled receptors (GPCRs), including *OGR1*, *GPR4*, and *TDAG8* was identified to be important for physiological pH homeostasis and inflammation. Thus we determined the function of proton-sensing OGR1 in the intestinal mucosa.

Design: *OGR1* expression in colonic tissues was investigated in controls and IBD patients. Expression of *OGR1* upon cell activation was studied in the Mono Mac 6 (MM6) cell line and primary human and murine monocytes by real-time PCR. *Ogr1* knockout mice were crossbred with *Il-10* deficient mice and studied over 200 days. Microarray profiling was performed using $Ogr1^{-/-}$ and $Ogr1^{+/+}$ (WT) residential peritoneal macrophages.

Results: IBD patients expressed higher levels of *OGR1* in the mucosa than non-IBD controls. Treatment of MM6 cells with TNF, led to significant up-regulation of *OGR1* expression, which could be reversed by the presence of NF-κB inhibitors. Kaplan-Meier survival analysis showed a significantly delayed onset and progression of rectal prolapse in female $Ogr1^{-/-}$// $Il\text{-}10^{-/-}$ mice. These mice displayed significantly less rectal prolapses. Up-regulation of gene expression, mediated by OGR1, in response to extracellular acidification in mouse macrophages was enriched for inflammation and immune response, actin cytoskeleton, and cell adhesion gene pathways.

Conclusion: *OGR1* expression is induced in cells of human macrophage lineage and primary human monocytes by TNF. NF-κB inhibition reverses the induction of *OGR1* expression by TNF. *OGR1* deficiency protects from spontaneous inflammation in the *Il-10* KO model. Our

data indicate a pathophysiological role for pH-sensing receptor *OGR1* during the pathogenesis of mucosal inflammation.

Word count 249

Key Words: GPCR; pH-sensing receptors; *OGR1*; IBD; microarrays; animal model

Abbreviations: CD, Crohn's disease; DSS, dextran sulphate sodium; GAPDH, glyceraldehyde-3-phosphate dehydrogenase; GPCR, G protein coupled receptor; *GPR4*, G protein coupled receptor 4; GPR65, G protein coupled receptor 65; GPR68, G protein coupled receptor 68; H&E, hematoxylin and eosin; HPRT, Hypoxanthine-guanine phosphoribosyltransferase; IBD, inflammatory bowel disease; IFN-γ, interferon gamma; IL, interleukin; MPO, myeloperoxidase; OGR1, ovarian cancer G-protein coupled receptor 1; OR, odds ratio; PBS, phosphate buffered saline; RT-PCR, reverse transcription polymerase chain reaction; *TDAG8,* T-cell death associated gene 8; TNF, tumour necrosis factor; UC, Ulcerative colitis

Grants

This work was supported by a collaborative grant from the Zürich Center for Integrative Human Physiology (ZIHP) to CW and GR, research grants from the Swiss National Science Foundation to GR (Grant No.314730-153380) and the Swiss IBD Cohort (Grant No 3347CO-108792). The funding institutions had no role in the study design, in the collection, analysis and interpretation of data and in the writing of the manuscript.

Competing interests:

The authors declare no competing interests.

Author contributions:

CdV performed experiments, analyzed the data and wrote the first draft of the manuscript; YW, SV, IC, MRS, IT, AT, M-GL, TS, performed experiments and were involved in data analysis, MF, GAK-U, IF-W, MS, JJE, KS, CAW, GR conceived, designed and supervised the study and respective experiments. All authors wrote, corrected and approved the manuscript.

INTRODUCTION

The mechanisms involved in the maintenance of mucosal homeostasis are important in our understanding of the pathophysiology of inflammatory bowel disease (IBD). Both forms of the disease, Crohn's disease (CD) and ulcerative colitis (UC), give rise to inflammation that is associated with extracellular acidification of mucosal tissue. Mucosal inflammation is interpreted as a local response to tissue damage and microbial invasion.

A number of studies suggest that an acidic environment affects the progression and resolution of inflammation.[1-3] Inflammation has been attributed to an increase in local proton concentration and lactate production[4] and subsequent pro-inflammatory cytokine production, such as tumour necrosis factor (TNF), interleukin-6 (IL-6), interferon-gamma (IFN-γ) and interleukin-1-beta (IL-1β). TNF is one of the characterizing cytokines in IBD[5, 6] and anti-TNF targeted therapies are successful in both CD and UC.[7-10] Activated macrophages, which are key cellular mediators of acute and chronic inflammation, are primary producers of TNF[11]. TNF activates the nuclear transcription factor kappa B (NF-κB), one of the key regulators in chronic mucosal inflammation.[12, 13]

G-protein-coupled receptors (GPCRs), cell-surface molecules involved in signal transduction, are targeted by key inflammatory cytokines.[14] The ovarian cancer G-protein coupled receptor 1 (*OGR1)* family of receptors, which include *OGR1*, G protein coupled receptor 4 *(GPR4)*, and T-cell death associated gene *(TDAG8)*, sense extracellular protons through histidine residues located on the extracellular region of the receptors, resulting in the modification of a variety of cell functions.[15, 16] Early signaling pathways of pH-sensing receptors triggered by acidification include phospholipase C activation, inositol trisphosphate formation and subsequent Ca^{2+} release[15] or cyclic adenosine monophosphate

(cAMP) production.[17, 18] The increase of intracellular calcium influx and accumulation of cAMP has been shown to regulate a vast range of cellular responses. Moreover, *OGR1* and *TDAG8* are alleged to act in opposition in a regulatory manner, either enhancing or inhibiting the production of proinflammatory cytokines respectively.[19]

TDAG8 mediated extracellular acidification inhibited lipopolysaccharide (LPS)-induced production of TNF and IL-6 in mouse peritoneal inflammatory macrophages.[2] Patients with CD demonstrate a defect in macrophage function resulting in an inadequate bacterial clearance from inflammatory sites.[20] In addition, macrophages from CD patients showed impaired TNF-alpha secretion in response to bacterial challenge.[21] Furthermore, association results and *in silico* analysis have recently identified a locus within the *TDAG8* gene as one of the susceptibility loci associated with CD.[22] Onozawa *et al*. suggest that *TDAG8* is a negative regulator of inflammation[23], which is mediated via a G_s-coupled mechanism.[2] In contrast, *OGR1* is reported to act predominately via a G_q-coupled mechanism to stimulate proinflammatory cytokines production upon extracellular acidification.[19]

To date, few data on the role of *OGR1* in inflammation in IBD have been published. *OGR1* may play an important role in the regulation of the inflammatory pathways in IBD, and it may represent an interesting target for innovative therapies. Therefore, we investigated the role and function of *OGR1* in gut inflammation, with a focus on myeloid cells. We used an immune-mediated inflammatory disease mouse model, namely interleukin-10 (*Il-10*) knockout (KO) mice, which spontaneously develop chronic colitis[24-26] and a human monocyte model. We show that *OGR1* expression is induced in monocytes by TNF and *OGR1* deficiency protects from spontaneous inflammation in the *Il-10* KO model.

Materials and Methods

Details of reagents used and methods for gene expression are provided in the Supplementary Materials and Methods section.

pH experiments

pH shift experiments were carried out in serum-free RPMI medium (1-41F24-I, Amimed), supplemented with 2 mM Glutamax (35050-038, Gibco), and 20 mM HEPES. The pH of all solutions was adjusted using a calibrated pH meter (Metrohm, Herisau, Switzerland) with NaOH or HCl, and the medium was equilibrated in a 5% CO_2 incubator for 36 h. All data presented are referenced to pH measured at room temperature.

Culture of cell lines

The monocytic cell line MonoMac 6 (MM6, obtained from DMSZ) was cultured in RPMI (Sigma-Aldrich, Munich, Germany) supplemented with 10% FCS, 1% nonessential amino acids, and 1% oxalacetic acid–pyruvate–insulin medium supplement (Sigma-Aldrich), and maintained according to the American Type Culture Collection (ATCC).

Patient tissue samples

Primary intact colonic epithelial cell crypts were isolated from normal human colonic tissue of patients undergoing bowel surgery as previously described.[27] Biopsies of human terminal ileum, colon, or rectum were taken from patients with CD or UC, or from control subjects undergoing colonoscopy for colon cancer screening. Biopsies from patients with colitis were taken endoscopically from inflamed areas. Written consent was obtained before specimen collection and studies were approved by the local ethics committee.

Isolation of human peripheral blood monocytes

Normal human peripheral blood monocytes, obtained from the Swiss Red Cross Blood Service, were isolated from buffy coat samples, by density gradient centrifugation using Lymphoprep (Axis-Shield, Norway). Purification was performed using EasySep™ Human Monocyte Enrichment Kit without CD16 Depletion and EasySep magnet (both from Stemcell, Canada) according to manufacturer's instructions. The purity of the monocytes was > 85% as assessed by fluoroscein isothiocyanate (FITC)-labelled anti-CD14 (#557742, BD Biosciences, USA) by flow cytometry (data not shown).

Animal models

All animal experiments were performed according to Swiss animal welfare laws and were approved by the Veterinary Authority of Basel-Stadt and the Veterinary Office of the Canton Zürich, Switzerland. *Ogr1*$^{-/-}$ (C57BL/6) mice, initially obtained from Deltagen, Inc. - San Mateo, Ca, USA, were generated as described.[28] *Il-10* $^{-/-}$ mice (C57BL/6) mice and *Ogr1*$^{-/-}$ mice were crossed to generate *Ogr1* $^{-/-}$ */Il-10* $^{-/-}$ colitis susceptible mice. Mice were observed until reaching either 200 days of age or suffering a prolapse. All mice were housed together in one room in a vivarium.

Genomic DNA extraction and genotyping

Genotyping was confirmed by PCR of tail genomic DNA. DNA extraction was performed according to standard NaOH methods. The PCR reactions used for *Ogr1* genotyping were performed as previously described[28], oligonucleotides used are listed in the supplementary material and methods.

Murine macrophage isolation and culture

Mature quiescent macrophages were isolated from the mouse peritoneal cavity without the aid of eliciting agents, as described by Zhang *et al.*[29] Animals were sacrificed by cervical dislocation to reduce influence on pH. Further details are described in the supplementary methods.

Evaluation of inflammation in murine colitis

Typical inflammatory parameters were evaluated as previously described.[30, 31]

Expression Profiling by Microarrays

Global whole-transcript analysis was performed using a GeneAtlas microarray system (Affymetrix) to compare response differences between *Ogr*1$^{+/+}$ and *Ogr*1$^{-/-}$ murine macrophages after 24 h acidic pH shift. Mature murine quiescent peritoneal macrophages were isolated as described above, from age matched female *Ogr*1 $^{-/-}$ and *Ogr*1 $^{+/+}$ mice (C57BL/6). Five replicates or mice per condition were used, and ≈ 1 x 10^6 macrophages/per mouse obtained. Cells were not pooled. Cells were treated with pH 6.7 equilibrated medium to activate *Ogr1,* and pH 7.7 to serve as negative controls. Cells were collected, and RNA and cDNA samples prepared. Biotin-labelled cDNA samples were hybridized to GeneChip Mouse Gene 1.1ST Array Strip (Affymetrix, P/N 901628) following protocols provided by Affymetrix. Data was summarized on gene-level using RMA (Robust Multi-array Average). Data quality was assessed using the bioconductor/R package 'arrayQualityMetrics'[32] and reproducibility was assessed using Pearson's correlation for all the filtered expression values and hierarchical clustering. For all pairwise comparisons, differentially expressed genes were selected using ≥2.0-fold-change, P<0.05 significance, as determined using ANOVA (as implemented by the R package, Linear Models for Microarray Data, 'limma') and F-test for

the complete experimental design. The results were analyzed by global ranked fold change and using Metacore software for pathway enrichment.

Statistical Analysis

For murine prolapse ratio comparison studies, statistical differences between genotypes were calculated by chi-square test with Fisher's exact test (exact significance, two sided) and risk estimate test from contingency tables. The prolapse survival analysis was performed using Kaplan-Meier survival analysis (log rank Mantel-Cox test) and estimated median survival time. Groups of data were compared using nonparametric Mann-Whitney U-test (mouse data) or Kruskal-Wallis one-way ANOVA followed by Dunn's multiple-comparison test (patient data). Data are presented as mean ± SEM for a series of n experiments. Probabilities (p, two tailed) of $p < 0.05$ were considered statistically significant. Monocyte/macrophage expression data were analyzed using a one-way analysis of variance (ANOVA) followed by the Tukey Post Hoc test. Throughout this manuscript, asterisks denote significant differences at *=p<0.05, **=p<0.01, ***=p<0.001.

RESULTS

OGR1 mRNA expression is increased in IBD patients

OGR1 mRNA expression in isolated crypts and terminal ileum, colon, or rectum specimens from IBD patients and control subjects was confirmed by RT-qPCR. Ct values from the isolated crypts from 4 patients ranged from 27 to 30, indicating moderate expression of *OGR1* in colonic epithelium (data not shown). Compared with normal control subjects, *OGR1* expression increased 2.3 -fold ($p<0.05$) in UC patients (n=8) and 2.2 -fold ($p<0.01$) in CD patients (n=29) (Figure 1).

OGR1 expression is regulated by TNF in myeloid cells

A local decrease in pH usually occurs at inflammatory sites, and monocytes are rapidly recruited, followed by an increase in pro-inflammatory cytokines. MM6 cells were treated with IFN-γ, IL-1β, IL-6, TNF or TGF-β, which are known to initiate immune and inflammatory responses in the mucosa. Stimulation by TNF resulted in significant up-regulation of *OGR1* expression (≈4-5-fold $p<0.001$, Figure 2A-B). No induction of *OGR1* occurred by IFN-γ, IL-1β, IL-6 or TGF-β at 6 h (Figure 2A-B) or at 1 h, 5 h or 24 h (data not shown). A concentration-dependent (0, 2.5, 10, 25, 50, 100 ng/ml) induction of *OGR1* mRNA expression in MM6 cells by TNF was confirmed at 4 and 8 h (Figure 2C). Maximal OGR1 induction, after 8 h treatment was reached at TNF concentration 50 ng/ml (Figure 2C). Induction of *OGR1* expression in MM6 cells by TNF returned to basal levels after 48 h (Figure 2D).

Treatment of MM6 cells with PMA, a known PKC activator but also commonly used to differentiate monocytes into macrophage-like cells[33], led to increased *OGR1* expression (14

-fold at 24 h, p< 0.001) (Figure 2E).

To confirm the relevance of our findings in MM6 cells, we tested OGR1 -induction by TNF and PMA in primary human monocytes and mouse peritoneal macrophages. Concentration-dependent TNF and PMA induction of *OGR1* mRNA was confirmed in human monocytes (Figure 3A-B). Similarly TNF -mediated OGR1 induction was observed in mouse macrophages (Figure 4). The intensity of the response to TNF was comparable in MM6 cells and primary mouse macrophages (Figure 2C-D MM6; Figure 4). The induction time of primary human monocytes was considerably slower but of similar intensity. Similarly, primary human monocytes exhibited a slower induction and lower response to PMA compared to MM6 cells. No induction of the other pH-sensing GPCRs *GPR4* and *TDAG8*, by any of the cytokines tested or by PMA was detected (data not shown).

TNF, LPS or PMA induced *OGR1* expression is reversed by Akt, MAP and PKC kinase and NF-κB inhibitors

To understand the pathways involved in TNF, PMA or LPS-mediated induction of *OGR1* expression we investigated the roles of Akt1/2 kinase, c-Jun N-terminal kinase (JNK) and PKC by using their specific inhibitors. Mitogen-activated protein kinases (MAPKs) play an important role in regulating the cellular response to various extracellular stimuli.[34] Signaling via PKC is known to activate MAPKs.[35] Activation occurs by sequential phosphorylation by JNK, ERK (extracellular-signal-regulated kinase) 1/2, p38 MAPK, ERK5 and ERK3/4.[36] Activated MAPK kinase pathways may stimulate activator protein 1 (AP-1).[37,38] Exposure of monocytes and macrophages to TNF, LPS and PMA results in activation of the AP-1, NF-κB, caspase and MAPK pathways.[39, 40] Akt is a serine-threonine kinase and has been implicated in TNF-mediated activation of NF-κB.[41, 42]

Based on our time course experiments (Figure 2D), cells were stimulated with PMA, TNF or LPS, in the presence of the appropriate kinase inhibitor, A6730 (9 μM), SP600125 (20 μM) and curcumin (25 μM), and harvested after 6 hours.

Exposure of MM6 cells to PMA, TNF and LPS induced *OGR1* expression 13.7, 8.2 and 10.3 -fold respectively. The Akt1/2 kinase inhibitor, A6730, significantly decreased TNF and LPS -induced *OGR1* expression, by 5.6 (68%) and 8.2 -fold (80%) respectively, but with less effect on PMA activation (4.8 -fold decrease, 35% decrease) (n=2, $p<0.001$ or 0.01, Figure 5A). SP600125, a JNK inhibitor, decreased *OGR1* induction by PMA 10.1 -fold, (73%) TNF 4.0 -fold (48%) and LPS 7.5 -fold (80%). These results suggest that the JNK/AP1 pathway may be involved in *OGR1* regulation. Curcumin is a potent inhibitor of protein kinase C[43] and inhibits NF-κB activation through inhibition of IκB kinase and Akt activation.[44] Curcumin abolished the induction of all three activating agents (PMA 12.7 -fold (93%), TNF 7.2 -fold 87% and LPS 9.9 -fold 96% decrease). These preliminary kinase inhibitor studies suggest that Akt1/2, JNK, PKC and IKK pathways play an important role in the induction of *OGR1* expression by PMA, TNF and LPS.

Prompted by the results we next tested a number of known NF-κB inhibitors. TNF-, PMA-, or LPS-mediated induction of *OGR1* was significantly reduced by simultaneous treatment of cells with NF-κB inhibitors: curcumin (25 μM), MG-132 (20 μM), AICAR (0.5 nM), BAY-11-7082 (20 μM), CAY10512 (0.3 μM), and SC-514 (25 μM) (Figure 5A-C). In the presence of the inhibitor MG132, TNF induced *OGR1* expression decreased 3.2 and 5.7 -fold respectively (TNF 95% decrease, PMA 89% decrease) (n=2, $p< 0.001$, Figure 5B).

AICAR (5-Aminoimidazole-4-carboxyamide) ribonucleoside blocks the expression of pro-inflammatory cytokines genes by a reduction in NF-κB DNA-binding activity[45]. BAY-11-7082

and SC-514 block NF-kB activation by inhibition of IκB kinase.[46, 47] The resveratrol analog CAY10512 is a specific NF-κB inhibitor. Treatment with PMA, TNF or LPS resulted in 10.2, 3.0 or 7.6 -fold increase in *OGR1* expression respectively, but in the presence of the NF-κB inhibitors induction of *OGR1* significantly decreased. *OGR1* expression decreased with inhibitor; AICAR 9.3-, 2.6- and 7.3 -fold / (91%, 88%, 96%) ; BAY 7082, 9.0-, 2.6- and 6.1 -fold / (88%, 87%, 81%); Cay 10512, 5.6-, 1.8- and 3.8 -fold / (56%, 62%, 49%), ; SC-514, 8.7-, 2.7- and 7.4 -fold (85%, 91%, 97%) on PMA, TNF and LPS stimulation, respectively (Figure 5C). The results collectively suggest that NF-κB plays a key role in the regulation of *OGR1*.

In silico analysis of the *OGR1* promoter

As the inhibitor studies suggested a strong role for AP-1[48] and NF-κB in the regulation of *OGR1* expression we next performed an *in silico* promoter analysis of *OGR1*. Two alternative predicted promoter variants ≈ 9 kpb apart, exist for the *OGR1* gene on chromosome 14. *In silico* analysis using MatInspector software[49] (http://www.genomatix.de/matinspector.html) revealed several putative DNA-binding sites for AP-1, NF-κB and HIF-1α within the proximal regions of the *OGR1* promoter variants. A schematic representation of these sites (TBSs) for *OGR1* variants 1 and 2 and binding sites are shown in Supplemental Figure S1 and S2, respectively.

Cellular responses upon *OGR1* activation by extracellular acidification in murine macrophages.

We further investigated the effect of OGR1 deficiency on intestinal inflammation. We conducted a microarray study and compared the global gene expression of wild type $Ogr1^{+/+}$ cells to $Ogr1^{-/-}$ cells in response to extracellular acidification. We selected the top 100 most

differentially expressed genes by comparing the ranked fold change upon pH shift in WT compared to KO macrophages. Figure 6A shows a heat map summarizing gene expression across all samples in the 4 experimental conditions for these 100 genes.

Acid-induced *OGR1*-mediated differentially up-regulated genes in WT macrophages compared to *OGR1* KO macrophages include inflammatory response genes (*Tnfrsf13c, Ccl24, Cxcl13, C1qa, Nr4a1)* and immune response genes (*Iglv1, Cd79a, H2-Eb1, Tinagl1, Lst1, C1qa, C1qb Cd83, Ccl17*). Furthermore, genes associated with adhesion and ECM (*Sparc, Cyr61, Timp1, Aebp1, Ebp1, Siglec1, Cdh2, Mmp11, Serpine2, Tgm2*), and actin cytoskeleton (*Inhba, Fscn1, Sorbs2, Tuba1c, Map1b, Parva, Cnn3*) were up-regulated by acidic activation of *OGR1* in WT but not in *OGR1* KO macrophages. Interestingly, cholesterol homeostasis genes, (*Cyp11a1, Ephx2*), glucose response and insulin processing genes, (*Inhba, Cpe, Cma1, Igfbp7, Htra1, Sfrp4*), differentiation and bone development gene *Bmp-2* and transcription factor gene *Nrbf2* also increased in WT $Ogr1^{+/+}$ compared to $Ogr1^{-/-}$ KO cells at acidic pH.

The scatter plot represents the ratio fold change low to high pH *OGR1* KO /fold change low to high pH WT macrophages (Figure 6B). The top 100 differentially expressed genes are shown in Supplementary Tables S2.A–B. In addition, a list of genes and enrichment pathways, generated in GeneGo by comparison of pairs of WT low pH vs. high pH to OGR1 KO low pH vs. high pH, is shown in supplementary Table S3 and Figure S3 respectively. Results discussed in this paper have been deposited in the NCBI Gene Expression Omnibus (GEO) Accession No. GSE60295 (http://www.ncbi.nlm.nih.gov/projects/geo).

OGR1 deficiency protects from development of spontaneous colitis in mice

To investigate whether the *OGR1* dependent changes upon acidification have functional consequences during IBD, we applied a mouse model of spontaneous colitis. Analysis of the occurrence of prolapse in the colon over the course of 200 days showed that, only 16.7% of female *Ogr1*$^{-/-}$/*Il-10*$^{-/-}$ mice (n=24) developed rectal prolapse. The incidence was significantly lower than that of female *Ogr1*$^{+/+}$/*Il-10*$^{-/-}$ littermate *mice* (66.7%, n=12) maintained in the same vivarium room during the same time period (p = 0.007**; Odds Ratio for female mice *Ogr1* $^{-/-}$/*Ogr1*$^{+/+}$ = 0.100 (95% CL 0.020~0.500), chi-square test with Fisher's exact test with two sides). Kaplan-Meier survival analysis showed a significantly delayed onset and progression of rectal prolapse in female *Ogr1*$^{-/-}$/*Il-10*$^{-/-}$ mice (estimated median survival time: >200 days vs. 123 days for female *Ogr1*$^{+/+}$/*Il-10*$^{-/-}$ mice, p=0.002 **, log rank (Mantel-Cox) test) (Figure 7). No prolapses were observed in control *Ogr1*$^{+/+}$/*Il-10*$^{+/+}$ mice (n > 100 animals).

Histologically, consistent with the prolapse ratios, *Ogr1*$^{-/-}$/*Il-10*$^{-/-}$ mice showed less inflammation (score 3.7±1.03) (Figure 8A), however, this difference did not reach statistical significance from *Ogr1*$^{+/+}$/*Il-10* $^{-/-}$ female mice (6.5±1.12) (p>0.05, Figure 8B). The same trend in MPO levels of female *Ogr1* $^{-/-}$/*Il10*$^{-/-}$ mice was observed (0.12±0.034 vs. 0.41±0.072, p>0.05, Figure 9A). There were no differences in colon length, relative spleen weight (Figure 9B-C) and in cytokines mRNA expression levels (Figure 10).

Discussion

Our manuscript provides evidence for a role of the pH-sensing receptor *OGR1*, in inflammatory processes such as intestinal inflammation. We show that *OGR1* mRNA expression is up-regulated ≈ 2 -fold during intestinal inflammation in IBD patients. To what extent this translates into up-regulated protein expression cannot currently be assessed due to a lack of suitable antibodies. We further show that the pro-inflammatory cytokine TNF, a major mediator in IBD associated inflammation induces *OGR1* expression in human and murine myeloid cells. TNF up-regulates *OGR1* expression for short periods (6 to 12 h), however, the effect is not sustained for longer periods, after 24 - 48 h *OGR1* expression returns to basal levels.

Similar to our findings, Lum and coworkers reported that expression of *GPR4*, a related proton sensing GPCR, is up-regulated several-fold by TNF and H_2O_2 in human brain microvascular endothelial cells.[50] TNF-mediated induction of *GPR4* occurred after 2 h and was sustained for 24 h.[50] However, in contrast to OGR1, we did not observe induction of *GPR4* and *TDAG8* expression upon treatment with TNF, PMA, or LPS in MM6 cells. *OGR1* expression induced by TNF, PMA or LPS was prevented by treatment with PI-3 (Akt1/2), MAP and PKC inhibitors and with NF-κB inhibitors AICAR, BAY-11-7082, CAY10512, and SC-514. LPS stimulates production of TNF in MM6 cells.[51, 52]

We further show that genetic deletion of *OGR1* ameliorates inflammation at least in female mice. Acidification and signaling via *OGR1* induced a multitude of cellular responses in the microarray analysis. In murine macrophages acid induced *OGR1*-mediated enriched up-regulated genes are involved in inflammatory responses, further supporting our finding that

OGR1 signaling upon pH changes may play an important role in mucosal inflammation. Notably, up-regulation of nuclear receptor subfamily 4 group A member 1 (NR4A1, also known as NUR77) was detected (Supplementary Table S3). NR4A1 functions as an immediate early-response gene and plays a key role in mediating inflammatory responses in macrophages.[53] Further affected pathways are actin cytoskeleton modulation and cell adhesion. This may also be relevant as anti-adhesion strategies for the treatment of IBD have been recently successful and vedolizumab as an antibody against $\alpha4\beta7$ integrin recently has been approved for therapy of Crohn's disease by the FDA and EMA. In an *OGR1*-overexpressing Caco2 model we also observed enrichment of inflammatory response, including NR4A1, actin cytoskeleton, and adhesion and ECM genes upon acidification (manuscript in submission). In the present study, the genes Inhba and Nr4a1 which are linked to the myocardin-related transcription factor (MRTF) pathway[54], were also found to be strongly regulated by pH change.

Another strongly regulated gene was activin. Activin A is released early in the cascade of circulatory cytokines during systemic inflammatory episodes, roughly coincident with TNF and before IL-6 and follistatin are elicited. Activin A protein is also elevated in IBD patients and in experimental colitis.[55] Recently activin A was identified to regulate macrophage switch between polarization states.[56] This skew towards a pro-inflammatory phenotype occurs by promoting the expression of M1 (GM-CSF) markers, and impairing the acquisition of M2 (M-CSF) markers, while down-regulating the production of *Il-10*.[56] Furthermore, *SPARC* (Secreted protein acidic and rich in cysteine) was found to be strongly regulated by *OGR1*. *SPARC* is a gene whose methylation has been related to IBD.[57, 58] *SPARC* exacerbates

colonic inflammatory symptoms in DSS-induced murine colitis. Compared to WT, *SPARC* KO mice had less inflammation with fewer inflammatory cells and more regulatory T cells.[59]

Why would pH-sensing be so important during intestinal inflammation? Firstly, pH homeostasis is important for the maintenance of normal cell function. pH is normally tightly controlled within a narrow range. Normal pH of blood and tissue is controlled at ≈ pH 7.2-7.4. Maintaining homeostasis requires cells to sense their external environment, communicate with each other, and respond rapidly to extracellular signals. This can be achieved by hydrophobic molecules, ion channels, catalytic receptor and G-protein-coupled receptors.[60]

Under physiological conditions there are also counterplayers of *OGR1* expressed in the mucosal tissue. *TDAG8* mediates extracellular proton-induced inhibition of proinflammatory cytokine production in mouse macrophages.[2] Onozawa *et al.* showed that *TDAG8* deficient mice exhibit enhanced arthritic symptoms compared to wild type animals; suggesting that *TDAG8* attenuates inflammation by negatively regulating the function of the macrophages, T cells and B cells.[23] In search for genetic components and causal genetic variants of IBD, genome-wide association (GWA) studies have identified numerous susceptibility regions that are marked by single nucleotide polymorphisms (SNPs).[22, 61, 62] Association results and *in silico* analysis identified a locus within the *TDAG8* gene as susceptibility locus in CD[22], supporting that *TDAG8* acts as a negative regulator of inflammation. Khor *et al.* propose that the presence of *TDAG8* as an IBD-risk loci is necessary to maintain intestinal homeostasis due to its immune modulatory effect.[63]

To summarize, ORG1 expression is induced in human and murine myeloid cells by TNF, PMA and LPS; whereby simultaneous treatment with NF-κB inhibitors caused a reversal of this effect. Up-regulated genes induced by extracellular low pH by proton-sensing OGR1 in murine macrophages were enriched for inflammatory and immune response, actin cytoskeleton and cell adhesion genes sets. The deficiency of pH-sensing receptor *OGR1* protects from spontaneous inflammation in the *Il-10* KO model. Thus, pH sensors may be interesting new targets for pharmacological intervention in intestinal inflammation.

Acknowledgements

We thank Jelena Kühn Georgijevic, Lennart Opitz, Michal Okoniewski and Hubert Rehrauer from the Functional Genomics Center Zürich for the microarray service/analysis and Andreas Sailer and Miroslava Vanek for providing human monocytes. Agnes Feige, Alexandra Cee, Christian Hiller and Silvia Lang are acknowledged for their expert technical assistance. The help from the ZIRP Rodent Phenotyping Facility is gratefully acknowledged.

Figure and table legends

Figure 1. OGR1 expression in human intestinal mucosa

IBD patients expressed higher levels of *OGR1* mRNA in the mucosa as compared to controls. Expression levels normalized to GAPDH. Biopsy specimens were taken from 29 CD patients, 8 UC patients and 17 non-IBD control patients. Asterisks denote significant differences from the respective control (*P < 0.05, **P < 0.01, ***P <0 .001).

Figure 2. TNF and PMA induce *OGR1* expression in human monocytes

A – B. MonoMac6 (MM6) cells were treated with cytokines for 6 hours. Treatment of MM6 cells with TNF led to significant up-regulation of *OGR1.* No induction of *OGR1* occurred with other cytokines (IFN-γ, IL-1β, IL-6, TGF-β) (50 ng/ml) tested. **C.** Concentration-dependent TNF (0, 2.5, 10, 25, 50, 100 ng/ml) induction of *OGR1* mRNA expression was confirmed at 4 and 8 h. Maximal *OGR*1 induction was reached at TNF concentration 50 ng/ml at 8 h. **D.** Induction of *OGR1* expression by TNF (50 ng/ml) returned to basal levels after 48 h. **E.** Monocytic-macrophagic differentiation of MM6 cells with phorbol 12-myristate 13-acetate (PMA) (25 nM), a specific activator of protein kinase C (PKC) and NF-κB, led to a significant increase in *OGR1* mRNA expression**.** Asterisks denote significant differences from the respective control (*P < 0.05, **P < 0.01, ***P <0 .001). Representative data of one of three qualitatively similar experiments shown unless indicated.

Figure 3. TNF- and PMA-dependent induction of *OGR1* mRNA in primary human monocytes. A. Dose-dependence of TNF (0, 2.5, 10, 25, 50 ng/ml) induction of *OGR1* mRNA was confirmed in primary human monocytes. **B.** PMA (0, 5, 25, 50, 75, 100 ng/ml) induction of *OGR1* mRNA was confirmed in primary human monocytes. Asterisks denote significant

differences from the respective control (*P < 0.05, **P < 0.01, ***P <0 .001). Representative data of one of two similar experiments shown.

Figure 4. TNF induces *OGR1* expression in murine macrophages. *OGR1* induction by TNF (25 ng/ml) was also confirmed in primary mouse residential peritoneal macrophages. Asterisks denote significant differences from the respective control (*P < 0.05, **P < 0.01, ***P <0 .001). Representative data of one of three similar experiments shown.

Figure 5. TNF-, PMA-, and LPS-mediated induction of *OGR1* in MM6 cells was reversed by simultaneous treatment of cells with kinase and NF-kB inhibitors. A. Kinase inhibitors, A6730 (9 μM), SP600125 (20 μM) and curcumin (25 μM), reduced or abolished TNF (25 ng/ml), PMA (25 nM), or LPS (1 μg/ml) mediated induction of *OGR1* in MM6 cells. **B.** Treatment with NF-kB inhibitor MG-132 (20 μM) significantly reduced TNF (50 ng/ml) or PMA (25 nM) mediated induction of *OGR1* in MM6 cells. **C.** AICAR (0.5 nM), BAY-11-7082 (20 μM), CAY10512 (0.3 μM), and SC-514 (25 μM) also reduced TNF (25 ng/ml), PMA (25 nM), or LPS (1 μg/ml) mediated induction of *OGR1.* Asterisks denote significant differences from the respective control (*P < 0.05, **P < 0.01, ***P <0 .001). Representative data of one of two similar experiments shown.

Figure 6. Global gene expression of acid response of mouse macrophages. A. Top 100 genes from the whole-transcript microarray analysis of acid response (pH 6.7) of wild type (WT) and Ogr1 KO murine macrophages**.** Control condition, pH 7.7 is shown on the left. Changes in gene expression within each comparison are represented as Log2-transformed fold changes (≥2.0-absolute-fold-change, P<0.05 significance). **B.** Differentially expressed genes for acid response in WT and *OGR1* KO macrophages. Fold changes in low to high pH shift of *OGR1* KO macrophages are depicted on y-axis and fold changes low to high pH WT

macrophages are shown on the x-axis. The highest ranking differentially expressed genes in the acid response of WT mouse macrophages are shown in the lower right quadrant of the scatter plot and the upper left quadrant shows the highest ranking differentially expressed genes in the acid response of *OGR1* KO mouse macrophages.

Figure 7. *OGR1* deficient mice show delayed onset and severity of prolapse in a spontaneous *IL-10* knock out mouse model. Kaplan-Meier survival analysis showed a significantly delayed onset and progression of rectal prolapse in female *Ogr1* $^{-/-}$*/Il-10*$^{-/-}$ *mice* (estimated median survival time: >200 days vs. 123 days, p=0.002 **, log rank (Mantel-Cox) test). Green solid lines, *Ogr1* $^{-/-}$*/Il-10* $^{-/-}$ mice (16.7% prolapses, n=24); blue solid line, *Ogr1* $^{+/+}$*/Il-10* $^{-/-}$ mice (66.7% prolapses, n=12); grey solid lines, *Ogr1*$^{+/+}$*/Il-10*$^{+/+}$ mice (0% prolapses, n=31). No rectal prolapses were detected in any of the *Ogr1*$^{+/+}$*/Il-10*$^{+/+}$ mice in the breeding colony in the study, 200 days.

Figure 8. *OGR1* deficient mice exhibit a trend to less inflammation in a spontaneous *IL-10* knock out mouse model A. Microscopic analysis of terminal colon sections from *Ogr1* $^{-/-}$*/Il-10* $^{-/-}$, *Ogr1*$^{+/+}$*/Il-10*$^{-/-}$ and *Ogr1*$^{+/+}$*/Il-10*$^{+/+}$ 80-day-old mice, staining by Hematoxylin and eosin. Representative images are shown. **B.** Histological score, based on evaluation of morphological changes of epithelium and immune cell infiltration, of distal colon from *Ogr1* $^{-/-}$*/Il-10* $^{-/-}$, *Ogr1*$^{+/+}$*/Il-10* $^{-/-}$ and *Ogr1*$^{+/+}$*/Il-10*$^{+/+}$ 80-day-old mice. Data presented as mean ± SEM; n ≥ 5 per group; Asterisks denote significant differences from the respective control (*P < 0.05, **P < 0.01, ***P <0 .001). All mice were female.

Figure 9. The development of IBD and progression of prolapse between *Ogr1* $^{-/-}$*/IL-10* $^{-/-}$ and *Ogr1*$^{+/+}$*/Il-10*$^{-/-}$ *female* mice. **A.** Comparison of MPO activity in colon tissue **B.**

Assessment of colon length. **C.** Relative spleen weight. No significant differences in OGR1 KO/Il-10 KO mice and controls in these parameters were observed.

Figure 10. Expression levels of cytokines in colons of female *Ogr1* $^{-/-}$*/Il-10* $^{-/-}$, *Ogr1* $^{+/+}$*/Il-10* $^{-/-}$ and *Ogr1* $^{+/+}$*/Il-10*$^{+/+}$ (WT control) mice were determined by real-time PCR and normalized to GAPDH. (n= 6~9 mice per group). The homogenate of each mouse colon sample was tested in triplicate. Data presented as mean ± SEM; Asterisks denote significant differences from the respective control (*P < 0.05, **P < 0.01, ***P <0 .001). No statistical difference between colon and mesenteric lymph nodes of female *Ogr1* $^{-/-}$*/Il-10*$^{-/-}$ mice and female *Ogr1* $^{+/+}$*/Il-10* $^{-/-}$ mice was observed (p>0.05, Kruskal-Wallis one-way ANOVA followed by Dunn's multiple-comparison test).

References

1. Hanly EJ, Aurora AA, Shih SP, et al. Peritoneal acidosis mediates immunoprotection in laparoscopic surgery. Surgery 2007;142:357-64.
2. Mogi C, Tobo M, Tomura H, et al. Involvement of Proton-Sensing TDAG8 in Extracellular Acidification-Induced Inhibition of Proinflammatory Cytokine Production in Peritoneal Macrophages. Journal of Immunology 2009;182:3243-3251.
3. Brokelman WJ, Lensvelt M, Borel Rinkes IH, et al. Peritoneal changes due to laparoscopic surgery. Surg Endosc 2011;25:1-9.
4. Lardner A. The effects of extracellular pH on immune function. J Leukoc Biol 2001;69:522-30.
5. van Heel DA, Udalova IA, De Silva AP, et al. Inflammatory bowel disease is associated with functional TNF polymorphism affecting OCT1/NF-kappa B interaction. Gut 2002;50:A30-A30.
6. Sandborn WJ, Targan SR. Biologic therapy of inflammatory bowel disease. Gastroenterology 2002;122:1592-1608.
7. Blam ME, Stein RB, Lichtenstein GR. Integrating anti-tumor necrosis factor therapy in inflammatory bowel disease: current and future perspectives. Am J Gastroenterol 2001;96:1977-97.
8. Danese S, Colombel JF, Peyrin-Biroulet L, et al. Review article: the role of anti-TNF in the management of ulcerative colitis -- past, present and future. Aliment Pharmacol Ther 2013;37:855-66.
9. Rutgeerts PJ. Review article: efficacy of infliximab in Crohn's disease--induction and maintenance of remission. Aliment Pharmacol Ther 1999;13 Suppl 4:9-15; discussion 38.
10. van Dullemen HM, van Deventer SJ, Hommes DW, et al. Treatment of Crohn's disease with anti-tumor necrosis factor chimeric monoclonal antibody (cA2). Gastroenterology 1995;109:129-35.
11. Grivennikov SI, Tumanov AV, Liepinsh DJ, et al. Distinct and nonredundant in vivo functions of TNF produced by t cells and macrophages/neutrophils: protective and deleterious effects. Immunity 2005;22:93-104.
12. Neurath MF, Pettersson S, Meyer zum Buschenfelde KH, et al. Local administration of antisense phosphorothioate oligonucleotides to the p65 subunit of NF-kappa B abrogates established experimental colitis in mice. Nat Med 1996;2:998-1004.
13. Rogler G, Brand K, Vogl D, et al. Nuclear factor kappaB is activated in macrophages and epithelial cells of inflamed intestinal mucosa. Gastroenterology 1998;115:357-69.
14. Hatoum OA, Binion DG, Gutterman DD. Paradox of simultaneous intestinal ischaemia and hyperaemia in inflammatory bowel disease. Eur J Clin Invest 2005;35:599-609.
15. Ludwig MG, Vanek M, Guerini D, et al. Proton-sensing G-protein-coupled receptors. Nature 2003;425:93-8.
16. Seuwen K, Ludwig MG, Wolf RM. Receptors for protons or lipid messengers or both? J Recept Signal Transduct Res 2006;26:599-610.
17. Mogi C, Tomura H, Tobo M, et al. Sphingosylphosphorylcholine antagonizes proton-sensing ovarian cancer G-protein-coupled receptor 1 (OGR1)-mediated inositol phosphate production and cAMP accumulation. J Pharmacol Sci 2005;99:160-7.
18. Tomura H, Wang JQ, Komachi M, et al. Prostaglandin I(2) production and cAMP accumulation in response to acidic extracellular pH through OGR1 in human aortic smooth muscle cells. J Biol Chem 2005;280:34458-64.
19. Ichimonji I, Tomura H, Mogi C, et al. Extracellular acidification stimulates IL-6 production and Ca2+ mobilization through proton-sensing OGR1 receptors in human airway smooth muscle cells. American Journal of Physiology-Lung Cellular and Molecular Physiology 2010;299:L567-L577.

20. Palmer CD, Rahman FZ, Sewell GW, et al. Diminished macrophage apoptosis and reactive oxygen species generation after phorbol ester stimulation in Crohn's disease. PLoS One 2009;4:e7787.
21. Campos N, Magro F, Castro AR, et al. Macrophages from IBD patients exhibit defective tumour necrosis factor-alpha secretion but otherwise normal or augmented pro-inflammatory responses to infection. Immunobiology 2011;216:961-70.
22. Franke A, McGovern DP, Barrett JC, et al. Genome-wide meta-analysis increases to 71 the number of confirmed Crohn's disease susceptibility loci. Nat Genet 2010;42:1118-25.
23. Onozawa Y, Komai T, Oda T. Activation of T cell death-associated gene 8 attenuates inflammation by negatively regulating the function of inflammatory cells. Eur J Pharmacol 2011;654:315-9.
24. Wirtz S, Neurath MF. Mouse models of inflammatory bowel disease. Adv Drug Deliv Rev 2007;59:1073-83.
25. Solomon L, Mansor S, Mallon P, et al. The dextran sulphate sodium (DSS) model of colitis: an overview. Comparative Clinical Pathology 2010;19:235-239.
26. Hibi T, Ogata H, Sakuraba A. Animal models of inflammatory bowel disease. J Gastroenterol 2002;37:409-17.
27. Rogler G, Daig R, Aschenbrenner E, et al. Establishment of long-term primary cultures of human small and large intestinal epithelial cells. Lab Invest 1998;78:889-90.
28. Mohebbi N, Benabbas C, Vidal S, et al. The Proton-activated G Protein Coupled Receptor OGR1 Acutely Regulates the Activity of Epithelial Proton Transport Proteins. Cellular Physiology and Biochemistry 2012;29:313-324.
29. Zhang X, Goncalves R, Mosser DM. The isolation and characterization of murine macrophages. Curr Protoc Immunol 2008;Chapter 14:Unit 14 1.
30. Bentz S, Pesch T, Wolfram L, et al. Lack of transketolase-like (TKTL) 1 aggravates murine experimental colitis. Am J Physiol Gastrointest Liver Physiol 2011;300:G598-607.
31. Fischbeck A, Leucht K, Frey-Wagner I, et al. Sphingomyelin induces cathepsin D-mediated apoptosis in intestinal epithelial cells and increases inflammation in DSS colitis. Gut 2011;60:55-65.
32. Kauffmann A, Gentleman R, Huber W. arrayQualityMetrics--a bioconductor package for quality assessment of microarray data. Bioinformatics 2009;25:415-6.
33. Auwerx J. The human leukemia cell line, THP-1: a multifacetted model for the study of monocyte-macrophage differentiation. Experientia 1991;47:22-31.
34. Widmann C, Gibson S, Jarpe MB, et al. Mitogen-activated protein kinase: conservation of a three-kinase module from yeast to human. Physiol Rev 1999;79:143-80.
35. Seger R, Krebs EG. The MAPK signaling cascade. FASEB J 1995;9:726-35.
36. Cargnello M, Roux PP. Activation and function of the MAPKs and their substrates, the MAPK-activated protein kinases. Microbiol Mol Biol Rev 2011;75:50-83.
37. Angel P, Karin M. The role of Jun, Fos and the AP-1 complex in cell-proliferation and transformation. Biochim Biophys Acta 1991;1072:129-57.
38. Karin M. The regulation of AP-1 activity by mitogen-activated protein kinases. J Biol Chem 1995;270:16483-6.
39. DeFranco AL, Crowley MT, Finn A, et al. The role of tyrosine kinases and map kinases in LPS-induced signaling. Prog Clin Biol Res 1998;397:119-36.
40. Englaro W, Bahadoran P, Bertolotto C, et al. Tumor necrosis factor alpha-mediated inhibition of melanogenesis is dependent on nuclear factor kappa B activation. Oncogene 1999;18:1553-9.
41. Kane LP, Shapiro VS, Stokoe D, et al. Induction of NF-kappaB by the Akt/PKB kinase. Curr Biol 1999;9:601-4.
42. Ozes ON, Mayo LD, Gustin JA, et al. NF-kappaB activation by tumour necrosis factor requires the Akt serine-threonine kinase. Nature 1999;401:82-5.

43. Aggarwal BB, Kumar A, Bharti AC. Anticancer potential of curcumin: Preclinical and clinical studies. Anticancer Research 2003;23:363-398.
44. Aggarwal S, Ichikawa H, Takada Y, et al. Curcumin (diferuloylmethane) down-regulates expression of cell proliferation and antiapoptotic and metastatic gene products through suppression of IkappaBalpha kinase and Akt activation. Mol Pharmacol 2006;69:195-206.
45. Katerelos M, Mudge SJ, Stapleton D, et al. 5-aminoimidazole-4-carboxamide ribonucleoside and AMP-activated protein kinase inhibit signalling through NF-kappaB. Immunol Cell Biol 2010;88:754-60.
46. Pierce JW, Schoenleber R, Jesmok G, et al. Novel inhibitors of cytokine-induced IkappaBalpha phosphorylation and endothelial cell adhesion molecule expression show anti-inflammatory effects in vivo. J Biol Chem 1997;272:21096-103.
47. Kishore N, Sommers C, Mathialagan S, et al. A selective IKK-2 inhibitor blocks NF-kappa B-dependent gene expression in interleukin-1 beta-stimulated synovial fibroblasts. J Biol Chem 2003;278:32861-71.
48. Fujioka S, Niu J, Schmidt C, et al. NF-kappaB and AP-1 connection: mechanism of NF-kappaB-dependent regulation of AP-1 activity. Mol Cell Biol 2004;24:7806-19.
49. Cartharius K, Frech K, Grote K, et al. MatInspector and beyond: promoter analysis based on transcription factor binding sites. Bioinformatics 2005;21:2933-42.
50. Lum H, Qiao J, Walter RJ, et al. Inflammatory stress increases receptor for lysophosphatidylcholine in human microvascular endothelial cells. Am J Physiol Heart Circ Physiol 2003;285:H1786-9.
51. Haas JG, Baeuerle PA, Riethmuller G, et al. Molecular mechanisms in down-regulation of tumor necrosis factor expression. Proc Natl Acad Sci U S A 1990;87:9563-7.
52. Ziegler-Heitbrock HW, Blumenstein M, Kafferlein E, et al. In vitro desensitization to lipopolysaccharide suppresses tumour necrosis factor, interleukin-1 and interleukin-6 gene expression in a similar fashion. Immunology 1992;75:264-8.
53. Pei L, Castrillo A, Tontonoz P. Regulation of macrophage inflammatory gene expression by the orphan nuclear receptor Nur77. Mol Endocrinol 2006;20:786-94.
54. Esnault C, Stewart A, Gualdrini F, et al. Rho-actin signaling to the MRTF coactivators dominates the immediate transcriptional response to serum in fibroblasts. Genes Dev 2014;28:943-58.
55. Zhang YQ, Resta S, Jung B, et al. Upregulation of activin signaling in experimental colitis. Am J Physiol Gastrointest Liver Physiol 2009;297:G768-80.
56. Sierra-Filardi E, Puig-Kroger A, Blanco FJ, et al. Activin A skews macrophage polarization by promoting a proinflammatory phenotype and inhibiting the acquisition of anti-inflammatory macrophage markers. Blood 2011;117:5092-101.
57. Lin Z, Hegarty JP, Cappel JA, et al. Identification of disease-associated DNA methylation in intestinal tissues from patients with inflammatory bowel disease. Clin Genet 2011;80:59-67.
58. Karatzas PS, Gazouli M, Safioleas M, et al. DNA methylation changes in inflammatory bowel disease. Ann Gastroenterol 2014;27:125-132.
59. Ng YL, Klopcic B, Lloyd F, et al. Secreted protein acidic and rich in cysteine (SPARC) exacerbates colonic inflammatory symptoms in dextran sodium sulphate-induced murine colitis. PLoS One 2013;8:e77575.
60. Aljarari NMH. The role of GPCR on various second messenger systems. Journal of Basic Medical and Allied Sciences 2012:1-7.
61. Anderson CA, Boucher G, Lees CW, et al. Meta-analysis identifies 29 additional ulcerative colitis risk loci, increasing the number of confirmed associations to 47. Nat Genet 2011;43:246-52.
62. Jostins L, Ripke S, Weersma RK, et al. Host-microbe interactions have shaped the genetic architecture of inflammatory bowel disease. Nature 2012;491:119-24.

63. Khor B, Gardet A, Xavier RJ. Genetics and pathogenesis of inflammatory bowel disease. Nature 2011;474:307-17.

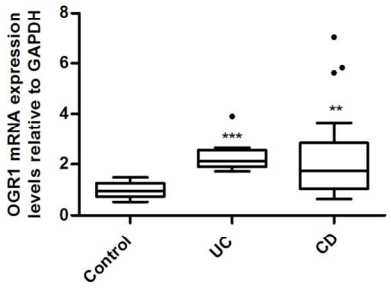

Figure 1. OGR1 expression in human intestinal mucosa
IBD patients expressed higher levels of OGR1 mRNA in the mucosa as compared to controls. Expression levels normalized to GAPDH. Biopsy specimens were taken from 29 CD patients, 8 UC patients and 17 non-IBD control patients. Asterisks denote significant differences from the respective control (*P < 0.05, **P < 0.01, ***P <0 .001).

215x279mm (300 x 300 DPI)

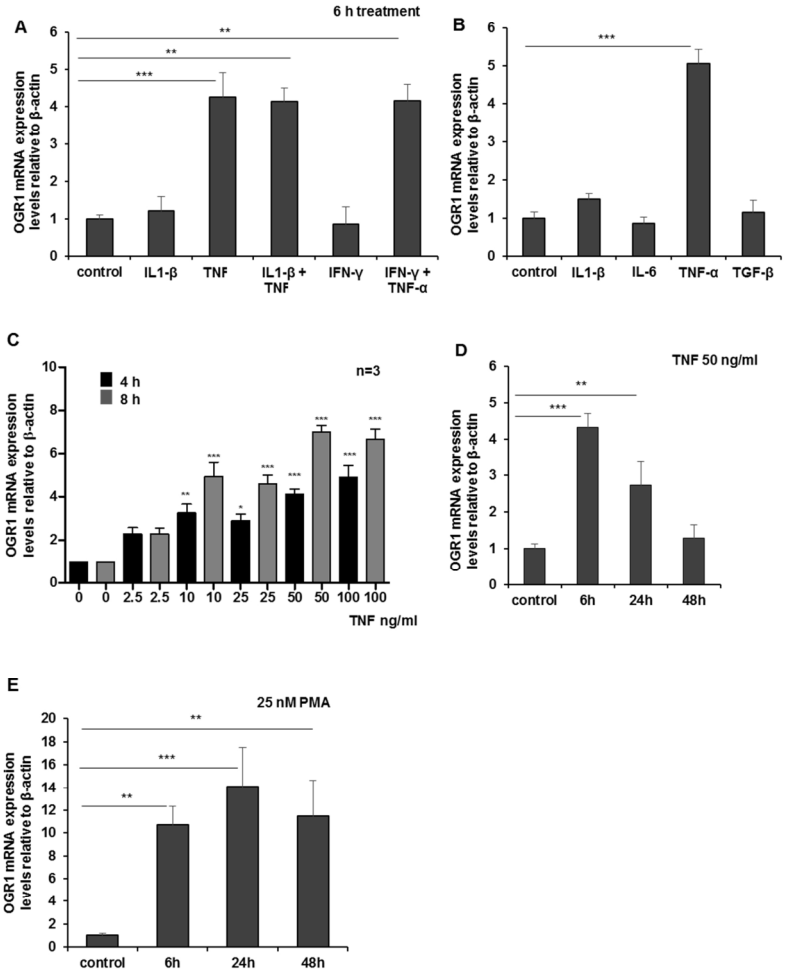

Figure 2. TNF and PMA induce OGR1 expression in human monocytes

A – B. MonoMac6 (MM6) cells were treated with cytokines for 6 hours. Treatment of MM6 cells with TNF led to significant up-regulation of OGR1. No induction of OGR1 occurred with other cytokines (IFN-γ, IL-1β, IL-6, TGF-β) (50 ng/ml) tested. C. Concentration-dependent TNF (0, 2.5, 10, 25, 50, 100 ng/ml) induction of OGR1 mRNA expression was confirmed at 4 and 8 h. Maximal OGR1 induction was reached at TNF concentration 50 ng/ml at 8 h. D. Induction of OGR1 expression by TNF (50 ng/ml) returned to basal levels after 48 h. E. Monocytic-macrophagic differentiation of MM6 cells with phorbol 12-myristate 13-acetate (PMA) (25 nM), a specific activator of protein kinase C (PKC) and NF-κB, led to a significant increase in OGR1 mRNA expression. Asterisks denote significant differences from the respective control (*P < 0.05, **P < 0.01, ***P <0 .001). Representative data of one of three qualitatively similar experiments shown unless indicated.

215x279mm (300 x 300 DPI)

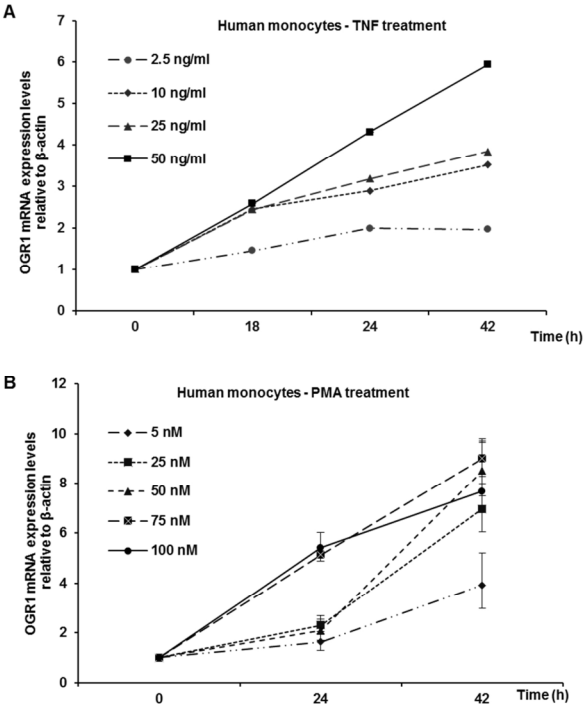

Figure 3. TNF- and PMA-dependent induction of OGR1 mRNA in primary human monocytes. A. Dose-dependence of TNF (0, 2.5, 10, 25, 50 ng/ml) induction of OGR1 mRNA was confirmed in primary human monocytes. B. PMA (0, 5, 25, 50, 75, 100 ng/ml) induction of OGR1 mRNA was confirmed in primary human monocytes. Asterisks denote significant differences from the respective control (*P < 0.05, **P < 0.01, ***P <0 .001). Representative data of one of two similar experiments shown.
215x279mm (300 x 300 DPI)

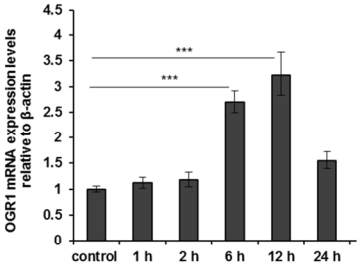

Figure 4. TNF induces OGR1 expression in murine macrophages. OGR1 induction by TNF (25 ng/ml) was also confirmed in primary mouse residential peritoneal macrophages. Asterisks denote significant differences from the respective control (*P < 0.05, **P < 0.01, ***P <0 .001). Representative data of one of three similar experiments shown.
215x279mm (300 x 300 DPI)

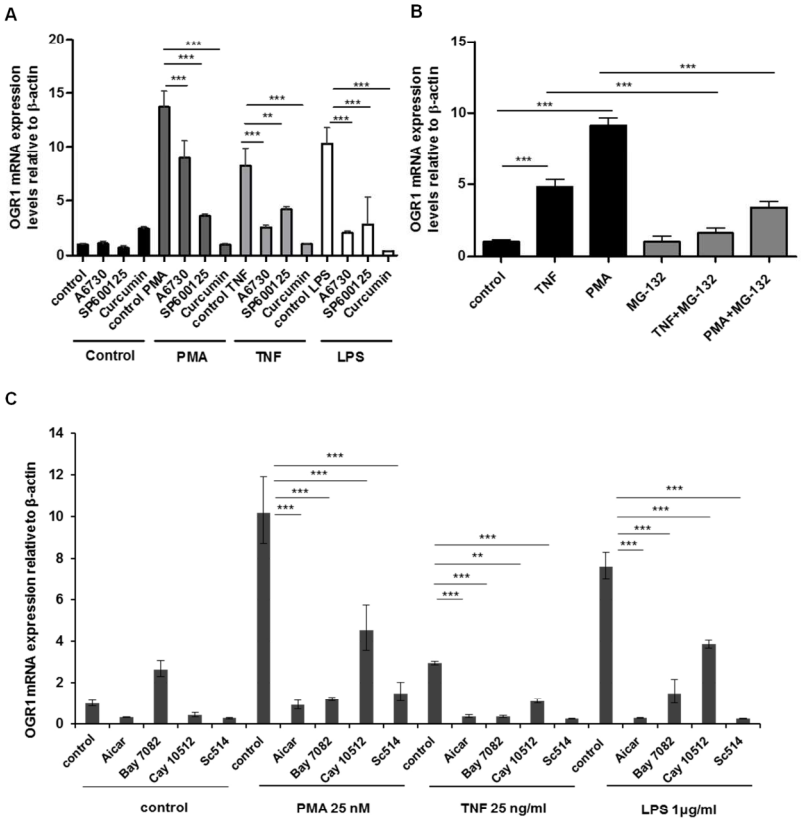

Figure 5. TNF-, PMA-, and LPS-mediated induction of OGR1 in MM6 cells was reversed by simultaneous treatment of cells with kinase and NF-kB inhibitors. A. Kinase inhibitors, A6730 (9 µM), SP600125 (20 µM) and curcumin (25 µM), reduced or abolished TNF (25 ng/ml), PMA (25 nM), or LPS (1 µg/ml) mediated induction of OGR1 in MM6 cells. B. Treatment with NF-kB inhibitor MG-132 (20 µM) significantly reduced TNF (50 ng/ml) or PMA (25 nM) mediated induction of OGR1 in MM6 cells. C. AICAR (0.5 nM), BAY-11-7082 (20 µM), CAY10512 (0.3 µM), and SC-514 (25 µM) also reduced TNF (25 ng/ml), PMA (25 nM), or LPS (1 µg/ml) mediated induction of OGR1. Asterisks denote significant differences from the respective control (*P < 0.05, **P < 0.01, ***P <0 .001). Representative data of one of two similar experiments shown.
215x279mm (300 x 300 DPI)

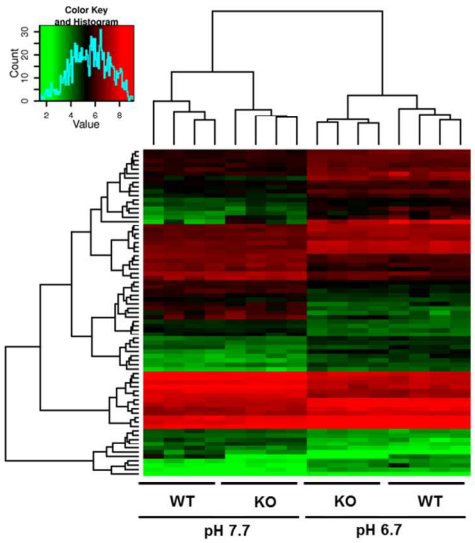

Figure 6.A Global gene expression of acid response of mouse macrophages. A. Top 100 genes from the whole-transcript microarray analysis of acid response (pH 6.7) of wild type (WT) and Ogr1 KO murine macrophages. Control condition, pH 7.7 is shown on the left. Changes in gene expression within each comparison are represented as Log2-transformed fold changes (≥2.0-absolute-fold-change, P<0.05 significance).
215x279mm (300 x 300 DPI)

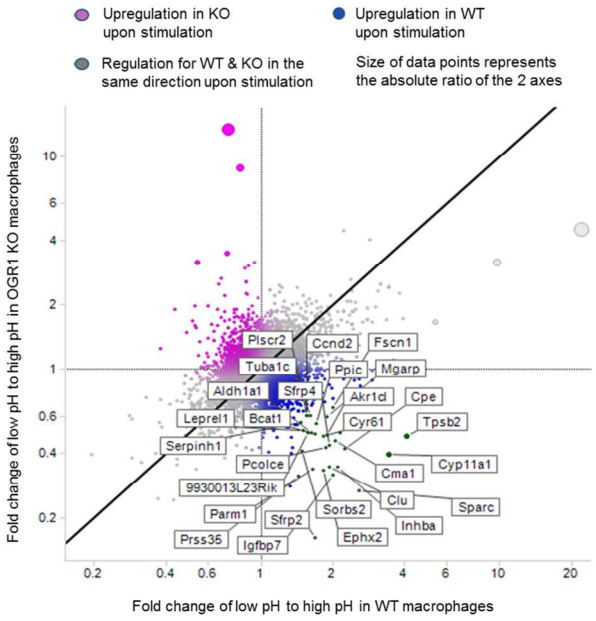

Figure 6.B Global gene expression of acid response of mouse macrophages. B. Differentially expressed genes for acid response in WT and OGR1 KO macrophages. Fold changes in low to high pH shift of OGR1 KO macrophages are depicted on y-axis and fold changes low to high pH WT macrophages are shown on the x-axis. The highest ranking differentially expressed genes in the acid response of WT mouse macrophages are shown in the lower right quadrant of the scatter plot and the upper left quadrant shows the highest ranking differentially expressed genes in the acid response of OGR1 KO mouse macrophages.
215x279mm (300 x 300 DPI)

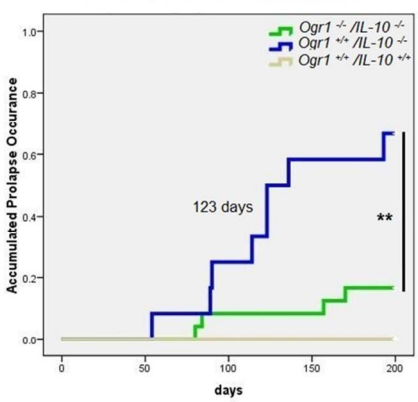

Figure 7. OGR1 deficient mice show delayed onset and severity of prolapse in a spontaneous IL-10 knock out mouse model. Kaplan-Meier survival analysis showed a significantly delayed onset and progression of rectal prolapse in female Ogr1 -/-/Il-10-/- mice (estimated median survival time: >200 days vs. 123 days, p=0.002 **, log rank (Mantel-Cox) test). Green solid lines, Ogr1 -/-/Il-10 -/- mice (16.7% prolapses, n=24); blue solid line, Ogr1 +/+/Il-10 -/- mice (66.7% prolapses, n=12); grey solid lines, Ogr1+/+/Il-10+/+ mice (0% prolapses, n=31). No rectal prolapses were detected in any of the Ogr1+/+/Il-10+/+ mice in the breeding colony in the study, 200 days.
215x279mm (300 x 300 DPI)

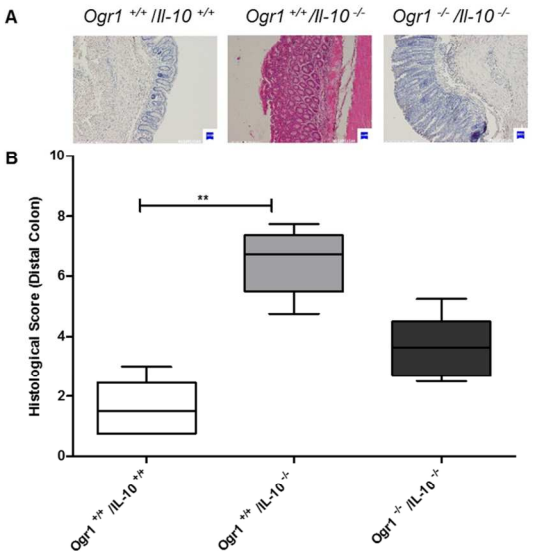

Figure 8. OGR1 deficient mice exhibit a trend to less inflammation in a spontaneous IL-10 knock out mouse model A. Microscopic analysis of terminal colon sections from Ogr1 -/-/Il-10 -/-, Ogr1+/+/Il-10-/- and Ogr1+/+/Il-10+/+ 80-day-old mice, staining by Hematoxylin and eosin. Representative images are shown. B. Histological score, based on evaluation of morphological changes of epithelium and immune cell infiltration, of distal colon from Ogr1 -/-/Il-10 -/-, Ogr1+/+/Il-10 -/- and Ogr1+/+/Il-10+/+ 80-day-old mice. Data presented as mean ± SEM; n ≥ 5 per group; Asterisks denote significant differences from the respective control (*P < 0.05, **P < 0.01, ***P <0 .001). All mice were female.
215x279mm (300 x 300 DPI)

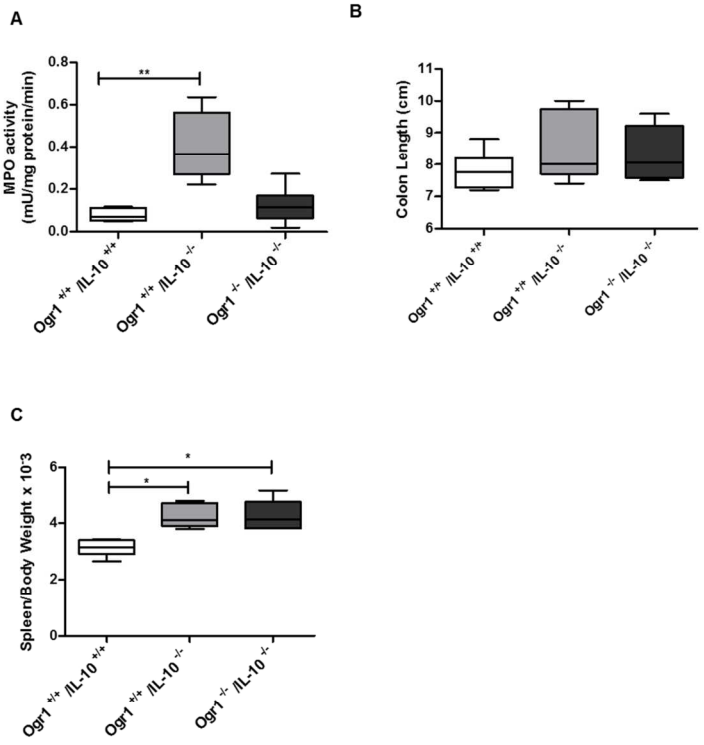

Figure 9. The development of IBD and progression of prolapse between Ogr1 -/-/IL-10 -/-and Ogr1+/+/Il-10-/- female mice. A. Comparison of MPO activity in colon tissue B. Assessment of colon length. C. Relative spleen weight. No significant differences in OGR1 KO/Il-10 KO mice and controls in these parameters were observed.
215x279mm (300 x 300 DPI)

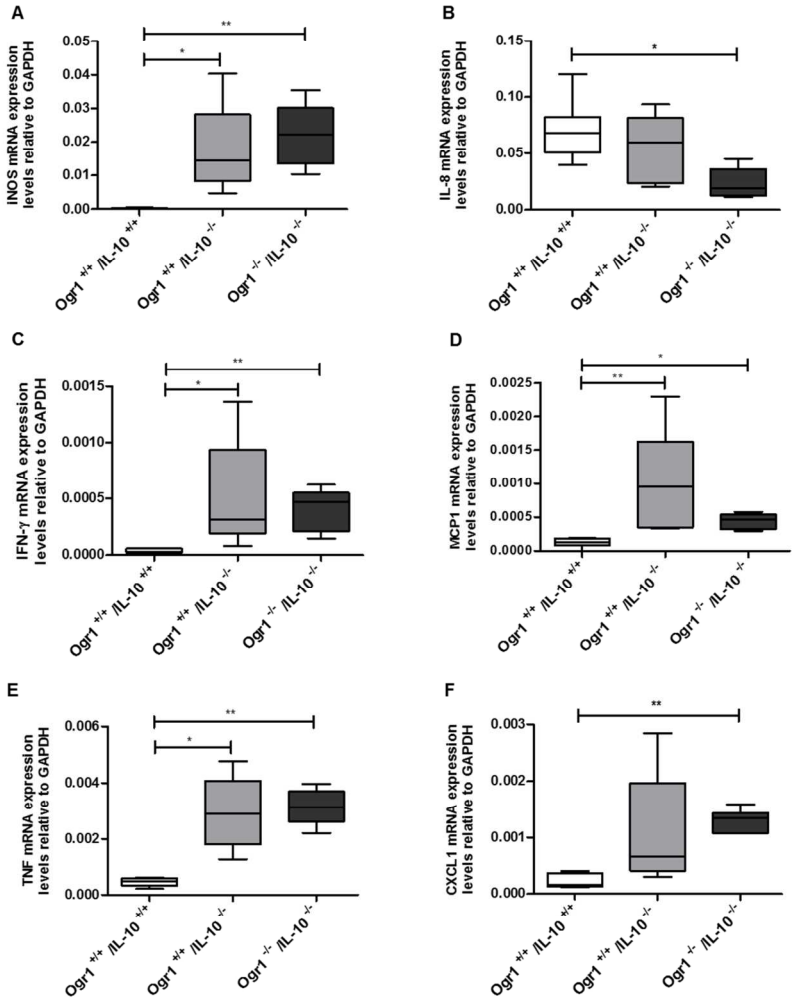

Figure 10. Expression levels of cytokines in colons of female Ogr1 -/-/Il-10 -/- , Ogr1 +/+/Il-10 -/- and Ogr1 +/+/Il-10+/+ (WT control) mice were determined by real-time PCR and normalized to GAPDH. (n= 6~9 mice per group). The homogenate of each mouse colon sample was tested in triplicate. Data presented as mean ± SEM; Asterisks denote significant differences from the respective control (*P < 0.05, **P < 0.01, ***P <0 .001). No statistical difference between colon and mesenteric lymph nodes of female Ogr1 -/-/Il-10-/- mice and female Ogr1 +/+/Il-10 -/- mice was observed (p>0.05, Kruskal-Wallis one-way ANOVA followed by Dunn's multiple-comparison test).
215x279mm (300 x 300 DPI)

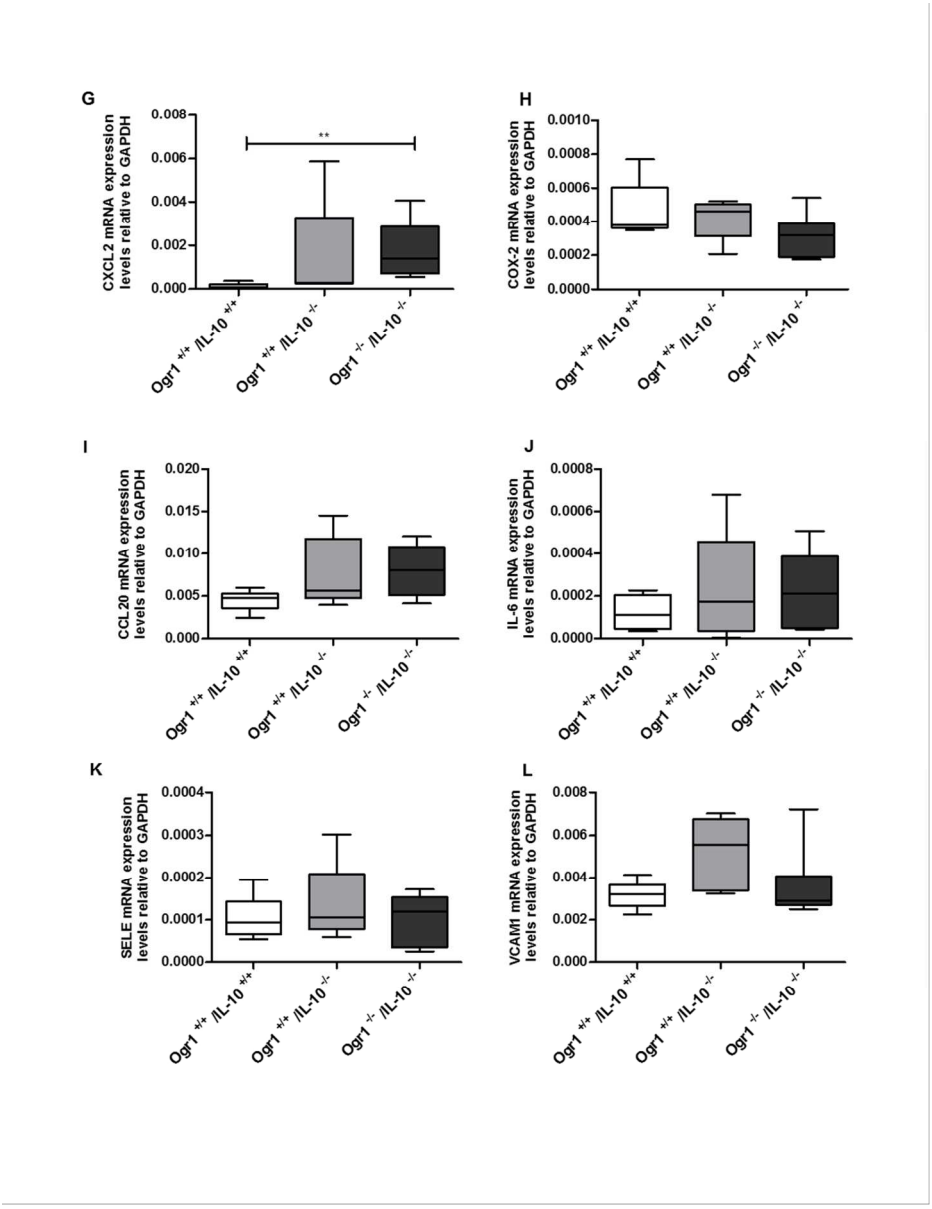

215x279mm (300 x 300 DPI)

De Vallière et al.

Supplementary Material

The G protein-coupled pH-sensing receptor *OGR1* is a regulator of intestinal inflammation

Materials and Methods

Chemicals

Cytokines were obtained from Sigma-Aldrich (St. Louis, MA, USA), unless otherwise stated. TNF (#654205) was purchased from Calbiochem (Merck Darmstadt, Germany). 5-aminoimidazole-4-carboxamide-1-beta-4-ribofuranoside (AICAR) (#100102-41), BAY-11-7082 (#100010266), CAY10512 (#10009536), Curcumin (#81025.1), SC-514 (Cayman#10010267), SP600125 (Cayman #100010466) were purchased from Cayman (Ann Arbor, Michigan, USA).

Genomic DNA extraction and genotyping

For PCR reactions, the oligonucleotides used were as follows:
Il-10 genotyping: 5'-GTGGGTGCAGTTATTGTCTTCCCG-3' (oIMR0086),
5'-GCCTTCAGTATAAAAGGGGGACC-3' (oIMR0087),
5'-CCTGCGTGCAATCCATCTTG-3' (oIMR0088),
Ogr-1 genotyping:
5'-ACCACC AGTGATGCCTAGATCCTG A-3' (P416),
5'-AAGATGACCACGGTGCTGAGC ACC A-3' (P417),
5'-CCATTCGACCACCAAGCG AAACAT C-3' (R3).

Murine macrophage isolation and culture

Peritoneal murine macrophages were centrifuged, washed in PBS and resuspended in RPMI 1640 medium containing 2 mM Glutamax (35050-038, Gibco), 10% fetal calf serum (2-

01F120-I, Amimed, Bio Concept, Allschwil, Switzerland), 100 U/ml penicillin, 100 µg/ml streptomycin (all obtained from Sigma–Aldrich, Buchs, Switzerland). Cells from each mouse were treated without pooling, after plating in 6 well plates (≈ 3 x 10^6 cells in 1 ml/well) at 37°C, 5% CO_2. After 2 h, non-adherent cells were removed. Macrophages were maintained in RPMI medium, 5% CO_2 for 24 h. Final number of cells per treatment (obtained from each mouse) was ≈ 1 x 10^6 cells. The resulting adherent population consisted of ≈ 88% peritoneal macrophages as determined by flow cytometry (data not shown).

RNA extraction and quantitative Real-Time RT-PCR.

Human and mouse tissue.

Tissue pieces used for RNA analysis were transferred immediately into RNAlater solution (Qiagen, Valencia, CA) and stored at −80°C. Tissue biopsies were disrupted in RLT buffer (Qiagen) using a 26G needle.

Cells and tissue samples. Total RNA was isolated using the RNeasy Mini Kit in the automated QIAcube following the manufacturer's recommendations (Qiagen, Hombrechtikon, Switzerland). For removal of residual DNA, DNase treatment, 15 min at room temperature, was integrated into the QIAcube program according to the manufacturer's instructions. For cDNA synthesis, the High-Capacity cDNA Reverse Transcription Kit (Applied Biosystems, Foster City, CA), was used, following the manufacturer's instructions. Determination of mRNA expression was performed by quantitative real-time PCR (qRT-PCR) on a 7900HT real-time PCR system (Applied Biosystems, Foster City, USA), under the following cycling conditions: 20 sec at 95 °C, then 45 cycles of 95 °C for 3 sec and 60 °C for 30 sec with the TaqMan Fast Universal Mastermix. Samples were analyzed as triplicates. Relative mRNA

expression was determined the by the comparative ΔΔCt method[1], which calculates the quantity of the target sequences relative to the endogenous control and a reference sample. TAQMAN Gene Expression Assays, (all from Applied Biosystems, Foster City, USA), used in this study are listed in the online supplementary Table S1.

Table S1. TaqMan assays

Gene Symbol	Gene Name	Assay ID
GPR68	Human G protein-coupled receptor 68, *OGR1*	Hs 00268858- s1
GPR4	Human G protein-coupled receptor 4	Hs 00270999 - s1
GPR65	Human G protein-coupled receptor 65, *TDAG8*	Hs 00269247 - s1
GAPDH	Human glyceraldehyde-3-phosphate dehydrogenase (GAPDH) Endogenous Control	4326317E
ACTB	Human ACTB (beta actin) Endogenous Control	4310881E
HuPo	Human acidic ribosomal protein (RPLPO) Endogenous Control	4310879E
HPRT1	Human Hypoxanthine guanine phosphoribosyl transferase 1	Hs01003268_g1
GPR68	Mouse G protein-coupled receptor 68, *OGR1*	Mm00558545_s1
GPR4	Mouse G protein-coupled receptor 4	Mm00558777_s1
GPR65	Mouse G protein-coupled receptor 65, *TDAG8*	Mm00433695_m1
CCL20	Mouse chemokine (C-C motif) ligand 20	Mm01268754_m1
COX-2	Mouse prostaglandin-endoperoxide synthase 2	Mm00478374_m1
CXCL1	Mouse chemokine (C-X-C motif) ligand 1	Mm04207460_m1
CXCL2	Mouse chemokine (C-X-C motif) ligand 2	Mm00436450_m1
IFN-γ	Mouse interferon gamma	Mm00801778_m1
IL-18	Mouse Interleukin 18	Mm00434225_m1
IL-6	Mouse Interleukin 6	Mm00446190_m1
iNOS	Mouse nitric oxide synthase 2	Mm01309893_m1
MCP-1	Mouse chemokine (C-C motif) ligand 2	Mm00441242_m1
SELE	Mouse selectin, endothelial cell	Mm00441278_m1
TNF-α	Mouse tumour necrosis factor alpha	Mm99999068_m1
VCAM1	Mouse vascular cell adhesion molecule 1	Mm01320970_m1
GAPDH	Mouse glyceraldehyde-3-phosphate dehydrogenase (GAPDH) Endogenous Control	Mm03302249_g1

Human β-actin 4310881E, Human hupo, 4310879E, Human GAPDH 4326317E, Human HPRT1 (hypoxanthine phosphoribosyltransferase 1) Hs01003268_g1 Cat. # 4331182
Human HuPo/ RPLP0 (large ribosomal protein) Endogenous Control (VIC / TAMRA Probe, Primer Limited), 4310879E, Human acidic ribosomal protein (HuPO), Hypoxanthine guanine phosphoribosyl transferase

Predictive location of OGR1 Promoter Variants 1 and 2 on Chromosome 14

Human G protein-coupled receptor 68 (GPR68), **transcript variant 1, mRNA** 2,880 bp linear mRNA
Human G protein-coupled receptor 68 (GPR68), **transcript variant 2, mRNA** 2,834 bp linear mRNA

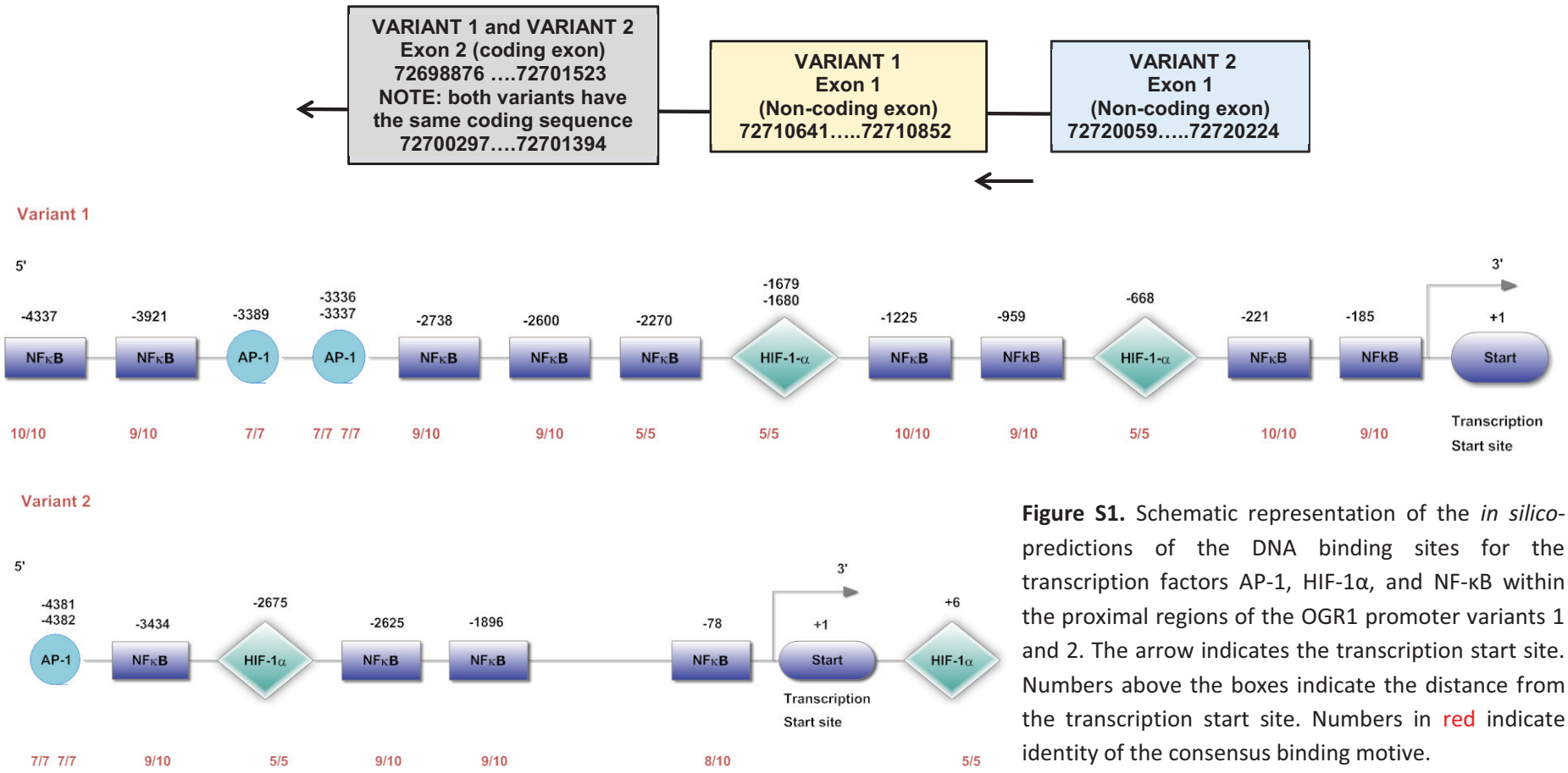

Figure S1. Schematic representation of the *in silico*-predictions of the DNA binding sites for the transcription factors AP-1, HIF-1α, and NF-κB within the proximal regions of the OGR1 promoter variants 1 and 2. The arrow indicates the transcription start site. Numbers above the boxes indicate the distance from the transcription start site. Numbers in red indicate identity of the consensus binding motive.

NFκB: 5' GGGRNYYYCC 3'

R = purine (A or G), Y = pyrimidine (T or C), N = any

- 396 (+) caGCGActtcccgca 9/10 -185
- 432 (-) ctggggatTTTCtag 10/10 -221
- 1170 (-) ctgggcctTTCCatc 9/10 -959
- 1436 (-) aaggggatTTCCtta 10/10 -1225
- 2481 (+) caGGGAttatcctgt 9/10 -2270
- 2811 (+) gagatgGGATttctc 9/10 -2600
- 2949 (+) atggggttTTGCcat 9/10 -2738
- 4132 (+) gatgggatTTCAccg 9/10 - 3921
- 4548 (-) aaGGGAtcctccctt 10/10 – 4337

(subtract 211 to obtain the location from the transcription start site)

HRE: 5' (A/G)CGTG 3'

- 879 (+) ggaagtgaCGTGccagc 5/5 -668
- 1890 (+) tagacacaCGTGctact 5/5 -1679
- 1891 (+) aagtagcaCGTGtgtct 5/5 -1680
- 3417 (-) ttaccttaCGTGgcaaa 5/5 -3206

(subtract 211 to obtain the location from the transcription start site)

AP-1: 5' TGACTCA 3'

- 85 (-) cattcaTGGGtcagtaaatca
- 98 (+) catgaaTGGGtcacaacccgc
- 1598 (-) ccGGCCtggtc
- 1972 (-) cactGCTAagtcagttctgtg
- 1974 (+) cagaacTGACttagcagtgac
- 2263 (-) atttGAGTaaaac
- 2300 (-) tcttacTGAGctagcatttca
- 2330 (-) agcacaTGAGagagcatgggc
- 2769 (+) caggcaTGTGtcactatgcct
- 3346 (+) caatGCTGgatcactccttac
- 3366 (-) cctaatcagCTGAccttaaag
- 3546 (-) taggcaTGAGtcacctcaccc
- 3547 (-) gcatgAGTCacct 7/7 3336
- 3547 (+) aggTGACtcatgc
- 3548 (+) gtgagGTGActcatgcctata 7/7 3337
- 3599 (-) aaacccTGAGtcaagcaatcc
- 3600 (+) gctTGACtcaggg 7/7 3389
- 3600 (-) cccTGAGtcaagc
- 3797 (+) aaaccaTGTGtcaagcaaaac
- 4901 (+) tgatgcCTCAcag
- 5162 (-) ggaGGCTgaggcggcaggatt

(subtract 211 to obtain position from transcription start site)

Figure S2. List of possible binding sites to the consensus elements AP-1, HIF1-α and NFκB in the *in silico* promoter analysis of OGR1.

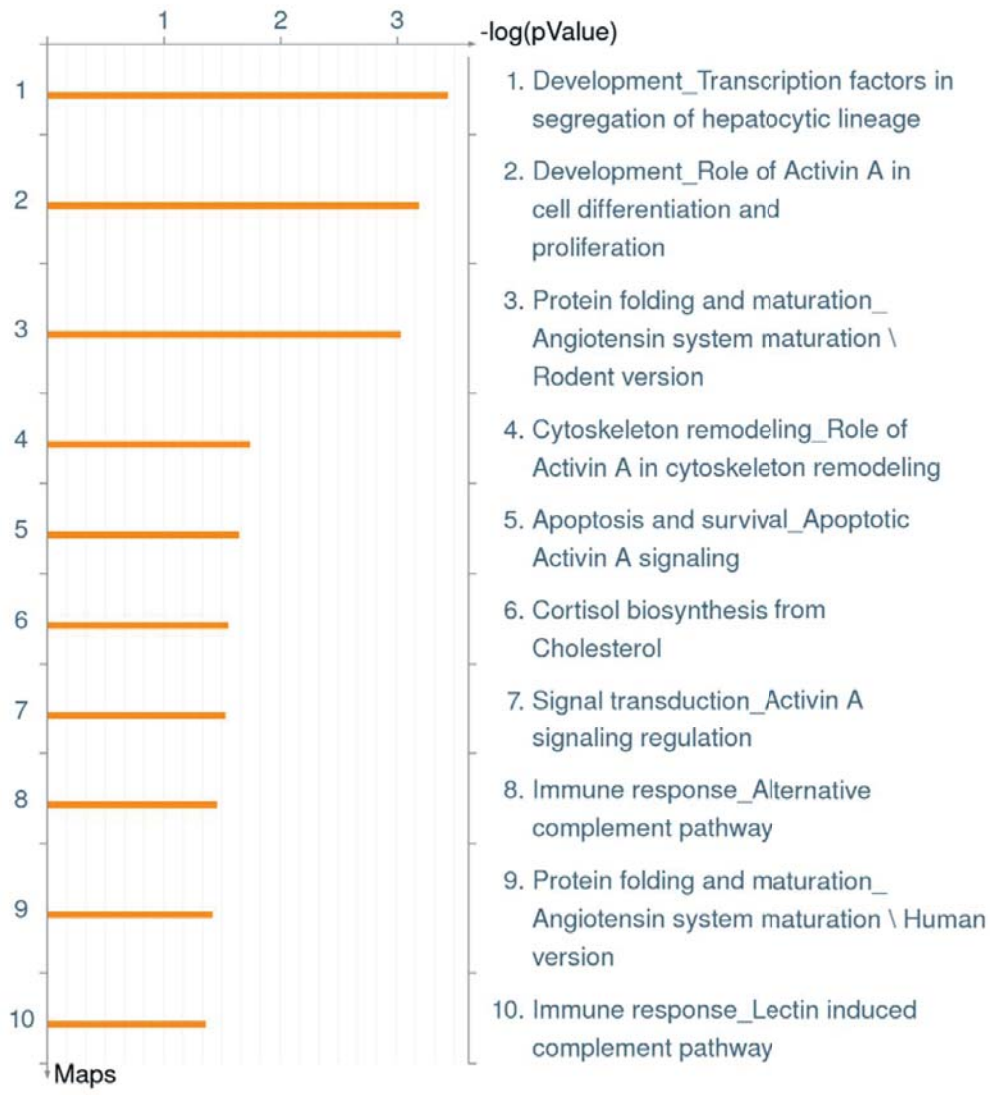

Figure S3. Enrichment analysis: Meta Core (Gene Go) Pathway Maps Ontology. Pairwise comparison of acidified WT vs. Ogr1 KO murine macrophages. pH 6.7 24 h. Extracellular acidosis activation of *Ogr1* in murine macrophages show that the most significantly enriched canonical pathways include Activin A associated pathways, immune response and actin cytoskeleton remodeling pathways.

Table S2.A-B. Differentially expressed genes following activation of OGR1 by acidic pH in mouse peritoneal macrophages pH 6.7 24 h. **A.** Gene List, including gene process **B.** Complete Table (Excel).

Rank WT/KO Ratio	Symbol	Full name	Involved in: (Reference: Gene Card, NCBI, JAX, Uniprot, unless otherwise indicated)
1.	*Cyp11a1*	Cholesterol side chain cleavage enzyme, mitochondrial (Cytochrome P450 11A1)	Cholesterol, lipid or steroid metabolism. Catalyses the side-chain cleavage reaction of cholesterol to pregnenolone.
2.	*Sparc*	Secreted acidic cysteine rich glycoprotein (Osteonectin, Basement membrane protein 40 (BM-40))	Cell adhesion, wound healing, ECM interactions, bone mineralization. Activates production and activity of matrix metalloproteinases.
3.	*Tpsb2*	Tryptase beta-2 or tryptase II (trypsin-like serine protease)	Inflammatory response, proteolysis.
4.	*Inhba*	Inhibin Beta A or Activin beta-A chain	Immune response and mediators of inflammation and tissue repair.[2-5]
5.	*Cpe*	Carboxypeptidase E	Insulin processing, proteolysis.
6.	*Igfbp7*	Insulin-like growth factor-binding protein 7	Stimulates prostacyclin (PGI2) production and cell adhesion. Induced by retinoic acid.
7.	*Clu*	Clusterin	Chaperone-mediated protein folding, positive regulation of NF-κB transcription factor activity. Protects cells against apoptosis and cytolysis by complement. Promotes proteasomal degradation of COMMD1 and IKBKB.
8.	*Cma1*	Chymase 1	Cellular response to glucose stimulus, interleukin-1 beta biosynthetic process. Possible roles: vasoactive peptide generation, extracellular matrix degradation.
9.	*Sfrp4*	Secreted frizzled-related protein 4	Negative regulation of Wnt signalling. Increases apoptosis during ovulation. Phosphaturic effects by specifically inhibiting sodium-dependent phosphate uptake.
10.	*Ephx2*	Bifunctional epoxide hydrolase	Cholesterol homeostasis, xenobiotic metabolism by degrading potentially toxic epoxides.
11.	*Pcolce*	Procollagen C-endopeptidase enhancer	Proteolysis. Collagen binding. Component in collagen and extracellular matrix.
12.	*Akr1cl*	Aldo-keto reductase family 1, member C-like	Oxidoreductase activity
13.	*Cyr61*	Cysteine rich protein 61	Cell adhesion, chemotaxis, cell proliferation, wound healing and angiogenesis.
14.	*Sfrp2*	Secreted frizzled-related protein 2	Differentiation, modulator of Wnt signalling pathway.
15.	*Parm1*	Prostate androgen-regulated mucin-like protein 1	Regulation of TLP1 expression and telomerase activity, enabling certain prostatic cells to resist apoptosis.
16.	*Bcat1*	Branched chain aminotransferase 1	Branched-chain amino acid biosynthetic process.
17.	*Mgarp*	Mitochondria localized glutamic acid rich protein, Hypoxia up-regulated mitochondrial movement regulator protein	Response to steroid hormone stimulus & hypoxia. Trafficking of mitochondria along microtubules. Aids steroidogenesis through maintenance of mitochondrial abundance & morphology.

18.	*Ppic*	Peptidyl-prolyl cis-trans isomerase C, cyclophilin C, cyp-20c	Accelerates protein folding.
19.	*Aldh1a1*	Retinal dehydrogenase 1, aldehyde dehydrogenase family 1, A1	9-cis-retinoic acid biosynthetic process. Converts/oxidizes retinaldehyde to retinoic acid.
20.	*9930013L23RikCemip*	Cell migration inducing protein	ER retention sequence binding, hyaluronic acid binding,
21.	*Fscn1*	Fascin homolog 1, actin bundling protein	Actin filament bundle assembly, cell migration. Organization of actin filament bundles, formation of microspikes, membrane ruffles, and stress fibres. Associates with beta-catenin.
22.	*Sorbs2*	Sorbin and SH3 domain containing 2	Actin filament organization, cell adhesion, cell migration.
23.	*Tuba1c*	Tubulin, alpha 1C	Microtubule-based process.
24.	*Leprel1*	Prolyl 3-hydroxylase 2 leprecan-like protein 1	Collagen metabolic process, negative regulation of cell proliferation.
25.	*Prss35*	Inactive serine protease 35	Serine protease homolog.
26.	*Plscr2*	Phospholipid scramblase 2	Cellular response to lipopolysaccharide.
27.	*Ccnd2*	Cyclin D2	Cell cycle, cell division, protein kinase binding.
28.	*Serpinh1*	Serpin H1	Stress response. Binds specifically to collagen. May be involved as a chaperone in the biosynthetic pathway of collagen.
29.	*Iglv1*	Immunoglobulin lambda variable 1	Immune Response
30.	*Tnfrsf13c*	Tumour necrosis factor receptor superfamily, member 13c	B, T cell costimulation, positive regulation of B and T cell proliferation, positive regulation of interferon-gamma biosynthetic process.
31.	*Timp1*	Metalloproteinase inhibitor 1, tissue inhibitor of metallo-proteinase 1	Response to cytokine, negative regulation of apoptotic process, wound healing. Complexes with metalloproteinases (such as collagenases) and irreversibly inactivates them by binding to their catalytic zinc cofactor.
32.	*Rpl18a*	Ribosomal protein L18A	Translation
33.	*Cd79a*	CD79A antigen (immunoglobulin-associated alpha)	Immune response
34.	*Ccl24*	Chemokine (C-C motif) ligand 24	Chemotaxis, Inflammatory response, cytoskeleton organization
35.	*Nrbf2*	Nuclear receptor (NR) binding factor 2	Transcription, transcription regulation. May modulate transcriptional activation by target NRs.
36.	*Gm9513*	Predicted gene 9513, Secreted tfp/ly-6/upar protein pate-p	N/A
37.	*Rpl35a*	Ribosomal protein L35A	rRNA processing
38.	*1700022KRikN4bp2os*	NEDD4 binding protein 2, opposite strand	N/A
39.	*H2-Eb1*	Histocompatibility 2, class II antigen E beta	Antigen processing and presentation of exogenous peptide antigen via MHC class II.
40.	*Map1b*	Microtubule-associated protein 1B	Microtubule bundle formation, actin binding, cytoskeletal regulatory protein binding.
41.	*Nrn1*	Neuritin 1	Axonogenesis
42.	*Tinagl1*	Tubulointerstitial nephritis antigen-like 1	Immune response, proteolysis, cysteine-type peptidase activity, laminin binding.
43.	*Gm11937*	Predicted gene 11937	Fibrous proteins rich in cysteine, keratin.
44.	*Olfr1004ps1*	Olfactory receptor 1004, pseudogene 1	Olfactory receptor

45.	*Cxcl13*	Chemokine (C-X-C motif) ligand 13	Chemotaxis, Inflammatory response.
46.	*Htra1*	Htra serine peptidase 1 or insulin-like growth factor binding protein 5 protease	Negative regulation of defense response to virus, TGFβ receptor and BMP signalling pathway
47.	*Parva*	Parvin, alpha	Actin cytoskeleton reorganization, actin-mediated cell contraction, cell polarity, substrate adhesion-dependent cell spreading, directed cell migration.
48.	*Aebp1*	AE binding protein 1, Adipocyte enhancer-binding protein 1	Cell adhesion, proteolysis. Isoform 2 may positively regulate NF-κB activity in macrophages by promoting phosphorylation and degradation of Iκ-B-α (NFKBIA), leading to enhanced macrophage inflammatory responsiveness.
49.	*Lst1*	Leukocyte specific transcript 1	Cell shape, immune response. Induces filopodia and microspikes, may be involved in dendritic cell maturation
50.	*Psmb5-ps*	Proteasome (prosome, macropain) subunit, beta type 5, pseudogene	Proteasome-mediated ubiquitin-dependent protein catabolic process, response to oxidative stress.
51.	*Trav13-2*	T cell receptor alpha variable 13-2	
52.	*Krtap6-2*	Keratin associated protein 6-2	Hair keratin-associated protein gene
53.	*Kcng2*	Potassium voltage-gated channel, subfamily G, member 2	Potassium ion transmembrane transport
54.	*Dab2*	Disabled 2, mitogen-responsive phosphoprotein	Apoptosis, Differentiation, Endocytosis, Protein transport, Transport, Wnt signalling.
55.	*Atp2a3*	Endoplasmic reticulum (ER) Ca^{2+} ATPase 3	Ca^{2+} transport, ion transport. Mg^{2+}-dependent enzyme, catalyses hydrolysis of ATP coupled with transport of Ca^{2+}. Transports Ca^{2+} from cytosol into sarcoplasmic/ER lumen
56.	*Siglec1*	Sialic acid binding Ig-like lectin 1, sialoadhesin	Cell adhesion, endocytosis
57.	*Gm6816 (Rps4lps)*	Ribosomal protein S4-like, pseudogene	Translation
58.	*Mmp11*	Matrix metallopeptidase 11	Basement membrane organization, Ca^{2} binding, metalloendopeptidase activity, Zn^{2+}-binding
59.	*Fdx1*	Ferredoxin 1	Cholesterol metabolic process, hormone biosynthetic process
60.	*Adamts1*	ADAM metallopeptidase with thrombospondin type 1 motif, 1	Inflammatory response
61.	*Fbxo32*	F-box protein 32	Protein ubiquitination
62.	*Uck2*	Uridine-cytidine kinase 2	UMP, CTP salvage, cellular response to oxygen levels.
63.	*Tm4sf19*	Transmembrane 4 L six family member 19	N/A
64.	*Gm10334*	Predicted gene 10334	Proteolysis
65.	*Rps2-ps13*	Ribosomal protein S2, pseudogene 13	N/A
66.	*Slc16a2*	Solute carrier family 16 (monocarboxylic acid transporters), member 2	Symporter activity
67.	*Cdh2*	Cadherin-2	Cell adhesion, calcium-dependent.
68.	*Gm13375*	Predicted gene 13375	N/A

69.	*Kifc5b*	Kinesin family member C5B	Microtubule binding and microtubule motor activity.
70.	*Slc7a8*	Solute carrier family 7 (cationic amino acid transporter, y+ system) member 8	Large and neutral amino acid transmembrane transport.
71.	*C1qa*	Complement component 1, q subcomponent, alpha polypeptide	Complement activation, classical pathway, immune system process,
72.	*Gm10540*	Predicted gene 10540	N/A
73.	*Gm10153*	Predicted gene 10153	N/A
74.	*Tsga10ip*	Testis specific 10 interacting protein	N/A
75.	*Cir1*	Corepressor interacting with RBPJ, 1 Recombining binding proteinsuppressor of hairless	Required for RBPJ-mediated repression of transcription
76.	*Hmgb3*	High mobility group box 3	Negative regulation of myeloid cell differentiation
77.	*Ormdl3*	ORM1-like 3	Ceramide metabolic process. Negative regulator of sphingolipid synthesis. May indirectly regulate endoplasmic reticulum-mediated calcium signalling
78.	*5430421N 21Rik*	RIKEN cdna 5430421N21 gene	Human homolog KRT83, keratin 83, intermediate filament (cytoskeleton)
79.	*Krt8*	Keratin, type II cytoskeletal 8, cytokeratin8	Maintains cellular structural integrity and cellular differentiation. TNF-mediated signalling pathway.
80.	*Cnn3*	Calponin 3, acidic	Thin filament-associated protein. Binds to actin, calmodulin, troponin C and tropomyosin. Interaction of calponin with actin inhibits actomyosin Mg-ATPase activity.
81.	*Acsf2*	Acyl-CoA synthetase family member 2	Acyl-CoA synthases catalyze the initial reaction in fatty acid metabolism.
82.	*F2r*	F2r coagulation factor II (thrombin) receptor, (Proteinase-activated receptor 1 (PAR1))	Regulation of thrombotic response.
83.	*C1qb*	C1qb complement component 1, q subcomponent, beta polypeptide	Immune and stress response.
84.	*Cd83*	CD83 antigen	Immune response, antigen presentation and cellular interactions that follow lymphocyte activation
85.	*Vmn2r4*	Vomeronasal 2, receptor 4	GPCR, putative pheromone receptor.
86.	*Hs6st2*	Heparan sulfate 6-O-sulfotransferase 2	Heparan sulfate proteoglycans are molecules in cell surface, ECM & basement membranes. Involved in cell growth, differentiation, adhesion, and migration. *Hs6st2* catalyzes the transfer of sulfate to HS.
87.	*Gm9025*	Predicted gene 9025	
88.	*H2-Aa*	H2-Aa histocompatibility 2, class II antigen A, alpha	Immune response
89.	*Vmn1r59*	Vomeronasal 1 receptor 59	GPCR, pheromone receptor.
90.	*Serpine2*	Serpine2 serine (or cysteine) peptidase inhibitor, clade E, member 2	Serine protease inhibitor with activity toward thrombin, trypsin, and urokinase. Promotes neurite extension by inhibiting thrombin. Binds heparin.
91.	*Hsd3b1*	Hydroxy-delta-5-steroid dehydrogenase, 3 beta- and steroid delta-isomerase 1	Possible steroid biosynthetic process

92.	*Ube2c*	Ubiquitin-conjugating enzyme E2C	Ubiquitin-protein ligase activity
93.	*Mcpt4*	Mast cell protease 4	Proteolysis
94.	*Tgm2*	Transglutaminase 2, C polypeptide	Protein crosslinking
95.	*Ptgs1*	Prostaglandin-endoperoxide synthase 1 (COX-1)	
96.	*Txlng*	Taxilin gamma	Intracellular vesicle trafficking
97.	*Igkv8-30*	Immunoglobulin kappa chain variable 8-30	Immune response
98.	*Lsm6*	Lsm6 homolog, U6 small nuclear RNA associated (S. cerevisiae)	Involved in RNA processing
99.	*Gm4968*	Predicted gene 4968	
100.	*Ccl17*	Chemokine (C-C motif) ligand 17	Induces chemotaxis in T cells

Table S3. Differentially expressed genes (≥2.0-absolute-fold-change, P<0.05) following proton activation of OGR1 in murine macrophages. pH 6.7 24 h.

Entrez Gene No.	Symbol/gene	Gene Name
20344	*Selp*	Selectin P (Granule Membrane Protein 140kDa)
13653	*Egr1*	Early Growth Response 1
20299	*Ccl22*	Chemokine (C-C Motif) Ligand 22
12156	*Bmp2*	Bone morphogenetic protein 2
18787	*PAI-1*	Serpine1
57349	*Ppbp*	Pro-platelet basic protein (chemokine (C-X-C motif) ligand 7)
23886	*Gdf15*	Growth Differentiation Factor
14131	*Fcgr3*	Fc receptor, IgG, low affinity III (CD16)
246256	*Fcgr4*	Fc receptor, IgG, low affinity IV (CD16-2)
15370	*Nr4a1*	Nuclear receptor subfamily 4
20343	*Sell*	Selectin, CD62L
54123	*Irf7*	Interferon Regulatory Factor 7
21825	*Thbs1*	Thrombospondin 1
67603	*Dusp6*	Dual Specificity Phosphatase 6
29817	*Igfbp7/8*	Insulin-Like Growth Factor Binding Protein 7
16323	*Inhba*	Activin
20692	*Sparc*	Osteonectin
17228	*Cma1*	Chymase
641340	*Nrbf2*	Nuclear receptor binding factor 2
17227	*Mcpt4*	Mcpt4 mast cell protease 4
20379	*Sfrp4*	Secreted frizzled-related protein 4
14129	*Fcgr1*	Fc Fragment Of IgG, High Affinity Ia, Receptor (CD64)
22339	*Vegfa*	Vascular endothelial growth factor A

References

1. Livak KJ, Schmittgen TD. Analysis of Relative Gene Expression Data Using Real-Time Quantitative PCR and the 2−ΔΔCT Method. *Methods.* 2001;25(4):402-408.
2. Xia Y, Schneyer AL. The biology of activin: recent advances in structure, regulation and function. *The Journal of endocrinology.* 2009;202(1):1-12.
3. Escribese MM, Sierra-Filardi E, Nieto C, et al. The prolyl hydroxylase PHD3 identifies proinflammatory macrophages and its expression is regulated by activin A. *J Immunol.* 2012;189(4):1946-1954.
4. Zhang YQ, Resta S, Jung B, Barrett KE, Sarvetnick N. Upregulation of activin signaling in experimental colitis. *American journal of physiology. Gastrointestinal and liver physiology.* 2009;297(4):G768-780.
5. Sierra-Filardi E, Puig-Kroger A, Blanco FJ, et al. Activin A skews macrophage polarization by promoting a proinflammatory phenotype and inhibiting the acquisition of anti-inflammatory macrophage markers. *Blood.* 2011;117(19):5092-5101.

Chapter 3
Discussion

3.1 Ameliorated colitis in mice lacking GPR4 or OGR1

This is the first study in which the role of pH sensing G-protein coupled receptors and intestinal inflammation was studied in some detail. Taken together, the results demonstrated that GPR4 knockout mice had a partially reduced susceptibility in the DSS induced chronic colitis model. The deficiency of the pH receptors GPR4 and OGR1 attenuated spontaneous inflammation and modulated the severity of disease in the *IL-10* $^{-/-}$ mouse model, indicating an important pathophysiological role for these G-protein coupled receptors during the pathogenesis of mucosal inflammation.

In the model of chronic DSS induced colitis, resembling UC, *Gpr4* $^{-/-}$ mice showed less body weight loss and lower histology scores compared with wildtype littermates, suggesting less severe inflammation. In contrast, we also observed shortening of colon length and higher colonoscopy scores in *Gpr4* $^{-/-}$ mice during DSS administration consistent with more severe inflammation. No significant difference was observed in MPO activity, spleen weight and cytokines expression between *Gpr4* $^{+/+}$ *and Gpr4* $^{-/-}$ mice group. Despite these apparently discrepant observations, the overall clinical picture suggests an improvement of colitis since the major indicators such as body weight and histology score were in favor of an improved course of disease. The reasons for these discrepancies are currently unclear but might be related to presence or absence and specific functions of the receptor in the different cell types forming the intestinal mucosa. Cell-specific knock-out of GPR4 may help to address this point. Moreover, the susceptibility to DSS highly varies between

animal species and mouse strains [93]. The C57BL/J6 strain of mice was found to be more susceptible to DSS induced colitis than the Balb/c strain [93]. We emphasize that we have consistently observed the same tendency and unbiased results in all three round of DSS induced chronic colitis (2 rounds of Balb/c and 1 round of C57BL/J6 background).

To further investigate the role of pH receptors, another IBD mouse model, the spontaneous colitis model, simulating CD, was introduced into the study. Kaplan-Meier analysis of prolaps onset showed that the deficiency of GPR4 or OGR1 significantly delayed the onset of rectal prolapses in female *Gpr4* $^{+/+}$ */Ogr1* $^{-/-}$ */IL-10* $^{-/-}$ and male & female Gpr4 $^{-/-}$ */Ogr1* $^{+/+}$ */IL-10* $^{-/-}$ mice rather than *Gpr4* $^{+/+}$ */Ogr1* $^{+/+}$ */IL-10* $^{-/-}$ mice, which was consistent with the protective role of deficient pH receptor. The finding was also supported by lower histology scores and MPO activity measurements.

The LPLs profiles in flow cytometric analysis showed that GPR4 knockout suppressed infiltration of $CD4^+$ (T helper) cells, mainly as Th1 cells, but not $CD8^+$ (T cytotoxic) cells, which were confirmed by the cytokine mRNA expression data. Female *Gpr4* $^{-/-}$ */Ogr1* $^{+/+}$ */IL-10* $^{-/-}$ mice had a significantly lower Th1 cytokine IFN-γ mRNA expression in colon compared with female *Gpr4* $^{+/+}$ */Ogr1* $^{+/+}$ */IL-10* $^{-/-}$ counterparts. IL-10 is a well-known anti-inflammatory cytokine and suppressor for Th1 cells and macrophages [94]. *IL-10* $^{-/-}$ mice undoubtedly have a high level of Th1 cells [86, 88, 89]. But our data showed *Gpr4* $^{-/-}$ */Ogr1* $^{+/+}$ */IL-10* $^{-/-}$ mice had a surprisingly low CD4+ T helper cells infiltration with significantly low IFN-γ expression, suggesting strong suppression of Th1 cells by the lack

of GPR4. Depleting GPR4 signaling replaced IL-10 to suppress Th1 cells or blocked the pathway of Th1 cells infiltration in *Gpr4* $^{-/-}$ */Ogr1* $^{+/+}$ */IL-10* $^{-/-}$ mice. Last, the anti-inflammatory effect of GPR4 deficiency seems not to be mediated by elevating Treg levels and enhancing its suppression because no significant changes in Treg were observed among *Gpr4* $^{+/+}$ */Ogr1* $^{+/+}$ */IL-10* $^{+/+}$, *Gpr4* $^{+/+}$ */Ogr1* $^{+/+}$ */IL-10* $^{-/-}$ and *Gpr4* $^{-/-}$ */Ogr1* $^{+/+}$ */IL-10* $^{-/-}$ mice.

3.2 The proposed mechanism of GPR4 mediated inflammation aggravation

Based on the above findings, the possible mechanism of GPR4-mediated inflammation aggravation is proposed (Figure 11). In spontaneous colitis model, the additional deletion of GPR4 in *IL-10* $^{-/-}$ mice leads to the loss of the proton sensors and defective downstream signaling pathway; induces suppression of Th1 cells and less production of IFN-γ in colon; offers protection against spontaneous inflammation; and finally delays the onset of rectal prolapse. Therefore, in turn, activation of GPR4 is likely to exacerbate intestinal inflammation and trigger the responses which promote inflammation via a Gs-cAMP-Th1-IFN-γ pathway. IFN-γ is widely known to aggravate inflammation by increasing inducible Nitric Oxide Synthase (iNOS) expression, activating macrophage and NK cells and inducing apoptosis [96, 97]. The excessive production of glycolytic metabolites in inflamed tissues may cause the accumulation of protons, which further activates GPR4, forming a positive feedback loop.

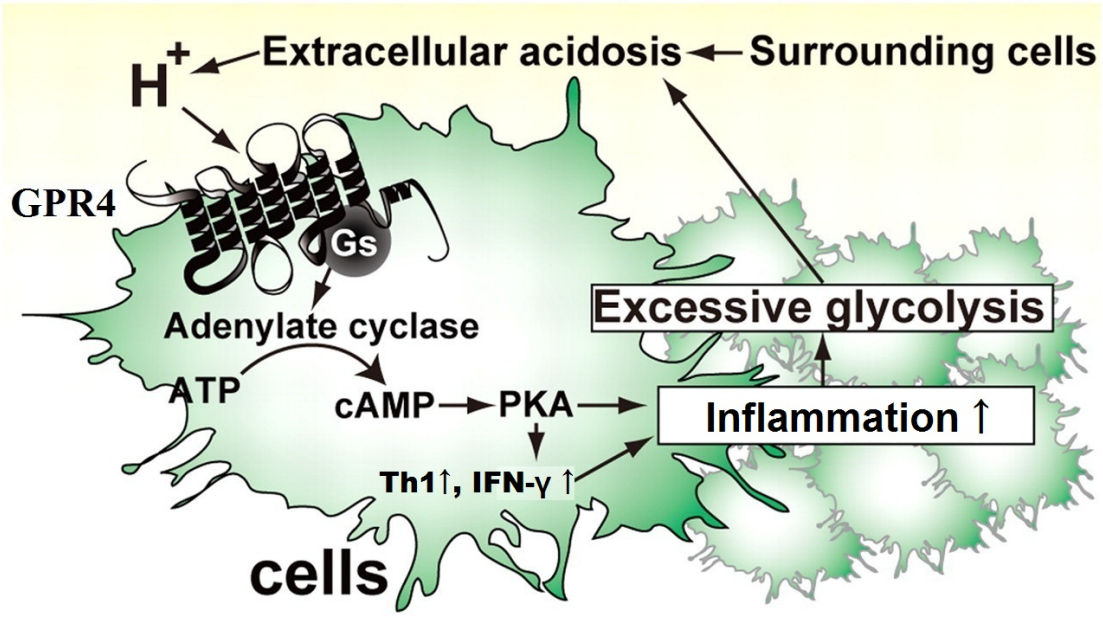

Figure 11 *The proposed mechanism of GPR4 mediated inflammation aggravation.* The excessive production of glycolytic metabolites in colonic tissue leads to the accumulation of proton, which in turn activates GPR4, forming a positive feedback loop. Therefore, activation of GPR4 is likely to exacerbate intestinal inflammation and trigger the responses that promote inflammation.

3.3 Several lines of evidence to support the destructive role of activated GPR4 in the progression of inflammation

The mRNA expression of GPR4 or OGR1 in human colon tissues provides a theoretical foundation for the functional involvement. The over-expression of GPR4 in variety of human cancer tissues including colon cancer has been reported [71]. In normal subjects, GPR4 mRNA is widely expressed. In small intestine and colon tissue, GPR4 shows a median expression level, as indicated by data provided by the National Center for Biotechnology Information (NCBI) Gene Expression Omnibus

(GEO) profile and Gene database (http://www.ncbi.nlm.nih.gov/sites/geo) and the BioGPS database of The Scripps Research Institute (http://biogps.org). Further evidence that GPR4 mRNA is strongly expressed in IBD patient's colon tissues was generated by our group and web-shared data (GEO Profile database ID: 12504653 and 4234799). Interestingly, GPR4 abundance in CD patients with remission, but not in severe and moderate CD or UC patients, was found to be significantly higher than the normal control level.

Recent publications on *Gpr4* $^{-/-}$ mice have reported several evidences to support the destructive role of activated GPR4 in the progress of inflammation. Seuwen and coworkers reported [73, 98], that *Gpr4* $^{-/-}$ mice showed an impaired response to VEGF-driven angiogenesis in a VEGF implant model and reduced tumor growth ability in a tumor-implant mouse model. Moreover, both GPR4 knockout and GPR4 inhibition by specific siRNAs resulted in decreased VEGFR2 (VEGF receptor 2, the main signaling receptor for VEGF on endothelial cells) levels, which might be one of the reasons for the reduced angiogenic response to VEGF [73, 98]. In an antigen induced arthritis mouse model, GPR4 deficient mice showed a significant inhibition of knee swelling and reduced severity of arthritis [98]. Also, reduced immune responses and attenuated airway hyperresponsiveness were observed in GPR4 deficient mice following ovalbumin exposure [98]. In the same ovalbumin-induced asthma mouse model, the decreased airway hyperresponsiveness in *Gpr4* $^{-/-}$ mice was associated with the reduction in the number of eosinophiles in bronchoalveolar lavage fluid, indicating a strong correlation between

GPR4 deficiency and inflammation inhibition [99]. In the cigarette smoke-induced COPD mouse model, *Gpr4* $^{-/-}$ mice showed an accelerated elimination of airway inflammation and enhanced neutrophil resolution [100], which, again, supports our observations.

3.4 Progress in GPR4 downstream signaling pathway studies

Up to date, only few efforts had been made to elucidate the GPR4 signaling pathway. Yang et al showed that acidosis/GPR4 signaling regulates endothelial cell adhesion mainly through the Gs/cAMP/Epac pathway [43]. The authors reported that the activation of GPR4 by acidosis increased the expression of multiple adhesion molecules such as E-selectin (SELE), Vascular cell adhesion molecule 1 (VCAM-1) and Intercellular Adhesion Molecule 1 (ICAM-1) in vitro and increased the adhesiveness of human umbilical vein endothelial cells (HUVECs) expressing endogenous GPR4 [43]. The mentioned adhesion molecules help to facilitate the binding of leukocytes and exacerbate the vascular inflammatory response. In our data, *Gpr4* $^{-/-}$ */IL-10* $^{-/-}$ female mice showed lower mRNA expression in iNOS, TNF-α, IFN-γ, IL-6, MCP-1, CXCL2, CXCL1, SELE and VCAM-1 rather than *Gpr4* $^{+/+}$ */IL-10* $^{-/-}$ female mice (no statistical significance except for IFN-γ), which at least in part is in agreement with the observations. The transcriptome analysis from the same research group reported that the NF-κB pathway was important for the acidosis and aGPR4-induced inflammatory gene expression [101].

Other data link GPR4 to the Extracellular Signal Regulated Kinase 1 and 2 (ERK 1⁄2) pathway. Bektas et al reported that activated GPR4 inhibited epidermal growth factor (EGF) induced ERK 1⁄2 activation [102]. But GPR4 was activated by the controversial agonist SPC, so the validity of this study must be questioned. Martinez et al reported that extracellular acidification induced human neutrophil activation through the activation of the P13K/Akt and ERK pathway, and low pH intensified acute inflammatory responses by delaying spontaneous apoptosis of neutrophil and extending the neutrophil functional lifespan [44, 45]. GPR4 may be among the mediators which are responsible for the acidification induced neutrophil activation. However, the presence of GPR4 has not been shown in these cells up to date. Considering other GPCRs, e.g. TDAG8 [72], angiotensin II type 2 receptor [103, 104] and sphingosine-1-phosphate receptor (S1P5) [105], also link to ERK pathway; Thus, the ERK pathway might be involved or partially involved in GPR4 signaling transduction and ultimately aggravate inflammation in an acidic environment. There are also some clues to link the ERK pathway to another pH sensing receptor, OGR1. An independent work reported low pH induced calcium mobilization and ERK phosphorylation in cancer progression [106]. Another work from a Japanese group reported extracellular acidosis induced IL-6 production and calcium mobilization, associated with the phosphorylation of ERK and p38MAPK [107]. The authors argued that it might be OGR1, but not GPR4, being responsible for the phosphorylation of ERK and Gq protein activation with calcium mobilization in response to extracellular protons.

cAMP has long been recognized as a “turn off button” and an

immunosuppressor to inhibit T cell functions [108, 109]. But recent studies demonstrated that cAMP also promotes T cell subset differentiation and T cell mediated immunity [110]. A conditional cAMP deficiency mouse model, in which the stimulatory Gα subunit (Gαs) was deleted in T cell, demonstrated that isolated $CD4^+$ T cell had reduced cAMP levels, fewer IFN-γ and IL-17 production, a weak Th1 and Th17 response but normal Th2 and Treg responses both in vitro and in vivo. The isolated $CD4^+$ T cell from same mouse model, short of cAMP production, showed reduced Th1/Th17 cell differentiation in vitro, and failed to induce colitis in the adoptive transfer mouse model (*Rag1* $^{-/-}$ recipients). The data provide further evidence for the contribution of cAMP to inflammation development, at least partially, supports the proposed mechanism of a GPR4-mediated inflammation aggravation and Gs-cAMP-Th1-IFN-γ pathway.

On all accounts, because there is a massive functional crosstalk among GPCRs, cAMP, Th1 cells, IFN-γ, other cytokines, kinases, transcription factors and promoters involved [96, 97], further analysis of downstream signaling networks of GPR4 will be of importance to elucidate the mechanisms underlying GPR4-mediated inflammation aggravation, as well as the complexity of the cytokine network in human IBD.

3.5 Progress in development of GPR4 inhibitors

A forward thinking strategy would also be to develop specific inhibitors or down-regulation modulators for IBD treatment. So far, two GPR4

inhibition agents were recently patented by Novartis [98, 111].

GPR4 antagonists, a group of imidazo-pyridine derivatives, were recently recognized and published [111]. For example: 2-Ethyl-3-{4-[3-(4-isopropyl-piperazin-1-yl)-prop-1-ynyl]-benzyl}-5- ,7-dimethyl-3H-imidazo[4,5-b] pyridine. The patent claimed to treat diseases and disorders which cover angiogenesis and/or pain, including autoimmune and inflammatory diseases using the compounds [111].

Another inhibitory modulator is siRNA specific for GPR4 [98]. The claims covered the treatment of cancer, anti-angiogenesis, macular degeneration, psoriasis, arthritis, multiple sclerosis or atherosclerosis by the inhibition of GPR4 [98].

3.6 OGR1 and inflammation

In agreement with our findings, there are several publications which describe the contribution of OGR1 to inflammation. Further, very interesting, OGR1 signaling transduction seems to be totally different from GPR4. Aoki et al [112, 113] reported *Ogr1* $^{-/-}$ mice exhibit diminished airway inflammation in the ovalbumin-induced asthma mouse model, including reduction in eosinophilia and mucus production, less goblet cell hyperplasia and significantly attenuated airway hyperresponsiveness. The diminished inflammation was achieved through Th2 responses, but not Th1 as in GPR4 deficient mice, because the *Ogr1* $^{-/-}$ mice showed impaired ability to generate Th2 associated cytokines IL-5, IL-4 and IgE [113].

A parallel project in our group has shown that OGR1 expression in Mono Mac 6 cells (derived from human macrophages and monocytes) was found to be induced by TNF-α, but not by other cytokines (IFN-γ, IL-1β, IL-6 and TGF-β), and the induction was reversed by NF-kB inhibitors (Cheryl de Valliere, unpublished data), further proving that OGR1 signaling differs from GPR4. Other publications associated OGR1 signaling with cyclooxygenase-2 (COX-2). Tomura et al [114] reported that protons/OGR1 signaling induced COX-2 expression and subsequent prostaglandin E-2 (PGE_2) production through Gq/11/phospholipase C/protein kinase C pathways, resulting bone calcium release and depletion. The effect was reversed by small interfering RNA (siRNA) specific to OGR1 and specific inhibitors for intracellular signaling pathways [114]. Liu et al reported activated OGR1 induced COX-2 expression, PGI_2 production and MKP-1 expression [115]. But in our data, we did not observe any change in COX-2 mRNA expression in both male and female *Gpr4* $^{+/+}$ */Ogr1* $^{-/-}$ */IL-10* $^{-/-}$ mice . How exactly the activated OGR1 boosts inflammation needs further efforts to resolve in the near future.

3.7 Gender dependent effect of OGR1

The gender difference exists also in immune response. The stronger response in female provides a better protection against infection, but may contribute to the higher incidence of autoimmune disease, e.g. Systemic lupus erythematosus (SLE), Rheumatoid arthritis (RA), Systemic sclerosis (SSc), rather than in male. The possible reasons for the gender difference are sex hormones or factors, including estrogen, testosterone

and Chromosome X, influencing the development, maturation, activation and apoptosis of immune cells. Unlike these female prevalent autoimmune diseases, as mentioned in Chapter 2.1, there seems to be only a slightly gender related difference in IBD incidence. UC is slightly more common in males, whereas CD shows a small female predominance [27].

By chance, we observed an obvious in-vivo gender difference in the spontaneous IBD mouse model. As shown in our data, the prolapse incidence in *Gpr4* $^{+/+}$ */Ogr1* $^{-/-}$ */IL-10* $^{-/-}$ male mice was significantly higher than in its female counterparts and Kaplan-Meier prolaps onset analysis showed that the onset of rectal prolapse in *Gpr4* $^{+/+}$ */Ogr1* $^{-/-}$ */IL-10* $^{-/-}$ female mice was significantly delayed as compared to their male litter mates, while no difference was observed in male and female mice for both *Gpr4* $^{+/+}$ */Ogr1* $^{+/+}$ */IL-10* $^{-/-}$ and *Gpr4* $^{-/-}$ */Ogr1* $^{+/+}$ */IL-10* $^{-/-}$ groups. The reason for the gender difference in prolapse incidence of *Gpr4* $^{+/+}$ */Ogr1* $^{-/-}$ */IL-10* $^{-/-}$ mice is not yet clear.

At the moment, we do not know whether sex hormones interfer with the regulation of OGR1 signalling pathways, or even if GPR4 and OGR1, respectively, are involved in different IBD types, UC and CD. More research work needs to be done to ascertain the involvement and role of estrogens, testosterone or other sex-based mediators in OGR1 signalling pathway.

3.8 Other proton sensors and the digestive system

pH receptors are not the only pH-sensing mechanism. Other than proton sensing GPCRs, there are many other receptors, enzymes, kinases and transporters functioning as sensors and regulators of extra- and intracellular protons [116], which also play important roles to maintain pH homeostasis, such as Na^+/H^+ exchanger (NHE family), Na^+/HCO_3^- transporters (biocarbonate transporters), acid sensing ion channels (ASICs), V-ATPases and so on.

A few representative members important for the digestive system are being shown here [116]. The Na^+/H^+ exchanger isoform 2 (SLC9A2/NHE2) is widely expressed in multiple tissues and responsible for fluid secretion in the digestive system [117, 118]. Na^+/H^+ exchanger isoform 3 (SLC9A3/NHE3) has a high abundance in kidney and intestines, and renal and intestinal absorption is defective in mice lacking SLC9A3/NHE3 [119, 120]. Diarrhea is the direct result of pathological SLC9A3/NHE3. Na^+/H^+ exchanger isoform 4 (SLC9A4/NHE4), a recognized risk loci for IBD [36], is abundantly expressed on stomach and kidney, whose pathophysiology is now being better understood. Histological analysis revealed that SLC9A4/NHE4 $^{-/-}$ mice were hypochlorhydric with reduced numbers of parietal cells and a loss of mature chief cells, indicating loss of SLC9A4/NHE4 corresponding to the impaired gastric acid secretion [121, 122].

Another kind of intracellular pH regulator is the mammalian bicarbonate transporter, which functions as acid extruder or acid loader to regulate intracellular protons. The acid extruding HCO_3^- transporters translocate Na^+ and HCO_3^- together in the same direction. Because the large

transmembrane Na^+ gradient is in favor of the net influx of HCO_3^-, which is equivalent to acid extrusion from the cells. For example, Na^+/HCO_3^- co-transporters SLC4a4/NBCe1 deficiency led to severe metabolic acidosis and intestinal obstruction [123, 124]. The acid loading Cl^-/HCO_3^- exchanger deal with the exchange of Cl^- for HCO_3^-. The inward Cl^- gradient provides the driving force for net HCO_3^- efflux in normal conditions. However, Cl^-/HCO_3^- exchanger SLC26a3/DRA's murin null phonotype showed a high chloride diarrhea and acidic luminal content in the colon [125]. Being of considerable interest, SLC26a3/DRA, predominantly expressed in the digestive system [126, 127], particularly abundant in duodenum and colon, was also identified as a risk loci for IBD [36] and its mutations caused congenital chloride diarrhea (CLD) [128-130].

We cannot rule out the involvement of any other proton sensor/transporter in the development of IBD. They may also compensate for GPR4 or OGR1. The previous work from our group reported that the pH sensitive kinase Pyk2 was upregulated in the proximal tubule of *Ogr1* $^{-/-}$ mice [79]. And GPR4 or OGR1 may regulate the activity and function of other proton sensors/transporters. A study demonstrated that chronic acidosis and GPR4 up-regulated the H^+-K^+-ATPase α subunit (HKα2) protein in HEK293 cells [78]. The previous work from our group also showed that OGR1 regulated the activity of two major plasma membrane proton transporters in HEK293 cells and renal proximal tubules, Na^+/H^+ exchanger (NHE_3) and H^+-ATPase [79]. Together with pH receptors, they may operate through complex interactions with each other.

Chapter 4
Future Perspectives

Some further areas of work come out as a consequence of our results:

- In this thesis, we firstly recognized that *Gpr4* $^{-/-}$ mice had a diminished mucosal inflammation by decreasing Th1 response and IFN-γ production. The reduced IFN-γ mRNA expression was shown in colon tissue of female *Gpr4* $^{-/-}$ */Ogr1* $^{+/+}$ */IL-10* $^{-/-}$ mice, but the IFN-γ protein level expression has not been tested yet. Therefore, the protein level expression of IFN-γ should be determined, e.g. by western blotting or ELISA.
- The intracellular cytokines could also be measured by intracellular cytokine staining of LPLs and FACS. Th1 associated cytokines (e.g. IFN-γ and IL-2) and Th2 cytokines (e.g. IL-4 and IL-10) staining could be measured, respectively, and Th1/Th2 ratio could be analyzed to verify GPR4 mediated inflammation aggravation through Th1 pathway.
- The protein level of GPR4 or OGR1 expression in human colon tissues could be validated by western blotting or immunofluorescence if corresponding antibodies would be available.
- It is necessary to test the in vivo anti-inflammatory properties of specific GPR4 antagonists in DSS induced chronic colitis mouse model and the spontaneous colitis mouse model.
- It is also necessary to test the proinflammatory effects of GPR4 or OGR1 activation with protons or other specific agonists in mouse colon, if these agonists are available.
- More in-vitro studies from GPR4 overexpressing cell lines would help to ascertain more detailed information on GPR4 activation as well as its downstream signaling pathway.

- The development and application of proton sensing receptors knockin mice (transgenic overexpression) would contribute to our better understanding of the molecular mechanism underlying pH receptor mediated inflammation aggravation.
- In this thesis, we observed an obvious gender difference in prolapse incidence and inflammatory progression in *Gpr4* $^{+/+}$ */Ogr1* $^{-/-}$ */IL-10* $^{-/-}$ mice group, while no difference existed for male and female mice for *Gpr4* $^{+/+}$ */Ogr1* $^{+/+}$ */IL-10* $^{-/-}$ and *Gpr4* $^{-/-}$ */Ogr1* $^{+/+}$ */IL-10* $^{-/-}$ mouse groups. More research work needs to be done to ascertain the involvement and role of estrogens, testosterone or other sex-based mediators in OGR1 signalling pathways.
- We investigated pH receptors GPR4 and OGR1 in this thesis. Another member of proton sensing receptor family, TDAG8, has not been studied in IBD. Especially, TDAG8 has been recognized as a risk locus in GWAS studies, which means it might play an even greater role in IBD pathogenesis. All the mentioned methodologies could be applied to TDAG8 studies, to further elucidate the precise role of TDAG8 in inflammation.

References

1. Kumar V, Robbins SL. Chapter 2 - Acute and Chronic Inflammation Robbins Basic Pathology. 8th ed. Philadelphia, PA: Saunders/Elsevier, 2007:31-58.
2. Kumar V, Robbins SL. Chapter 2 - Inflammation and Repair. Robbins Basic Pathology. 9th ed. Philadelphia, PA: Saunders/Elsevier, 2012:29-72.
3. Katzung BG. Chapter 55 - Immunopharmacology. Basic & Clinical Pharmacology. 9th Ed ed. New York: Lange Medical Books/McGraw Hill, 2004:977-980.
4. Rubin E, Reisner HM. Chapter 3 - Repair, Regeneration and Fibrosis. Essentials of Rubin's Pathology. 5th ed. Philadelphia: Wolters Kluwer Health/Lippincott Williams & Wilkins, 2009:36-52.
5. Dolgachev V, Lukacs NW. Chapter 2 - Acute and Chronic Inflammation Induces Disease Pathogenesis. Essential Concepts in Molecular Pathology. 1st Ed ed. San Diego: Academic Press, 2010:15-24.
6. Fitch FW, Editor-in-Chief: Peter JD. Helper T Lymphocytes. Encyclopedia of Immunology (Second Edition). Oxford: Elsevier, 1998:1158-1161.
7. Heath WR, Editor-in-Chief: Peter JD. T Lymphocytes. Encyclopedia of Immunology (Second Edition). Oxford: Elsevier, 1998:2341-2343.
8. Mason D, Editor-in-Chief: Peter JD. Lymphocytes. Encyclopedia of Immunology (Second Edition). Oxford: Elsevier, 1998:1625-1627.
9. Taub DD, Editor-in-Chief: Peter JD. Effector Lymphocytes. Encyclopedia of Immunology (Second Edition). Oxford: Elsevier, 1998:789-790.
10. Ward SG, June CH, Editor-in-Chief: Peter JD. T Lymphocyte Activation. Encyclopedia of Immunology (Second Edition). Oxford: Elsevier, 1998:2323-2329.
11. Braciale VL, Editor-in-Chief: Peter JD. Cytotoxic T Lymphocytes. Encyclopedia of Immunology (Second Edition). Oxford: Elsevier, 1998:725-730.
12. Stollar BD, Editor-in-Chief: Peter JD. B Lymphocytes. Encyclopedia of Immunology (Second Edition). Oxford: Elsevier, 1998:363-367.
13. Miossec P, Korn T, Kuchroo VK. Interleukin-17 and type 17 helper T cells. N Engl J Med 2009;361:888-98.
14. Bettelli E, Oukka M, Kuchroo VK. T(H)-17 cells in the circle of immunity and autoimmunity. Nat Immunol 2007;8:345-50.
15. Korn T, Bettelli E, Oukka M, Kuchroo VK. IL-17 and Th17 Cells. Annu Rev Immunol 2009;27:485-517.
16. Nomura T, Sakaguchi S. Foxp3 and Aire in thymus-generated Treg cells: a link in self-tolerance. Nat Immunol 2007;8:333-4.
17. Hill JA, Benoist C, Mathis D. Treg cells: guardians for life. Nat Immunol 2007;8:124-5.
18. Khattri R, Cox T, Yasayko SA, Ramsdell F. An essential role for Scurfin in CD4+CD25+ T regulatory cells. Nat Immunol 2003;4:337-42.
19. Walker MR, Kasprowicz DJ, Gersuk VH, Benard A, Van Landeghen M, et al.

Induction of FoxP3 and acquisition of T regulatory activity by stimulated human CD4+CD25- T cells. J Clin Invest 2003;112:1437-43.
20. Kim JM, Rasmussen JP, Rudensky AY. Regulatory T cells prevent catastrophic autoimmunity throughout the lifespan of mice. Nat Immunol 2007;8:191-7.
21. Abraham C, Cho JH. Inflammatory bowel disease. N Engl J Med 2009;361:2066-78.
22. Podolsky DK. Inflammatory bowel disease. N Engl J Med 2002;347:417-29.
23. Baumgart DC, Carding SR. Inflammatory bowel disease: cause and immunobiology. Lancet 2007;369:1627-40.
24. Baumgart DC, Sandborn WJ. Inflammatory bowel disease: clinical aspects and established and evolving therapies. Lancet 2007;369:1641-57.
25. Sellin J. Treatment targets in inflammatory bowel disease. Adv Drug Deliv Rev 2005;57:217-8.
26. WGO. World Gastroenterology Organisation Global Guidelines - Inflammatory bowel disease: a global perspective. http://www.worldgastroenterology.org/inflammatory-bowel-disease.html June 2009.
27. Loftus EV, Jr. Clinical epidemiology of inflammatory bowel disease: Incidence, prevalence, and environmental influences. Gastroenterology 2004;126:1504-17.
28. Endo K, Shiga H, Kinouchi Y, Shimosegawa T. [Inflammatory bowel disease: IBD]. Rinsho Byori 2009;57:527-32.
29. Strober W, Fuss I, Mannon P. The fundamental basis of inflammatory bowel disease. J Clin Invest 2007;117:514-21.
30. Weigmann B, Tubbe I, Seidel D, Nicolaev A, Becker C, et al. Isolation and subsequent analysis of murine lamina propria mononuclear cells from colonic tissue. Nat Protoc 2007;2:2307-11.
31. Lefrancois L, Lycke N. Isolation of mouse small intestinal intraepithelial lymphocytes, Peyer's patch, and lamina propria cells. Curr Protoc Immunol 2001;Chapter 3:Unit 3 19.
32. Xavier RJ, Podolsky DK. Unravelling the pathogenesis of inflammatory bowel disease. Nature 2007;448:427-34.
33. Papadakis KA, Targan SR. Role of cytokines in the pathogenesis of inflammatory bowel disease. Annu Rev Med 2000;51:289-98.
34. Bamias G, Nyce MR, De La Rue SA, Cominelli F. New concepts in the pathophysiology of inflammatory bowel disease. Ann Intern Med 2005;143:895-904.
35. Strober W, Fuss IJ. Proinflammatory cytokines in the pathogenesis of inflammatory bowel diseases. Gastroenterology 2011;140:1756-67.
36. Khor B, Gardet A, Xavier RJ. Genetics and pathogenesis of inflammatory bowel disease. Nature 2011;474:307-17.
37. Manolio TA. Genomewide association studies and assessment of the risk of disease. N Engl J Med 2010;363:166-76.
38. Mathew CG. New links to the pathogenesis of Crohn disease provided by

genome-wide association scans. Nat Rev Genet 2008;9:9-14.
39. Anderson CA, Boucher G, Lees CW, Franke A, D'Amato M, et al. Meta-analysis identifies 29 additional ulcerative colitis risk loci, increasing the number of confirmed associations to 47. Nat Genet 2011;43:246-52.
40. Barrett JC, Hansoul S, Nicolae DL, Cho JH, Duerr RH, et al. Genome-wide association defines more than 30 distinct susceptibility loci for Crohn's disease. Nat Genet 2008;40:955-962.
41. Franke A, McGovern DPB, Barrett JC, Wang K, Radford-Smith GL, et al. Genome-wide meta-analysis increases to 71 the number of confirmed Crohn's disease susceptibility loci. Nat Genet 2010;42:1118-1125.
42. James L. Lewis I, MD (Last full review/revision February 2013). Acid-Base Regulation and Disorders, The Merck Manual. http://www.merckmanuals.com/professional/endocrine_and_metabolic_disorders/acid-base_regulation_and_disorders/acid-base_regulation.html. Merck & Co., Inc., 2013.
43. Chen A, Dong L, Leffler NR, Asch AS, Witte ON, et al. Activation of GPR4 by acidosis increases endothelial cell adhesion through the cAMP/Epac pathway. PLoS One 2011;6:e27586.
44. Trevani AS, Andonegui G, Giordano M, Lopez DH, Gamberale R, et al. Extracellular acidification induces human neutrophil activation. J Immunol 1999;162:4849-57.
45. Martinez D, Vermeulen M, Trevani A, Ceballos A, Sabatte J, et al. Extracellular acidosis induces neutrophil activation by a mechanism dependent on activation of phosphatidylinositol 3-kinase/Akt and ERK pathways. J Immunol 2006;176:1163-71.
46. Vermeulen M, Giordano M, Trevani AS, Sedlik C, Gamberale R, et al. Acidosis improves uptake of antigens and MHC class I-restricted presentation by dendritic cells. J Immunol 2004;172:3196-204.
47. Vermeulen ME, Gamberale R, Trevani AS, Martinez D, Ceballos A, et al. The impact of extracellular acidosis on dendritic cell function. Crit Rev Immunol 2004;24:363-84.
48. Martinez D, Vermeulen M, von Euw E, Sabatte J, Maggini J, et al. Extracellular acidosis triggers the maturation of human dendritic cells and the production of IL-12. J Immunol 2007;179:1950-9.
49. Jancic CC, Cabrini M, Gabelloni ML, Rodriguez Rodrigues C, Salamone G, et al. Low extracellular pH stimulates the production of IL-1beta by human monocytes. Cytokine 2012;57:258-68.
50. Rubartelli A, Bajetto A, Allavena G, Cozzolino F, Sitia R. Post-translational regulation of interleukin 1 beta secretion. Cytokine 1993;5:117-24.
51. Eltzschig HK, Carmeliet P. Hypoxia and inflammation. N Engl J Med 2011;364:656-65.
52. Fallingborg J, Christensen LA, Jacobsen BA, Rasmussen SN. Very low intraluminal colonic pH in patients with active ulcerative colitis. Dig Dis Sci 1993;38:1989-93.

53. Raimundo AH, Evans DF, Rogers J, Silk DBA. Gastrointestinal pH profiles in ulcerative colitis. Gastroenterology 1992;102:A681.
54. Nugent SG, Kumar D, Rampton DS, Evans DF. Intestinal luminal pH in inflammatory bowel disease: possible determinants and implications for therapy with aminosalicylates and other drugs. Gut 2001;48:571-7.
55. Ileostomy Care. http://ileostomycare.com/ileostomy-care/ 2009.
56. Press AG, Hauptmann IA, Hauptmann L, Fuchs B, Fuchs M, et al. Gastrointestinal pH profiles in patients with inflammatory bowel disease. Aliment Pharmacol Ther 1998;12:673-8.
57. Ewe K, Schwartz S, Petersen S, Press AG. Inflammation does not decrease intraluminal pH in chronic inflammatory bowel disease. Dig Dis Sci 1999;44:1434-9.
58. Hou JK, Abraham B, El-Serag H. Dietary intake and risk of developing inflammatory bowel disease: a systematic review of the literature. Am J Gastroenterol 2011;106:563-73.
59. Cummings JH, Englyst HN. Gastrointestinal effects of food carbohydrate. Am J Clin Nutr 1995;61:938S-945S.
60. Gibson GR, Roberfroid MB. Dietary modulation of the human colonic microbiota: introducing the concept of prebiotics. J Nutr 1995;125:1401-12.
61. Seuwen K, Ludwig MG, Wolf RM. Receptors for protons or lipid messengers or both? J Recept Signal Transduct Res 2006;26:599-610.
62. Choi JW, Lee SY, Choi Y. Identification of a putative G protein-coupled receptor induced during activation-induced apoptosis of T cells. Cell Immunol 1996;168:78-84.
63. Sphingosylphosphorylcholine and lysophosphatidylcholine are ligands for the G protein-coupled receptor GPR4. J Biol Chem 2005;280:43280.
64. Retraction. Sphingosylphosphorylcholine is a ligand for ovarian cancer G-protein-coupled receptor 1. Nat Cell Biol 2006;8:299.
65. Kabarowski JH, Zhu K, Le LQ, Witte ON, Xu Y. Lysophosphatidylcholine as a ligand for the immunoregulatory receptor G2A. Science 2001;293:702-5.
66. Xu Y, Zhu K, Hong G, Wu W, Baudhuin LM, et al. Sphingosylphosphorylcholine is a ligand for ovarian cancer G-protein-coupled receptor 1. Nat Cell Biol 2000;2:261-7.
67. Zhu K, Baudhuin LM, Hong G, Williams FS, Cristina KL, et al. Sphingosylphosphorylcholine and lysophosphatidylcholine are ligands for the G protein-coupled receptor GPR4. J Biol Chem 2001;276:41325-35.
68. Ludwig MG, Vanek M, Guerini D, Gasser JA, Jones CE, et al. Proton-sensing G-protein-coupled receptors. Nature 2003;425:93-8.
69. Ishii S, Kihara Y, Shimizu T. Identification of T cell death-associated gene 8 (TDAG8) as a novel acid sensing G-protein-coupled receptor. J Biol Chem 2005;280:9083-7.
70. Wang JQ, Kon J, Mogi C, Tobo M, Damirin A, et al. TDAG8 is a proton-sensing and psychosine-sensitive G-protein-coupled receptor. J Biol Chem 2004;279:45626-33.

71. Sin WC, Zhang Y, Zhong W, Adhikarakunnathu S, Powers S, et al. G protein-coupled receptors GPR4 and TDAG8 are oncogenic and overexpressed in human cancers. Oncogene 2004;23:6299-303.
72. Ihara Y, Kihara Y, Hamano F, Yanagida K, Morishita Y, et al. The G protein-coupled receptor T-cell death-associated gene 8 (TDAG8) facilitates tumor development by serving as an extracellular pH sensor. Proc Natl Acad Sci U S A 2010;107:17309-14.
73. Wyder L, Suply T, Ricoux B, Billy E, Schnell C, et al. Reduced pathological angiogenesis and tumor growth in mice lacking GPR4, a proton sensing receptor. Angiogenesis 2011;14:533-44.
74. Li H, Wang D, Singh LS, Berk M, Tan H, et al. Abnormalities in osteoclastogenesis and decreased tumorigenesis in mice deficient for ovarian cancer G protein-coupled receptor 1. PLoS One 2009;4:e5705.
75. Castellone RD, Leffler NR, Dong L, Yang LV. Inhibition of tumor cell migration and metastasis by the proton-sensing GPR4 receptor. Cancer Lett 2011;312:197-208.
76. Singh LS, Berk M, Oates R, Zhao Z, Tan H, et al. Ovarian cancer G protein-coupled receptor 1, a new metastasis suppressor gene in prostate cancer. J Natl Cancer Inst 2007;99:1313-27.
77. Sun X, Yang LV, Tiegs BC, Arend LJ, McGraw DW, et al. Deletion of the pH sensor GPR4 decreases renal acid excretion. J Am Soc Nephrol 2010;21:1745-55.
78. Codina J, Opyd TS, Powell ZB, Furdui CM, Petrovic S, et al. pH-dependent regulation of the alpha-subunit of H+-K+-ATPase (HKalpha2). Am J Physiol Renal Physiol 2011;301:F536-43.
79. Mohebbi N, Benabbas C, Vidal S, Daryadel A, Bourgeois S, et al. The proton-activated G protein coupled receptor OGR1 acutely regulates the activity of epithelial proton transport proteins. Cell Physiol Biochem 2012;29:313-24.
80. Nakakura T, Mogi C, Tobo M, Tomura H, Sato K, et al. Deficiency of proton-sensing ovarian cancer G protein-coupled receptor 1 attenuates glucose-stimulated insulin secretion. Endocrinology 2012;153:4171-80.
81. Giudici L, Velic A, Daryadel A, Bettoni C, Mohebbi N, et al. The proton-activated receptor GPR4 modulates glucose homeostasis by increasing insulin sensitivity. Cell Physiol Biochem 2013;32:1403-16.
82. He XD, Tobo M, Mogi C, Nakakura T, Komachi M, et al. Involvement of proton-sensing receptor TDAG8 in the anti-inflammatory actions of dexamethasone in peritoneal macrophages. Biochem Biophys Res Commun 2011;415:627-31.
83. Mogi C, Tobo M, Tomura H, Murata N, He XD, et al. Involvement of proton-sensing TDAG8 in extracellular acidification-induced inhibition of proinflammatory cytokine production in peritoneal macrophages. J Immunol 2009;182:3243-51.
84. Kottyan LC, Collier AR, Cao KH, Niese KA, Hedgebeth M, et al. Eosinophil

viability is increased by acidic pH in a cAMP- and GPR65-dependent manner. Blood 2009;114:2774-82.
85. Hikiji H, Endo D, Horie K, Harayama T, Akahoshi N, et al. TDAG8 activation inhibits osteoclastic bone resorption. FASEB J 2014;28:871-9.
86. Hibi T, Ogata H, Sakuraba A. Animal models of inflammatory bowel disease. J Gastroenterol 2002;37:409-17.
87. Eckmann L. Animal models of inflammatory bowel disease: lessons from enteric infections. Ann N Y Acad Sci 2006;1072:28-38.
88. Wirtz S, Neurath MF. Mouse models of inflammatory bowel disease. Adv Drug Deliv Rev 2007;59:1073-83.
89. Solomon L, Mansor S, Mallon P, Donnelly E, Hoper M, et al. The dextran sulphate sodium (DSS) model of colitis: an overview. Comparative Clinical Pathology. Volume 19: Springer London, 2010:235-239.
90. Okayasu I, Hatakeyama S, Yamada M, Ohkusa T, Inagaki Y, et al. A novel method in the induction of reliable experimental acute and chronic ulcerative colitis in mice. Gastroenterology 1990;98:694-702.
91. Ni J, Chen SF, Hollander D. Effects of dextran sulphate sodium on intestinal epithelial cells and intestinal lymphocytes. Gut 1996;39:234-41.
92. Dieleman LA, Palmen MJ, Akol H, Bloemena E, Pena AS, et al. Chronic experimental colitis induced by dextran sulphate sodium (DSS) is characterized by Th1 and Th2 cytokines. Clin Exp Immunol 1998;114:385-91.
93. Mahler M, Bristol IJ, Leiter EH, Workman AE, Birkenmeier EH, et al. Differential susceptibility of inbred mouse strains to dextran sulfate sodium-induced colitis. Am J Physiol 1998;274:G544-51.
94. Moore KW, de Waal Malefyt R, Coffman RL, O'Garra A. Interleukin-10 and the interleukin-10 receptor. Annu Rev Immunol 2001;19:683-765.
95. Yang H, Jiang W, Furth EE, Wen X, Katz JP, et al. Intestinal inflammation reduces expression of DRA, a transporter responsible for congenital chloride diarrhea. Am J Physiol 1998;275:G1445-53.
96. Perez-Rodriguez R, Roncero C, Olivan AM, Gonzalez MP, Oset-Gasque MJ. Signaling mechanisms of interferon gamma induced apoptosis in chromaffin cells: involvement of nNOS, iNOS, and NFkappaB. J Neurochem 2009;108:1083-96.
97. Schroder K, Hertzog PJ, Ravasi T, Hume DA. Interferon-gamma: an overview of signals, mechanisms and functions. J Leukoc Biol 2004;75:163-89.
98. Seuwen; Klaus; (Basel CBEB, CH) ; Suply; Thomas; (Basel, CH) ; Wyder; Lorenza; (Basel, CH) ; Dawson King; Janet; (Basel, CH) ; Ludwig; Marie-Gabrielle; (Basel, CH) ; Mueller; Matthias; (Basel, CH) ; Nath; Puneeta; (Horsham, GB) ; Jones; Carol Elizabeth; (Horsham, GB). Inhibition of gpr4, US20100144835. In: USPTO, ed. Volume 20100144835. USA, 2010:1-50.
99. P Nath JM, M Freeman, C Poll, KH Banner, T Suply, A Trifilief, and C Jones. Effect of GPR4 Inhibition in a Murine Model of Allergic Asthma. D22 MODULATORS OF INFLAMMATORY PATHWAYS IN AIRWAY DISEASE. American Thoracic Society 2009 International Conference. Volume 179. San

Diego,CA, US: Am J Respir Crit Care Med, 2009:A5449.
100. Puneeta Nath CS, Mark Freeman, Chris Poll, Katharine Banner, Thomas Suply, Alexandre Triffilief, Carol Jones. Effect of GPR4 inhibition in a murine tobacco smoke model of chronic obstructive pulmonary disease. British Pharmacological Society Winter Meeting December 2008. Volume 6. Brighton, UK: Proceedings of the British Pharmacological Society, 2008:017P.
101. Dong L, Li Z, Leffler NR, Asch AS, Chi JT, et al. Acidosis activation of the proton-sensing GPR4 receptor stimulates vascular endothelial cell inflammatory responses revealed by transcriptome analysis. PLoS One 2013;8:e61991.
102. Bektas M, Barak LS, Jolly PS, Liu H, Lynch KR, et al. The G protein-coupled receptor GPR4 suppresses ERK activation in a ligand-independent manner. Biochemistry 2003;42:12181-91.
103. Bedecs K, Elbaz N, Sutren M, Masson M, Susini C, et al. Angiotensin II type 2 receptors mediate inhibition of mitogen-activated protein kinase cascade and functional activation of SHP-1 tyrosine phosphatase. Biochem J 1997;325 (Pt 2):449-54.
104. Huang XC, Sumners C, Richards EM. Angiotensin II stimulates protein phosphatase 2A activity in cultured neuronal cells via type 2 receptors in a pertussis toxin sensitive fashion. Adv Exp Med Biol 1996;396:209-15.
105. Malek RL, Toman RE, Edsall LC, Wong S, Chiu J, et al. Nrg-1 belongs to the endothelial differentiation gene family of G protein-coupled sphingosine-1-phosphate receptors. J Biol Chem 2001;276:5692-9.
106. Huang WC, Swietach P, Vaughan-Jones RD, Glitsch MD. Differentiation impairs low pH-induced Ca2+ signaling and ERK phosphorylation in granule precursor tumour cells. Cell Calcium 2009;45:391-9.
107. Ichimonji I, Tomura H, Mogi C, Sato K, Aoki H, et al. Extracellular acidification stimulates IL-6 production and Ca(2+) mobilization through proton-sensing OGR1 receptors in human airway smooth muscle cells. Am J Physiol Lung Cell Mol Physiol 2010;299:L567-77.
108. Mosenden R, Tasken K. Cyclic AMP-mediated immune regulation--overview of mechanisms of action in T cells. Cell Signal 2011;23:1009-16.
109. Bender AT, Beavo JA. Cyclic nucleotide phosphodiesterases: molecular regulation to clinical use. Pharmacol Rev 2006;58:488-520.
110. Li X, Murray F, Koide N, Goldstone J, Dann SM, et al. Divergent requirement for Galphas and cAMP in the differentiation and inflammatory profile of distinct mouse Th subsets. J Clin Invest 2012;122:963-73.
111. Taracido; Ivan Cornella; (Somerville MHEMP, MA) ; Hersperger; Rene; (Basel, CH) ; Lattmann; Rene; (Basel, CH) ; Miltz; Wolfgang; (Basel, CH) ; Weigand; Klaus; (Basel, CH). Imidazo pyridine derivatives, US20090291942. In: USPTO, ed. USA, 2009:1-50.
112. H. Aoki CM, T. Hisada, T. Ishizuka, K. Dobashi, M. Mori, F. Okajima. Effect of GPR4 Inhibition in a Murine Model of Allergic Asthma. D35 MODULATORS OF AIRWAY INFLAMMATION. American Thoracic Society 2010 International

Conference. Volume 181. New Orleans,LA, US: Am J Respir Crit Care Med, 2010:A5687.

113. H. Aoki CM, T. Hisada, T. Ishizuka, K. Dobashi, M. Mori, F. Okajima. Improving of experimental allergic asthma by decreased Th2 responses in OGR-1 knockout mice. E-Communication Session : Animal models of asthma and lung inflammation. European Respiratory Society Annual Congress 2010. Barcelona,Spain: https://www.ersnetsecure.org/public/prg_congres.abstract?ww_i_presentation=47174, 2010:5648.
114. Tomura H, Wang JQ, Liu JP, Komachi M, Damirin A, et al. Cyclooxygenase-2 expression and prostaglandin E2 production in response to acidic pH through OGR1 in a human osteoblastic cell line. J Bone Miner Res 2008;23:1129-39.
115. Liu JP, Komachi M, Tomura H, Mogi C, Damirin A, et al. Ovarian cancer G protein-coupled receptor 1-dependent and -independent vascular actions to acidic pH in human aortic smooth muscle cells. Am J Physiol Heart Circ Physiol 2010;299:H731-42.
116. Casey JR, Grinstein S, Orlowski J. Sensors and regulators of intracellular pH. Nat Rev Mol Cell Biol 2010;11:50-61.
117. Park K, Evans RL, Watson GE, Nehrke K, Richardson L, et al. Defective fluid secretion and NaCl absorption in the parotid glands of Na+/H+ exchanger-deficient mice. J Biol Chem 2001;276:27042-50.
118. Schultheis PJ, Clarke LL, Meneton P, Harline M, Boivin GP, et al. Targeted disruption of the murine Na+/H+ exchanger isoform 2 gene causes reduced viability of gastric parietal cells and loss of net acid secretion. J Clin Invest 1998;101:1243-53.
119. Gekle M, Volker K, Mildenberger S, Freudinger R, Shull GE, et al. NHE3 Na+/H+ exchanger supports proximal tubular protein reabsorption in vivo. Am J Physiol Renal Physiol 2004;287:F469-73.
120. Schultheis PJ, Clarke LL, Meneton P, Miller ML, Soleimani M, et al. Renal and intestinal absorptive defects in mice lacking the NHE3 Na+/H+ exchanger. Nat Genet 1998;19:282-5.
121. He P, Yun CC. Mechanisms of the regulation of the intestinal Na+/H+ exchanger NHE3. J Biomed Biotechnol 2010;2010:238080.
122. Gawenis LR, Greeb JM, Prasad V, Grisham C, Sanford LP, et al. Impaired gastric acid secretion in mice with a targeted disruption of the NHE4 Na+/H+ exchanger. J Biol Chem 2005;280:12781-9.
123. Burnham CE, Amlal H, Wang Z, Shull GE, Soleimani M. Cloning and functional expression of a human kidney Na+:HCO3- cotransporter. J Biol Chem 1997;272:19111-4.
124. Gawenis LR, Bradford EM, Prasad V, Lorenz JN, Simpson JE, et al. Colonic anion secretory defects and metabolic acidosis in mice lacking the NBC1 Na+/HCO3- cotransporter. J Biol Chem 2007;282:9042-52.
125. Schweinfest CW, Spyropoulos DD, Henderson KW, Kim JH, Chapman JM, et al. slc26a3 (dra)-deficient mice display chloride-losing diarrhea, enhanced

colonic proliferation, and distinct up-regulation of ion transporters in the colon. J Biol Chem 2006;281:37962-71.
126. Jacob P, Rossmann H, Lamprecht G, Kretz A, Neff C, et al. Down-regulated in adenoma mediates apical Cl-/HCO3- exchange in rabbit, rat, and human duodenum. Gastroenterology 2002;122:709-24.
127. Mount DB, Romero MF. The SLC26 gene family of multifunctional anion exchangers. Pflugers Arch 2004;447:710-21.
128. Hoglund P. SLC26A3 and congenital chloride diarrhoea. Novartis Found Symp 2006;273:74-86; discussion 86-90, 261-4.
129. Makela S, Kere J, Holmberg C, Hoglund P. SLC26A3 mutations in congenital chloride diarrhea. Hum Mutat 2002;20:425-38.
130. Wedenoja S, Pekansaari E, Hoglund P, Makela S, Holmberg C, et al. Update on SLC26A3 mutations in congenital chloride diarrhea. Hum Mutat 2011;32:715-22.

Curriculum Vitae

Name:	**Yu WANG (王瑜)**
E-mail:	wangyudoctor@gmail.com
Sex / Marital Status:	Male / Married
Date of Birth:	22/Apr/1979
Nationality:	Chinese

Education:

July, 2009 ~ Current	**PhD Candidate in Integrative Molecular Medicine (imMed)** ETH/UniZH, The Life Science Zürich Graduate School. Supervisor: Prof. Carsten Wagner (Physiology, University of Zürich), Prof. Gerhard Rogler (Gastroenterology, University Hospital Zürich). Thesis: Role of pH receptors in intestinal inflammation.
Oct,2007 ~ May, 2009	**PhD Candidate and research assistant** King's College London. Thesis: S-Nitrosoglutathione Reductase (GSNOR): functional activity and structural studies.Mechanism of asthma and novel therapeutic target validation.
Sep, 2001 ~ June, 2004	**M.Sc in Pharmacology** Xi'an Jiaotong University (Top Ten in CHINA), Xi'an, Shaanxi, China.
Sep, 1996 ~ July, 2001	**Bachelor of Medicine/Medical Doctor training** Medical College of Chinese People's Police, Tianjin, China. 3.5 years training in medical school and 1.5 years intern in hospital (Rotation in Cardiology, Gastroenterology, Emergency Med, Oncology, Nephrology and dialysis, General Surgery, Imaging, Diagnostics and Clinical Chemistry).

Professional Experience:

June, 2006 ~ Sep, 2007	**Contract Researcher II (FTE for Pfizer)** Biology Service Department, WuXi PharmaTech Co. Ltd (NYSE:WX). ShangHai, China. (The most leading R&D outsourcing supplier and CRO in China)

1. Developed high throughput screening assays for cervical and breast cancer;
2. Applications of fluorescent cell-based assays in GPCR drug discovery;
3. Performed outsourcing projects strategy planning;
4. Helped to handle Pharm R&D projects portfolio management and priority analysis.

June, 2004 ~ June, 2006	**Research Assistant** Preclinical Research Center, Guangzhou Institute of Biomedicine and Health (GIBH), Chinese Academy of Sciences (CAS). GuangZhou, China.

Led, supervised and performed the following projects with team of 4 students:

1. In vitro ADME/Tox profiling and Preclinical drug development;
2. The Caco-2 permeability assay for intestinal absorption and transport studies;
3. Hepatocytes sandwich cultures for metabolic stability, P450 induction and inhibition;
4. Drug-drug interaction and drug safety evaluation.

Professional Training and Certifications:

1. **NIH Clinical Research Training** online course (NIH Clinical Center, US, 2012)
2. **2011 Merck Serono Innovation Cup Competition** (1⁄20 selected participants from all over the world, Merck Serono S.A., Seeheim-Jugenheim, Germany, 2011)
3. **Clinical Data Management** summer training and certificate (SMMU / Roche R&D center in ShangHai, 2010)
4. Intensive training course in **Epidemiology and Biostatistics** in Biomedical Research (Bio410, Institute of Social and Preventive Medicine, UZH, 2010)
5. Intensive training course in **Developing New Medicines** (Bio429, UZH, 2010)
6. **Patenting in Life Science and IP protection** (The Life Science Zürich Graduate School, 2010)
7. **Data analysis using the statistical software R-1** (The Life Science Zürich Graduate School, 2010)
8. **Project Management** Training (Zürich Center for Integrative Human Physiology, ZIHP, 2010)

Language skills:

English (Excellent); Chinese Mandarin (Mother language); Deutsch (Basic); Cantonese (Middle).

Computer skills:

1. Microsoft Word, Outlook and Powerpoint;
2. SPSS and Microsoft Excel for spreadsheet analysis;
3. SAS (Basic programming for biostatistics);
4. GenSight (Project portfolio management and prioritizing matrix);
5. Winnoline (PK/PD modeling);
6. Clinical trial protocol, Statistical analysis planning and Clinical study report;
7. Case Report Form (CRF) database (Clinical trial and data management);
8. Adverse Drug Reaction (ADR) database (Data processing and analysis);
9. GraphPad Prism and SigmaPlot (Biostatistics and plotting);
10. Instruments & Software & Database (Many, upon request).

Other Activities:

Organizing committee member of Zürich Life Science Day Career Fair Event (2012 and 2013).

1. Being responsible to look for and communicate with sponsors.
2. Coordinate and organize the event.

Board member of Chinese Association of Life Science in Switzerland (CALSS).

1. Coordinate and organize the annual event, networking Apéro.
2. Being responsible to look for scientific partnership and partnership funding for both China and Swiss, contributing to a better understanding and collaboration.

Acknowledgements

I would like to thank:

- Prof. Carsten A. Wagner, Prof. Gerhard Rogler and Dr. Isabelle Frey-Wagner, my thesis supervisors for giving me the opportunity to work in the group and with this exciting project, their valuable guidance and support throughout the years of my thesis would be most appreciated. Their rigorous and conscientious attitude and constantly striving for excellence will always inspire me for the rest of my life.

- Dr. Klaus Seuwen (Novartis NIBR Basel, GPCR Biology), as one of the thesis committee members, for the kind supply of knockout mice used in the study.

- Martin Hausmann and Silvia Lang, the regular audience of my work in progress meetings at USZ, for their helpful discussion and precious advices in scientific and technical issues.

- Irina Leonardi, Sven Gruber, Kirstin Atrott for their great contribution to the experiments and always giving good input into the planning of experiments.

- Katharina Leucht, Lutz Wolfram, Alexandra Gerstgrasser, for their inexhaustible patience to read my working protocols, guide me to use machines and support me both physically and psychologically.

- All the people from Prof. Gerhard Rogler's group who contributed to the project with their work and expertise:
Cheryl de Valliere, Michaela Krebs, Ragam Attinkara, Belen Moron Flores , Anne Fischbeck, Susanne Bentz, Helen Mareike, Kacper Wojtal, Joba Arrikat, Aretussa Apladas, Sandra Frei, Kathrin Schlesinger, Annika Wyss, Marianne Spalinger, Susan Bengs, Claudia Stanzel , Eugenia Becker.

- Prof. Jürg Biber, Nilufar Mohebbi, Nati Hernando and Nicole Kampik, the regular audience of my work in progress meetings at Irchel, for their valuable suggestions and advice concerning my project.

- Abhijeet Todkar and Yang LIU from Dr. Andreas Serra's group for their

kind help to take care of my mice during my absence. Especially Abhijeet has been a good source for discussions and problem solving when needed.

- Marija Mihailova and Petra Seebeck for offering help to look after my mice.

- Nicolas Picard, Olga Andrini and Monica Patti for all technical advice and help.

- All the people from Prof. Carsten A. Wagner's group and J floor who contributed to the project with their work and expertise:
Soline Bourgeois, Isabel Rubio Aliaga, Arezoo Daryadel, Udo Schnitzbauer, Carla Bettoni, Thomas Knöpfel, Reto Mühlemann, Marta Ferreira Lopes de Figueiredo, Justyna Ruminska, Kessara Chan, Lisa Bounoure, Remy Bürki, Chahira Benabbas, Luca Giudici, Maria Haller, Meisam Khorrami, Ming ZENG, Hongbo ZHANG, Gerti Stange, Ursula Lüthi, Myakala Komuraiah, Linto Thomas.

- Prof. Onur Boyman, Dr. Carsten Krieg and Koray Thomasson from the Laboratory of Applied Immunobiology, University of Zurich, for the kind supply of the FACS machine and antibodies, and their work and expertise contributing to this project.

- The Zurich Center for Integrative Human Physiology (ZIHP)/cooperative projects for financing the challenging project and The PhD Program in Integrative Molecular Medicine (imMed), Life Science Zurich Graduate School, for the PhD student membership.

- Hartmann Müller-Stiftung and Swiss Physiological Society for supplying fundinge to cover my US trips to Digestive Disease Week (DDW) 2011 and 2012.

Furthermore, I would like to thank:

- My parents (Mr. Yuanhua WANG and Ms. Sujuan YU), Jia's mum Ms. Yahua DING for their great support and patience during all the years of my studies and my PhD.

- My wife Jiajia for her love and especially for her patience during the

though time of my PhD; and the coming son of ours (Oscar Yichen WANG) for the hope and anxious waiting of birth.

- Reto Mühlemann, my first gross man in my wedding and a good friend, for his wonderful personality and positive attitude, encouraging me and making my life easier.

- Sven Gruber, for his great efforts to translate the summary of my thesis into German. His help is also a constant source of inspiration.

List of Abstracts

Abstracts:

1. **Yu Wang**, Gerhard Rogler, Carsten Wagner, et al. Deficiency of the pH receptors OGR1 or GPR4 ameliorates inflammatory bowel disease. ***Annual Meeting of the Swiss Physiological Society and Young Investigator Award*** 2012. Sep 2012 in Fribourg, Switzerland. (Abstract and Oral Presentation)
2. **Yu Wang**, Gerhard Rogler, Carsten Wagner, et al. pH receptor deficiency delays the onset and progression of spontaneous colitis in IL-10 knockout mice. ***Digestive Disease Week (DDW)*** 2012. May 2012 in San Diego, US. (Abstract and poster)
3. **Yu Wang**, Gerhard Rogler, Carsten Wagner, et al. Role of pH receptors in inflammatory bowel disease mouse model. ***Digestive Disease Week (DDW)*** 2011. May 2011 in Chicago, US. (Abstract and poster)
4. **Yu Wang**, Isabelle Frey-Wagner, Cheryl de Valliere et al. Role of pH receptors in murine experimental colitis. ***7th Symposium of the ZIHP 2011***. Aug 2011 in Zürich, Switzerland. (Abstract and poster)
5. **Yu Wang**, Aretussa Apladas, et al. Role of proton-activated receptors in inflammatory bowel disease in mice. ***6th Symposium of the ZIHP 2010***. Aug 2010 in Zürich, Switzerland. (Abstract and poster)

Publications:

1. **Yu Wang***, Cheryl de Valliere*, Gerhard Rogler, Carsten Wagner, et al. The proton-activated receptor GPR4 modulates intestinal inflammation. 2015.
* contributed equally to this work. Submitted.

2. Cheryl de Valliere*, **Yu Wang***, Gerhard Rogler, Carsten Wagner, et al. The G-protein-coupled pH-sensing *OGR1* is a regulator of intestinal inflammation. 2015. Inflammatory Bowel Diseases.
* contributed equally to this work. Accepted.

3. Sven Gruber*, **Yu Wang***, Carsten Wagner, et al. Role of LRRK2 in inflammatory bowel disease. 2015.

* contributed equally to this work. In preparation.